RODRIGO CASTELAN CARLSON

MAINSTREAM TRAFFIC FLOW CONTROL ON MOTORWAYS

CHANIA, GREECE
2011

TECHNICAL UNIVERSITY OF CRETE

DEPARTMENT OF PRODUCTION ENGINEERING AND MANAGEMENT

MAINSTREAM TRAFFIC FLOW CONTROL ON MOTORWAYS

Thesis submitted in partial fulfillment of
the requirements for the degree of
Doctor of Philosophy
by

RODRIGO CASTELAN CARLSON

Chania, Greece, September 2011

Typeset in LaTeX with Texmaker and MiKTeX.

Figures created with Inkscape and the `textext` plugin.

Plots generated with Matlab® and the `matlabfrag` function.

MAINSTREAM TRAFFIC FLOW CONTROL ON MOTORWAYS

Rodrigo Castelan Carlson

'This Ph.D. Thesis is approved by:'

Advisory committee:

Markos Papageorgiou (Supervisor)
Professor, Department of Production Engineering and Management
Technical University of Crete

Ioannis Papamichail (Co-supervisor)
Assistant Professor, Department of Production Engineering and Management
Technical University of Crete

Elias Kosmatopoulos (Member of the advisory committee)
Associate Professor, Department of Electrical and Computer Engineering
Democritus University of Thrace

Thesis committee:

Vassilis Kouikoglou
Professor, Department of Production Engineering and Management
Technical University of Crete

Georgios Stavroulakis
Professor, Department of Production Engineering and Management
Technical University of Crete

Dimitrios Rovas
Assistant Professor, Department of Production Engineering and Management
Technical University of Crete

Iasson Karafyllis
Assistant Professor, Department of Environmental Engineering
Technical University of Crete

To Anamaria.

ACKNOWLEDGEMENTS

Living four years in Greece was an adventure and I could not have a better company than my wife Anamaria and, in the last few months, our baby to be, to whom I am extremely grateful. Our families had and indisputable role supporting us in these four years and we are grateful to all of them, specially to my father Renato Carlson and his wife Suzana Carlson; to my brothers Augusto Castelan Carlson, Victor Emmanuel Carlson, Luiz Henrique Castelan Carlson and their families; to my father-in-law Cleber Teixeira dos Santos, to my mother-in-law Maria Elisabeth Pereira Rego, and to Anamaria's aunt Sonia Mascarello. In memory of my mother, I would like to thank her for her important role in my education.

During this work I had the privilege of being supervised by Prof. Markos Papageorgiou. I feel honoured of having had him as my supervisor and I wish I could stay longer and learn even more from him. His support went far beyond academic advice without which it would have been very difficult to stay in Greece. I am also grateful to my co-advisor Dr. Ioannis Papamichail for the constant support and patience.

I really appreciate the assistance of the secretaries and professors of the Department of Production Engineering and Management that were involved in one way or another with my studies at the Technical University of Crete. I am also grateful to the professors who participated in my thesis committee.

I would like to thank my colleagues at DSSL, Athina Tymbakianaki, Gerasimos Loutos, Giorgos Sarros, Kostas Aboudoulas, Mehdi Keyvan Ekbatani, Natasa Spiliopoulou and Tasos Kouvelas; and DSSL staff Vangelis Voudourakis and Dimitra Tsimpinou.

I thank Dr. Albert Messmer for incorporating Variable Speed Limits in the METANET simulator and in the AMOC optimal control tool.

I am extremely grateful to Katerina and Efi Frantzikinaki, our hosts in the last four years, for their love and support.

I thank the staff of TUC's restaurant when operated by First Class A.B.E.T.E., specially the restaurant's chef and friend Giorgos Liontaras.

I thank the members and participants of the Multitude Project (http://www.multitude-project.eu/) funded by the European Union COST programme. The experience of participating in this project and interacting with its members and participants was invaluable.

Several friends changed their holidays destination and saved their hard earned money to visit us in Greece. Their company during the few days of their visits but also their support during our stay in Greece was invaluable: Júlio Cordioli, Manoel Vieira, Maria Isabel Vieira e Regina Melin Cunha; Eduardo Nickel; Eduardo Henrique Bastos e Maíra Queiroz dos Santos; Cristiano da Silva Teixeira e Leila Procópia Nascimento; e Manoel P. R. T. dos Santos. I thank many other friends that were unable to visit us but kept in touch giving their support and following closely our progress.

Rock climbing in Crete was a great experience and I am thankful to all my climbing partners during my stay in Greece, particularly Manolis Katsanevas and Kostas Kavalinakis.

I appreciate the support of several professors and staff at the Department of Automation and Systems at the Federal University of Santa Catarina during my application for the scholarship for studies abroad and during my stay in Greece. I am particularly grateful to my former advisor Prof. Werner Kraus Junior for the support and cooperation during these four years and for serving as my CAPES' Tutor.

Finally, I would like to thank the CAPES Foundation, Ministry of Education of Brazil, for funding my studies abroad and all the staff involved in the whole process, as well as the Brazilian taxpayers who were ultimately the funders of this work.

SHORT BIOGRAPHY

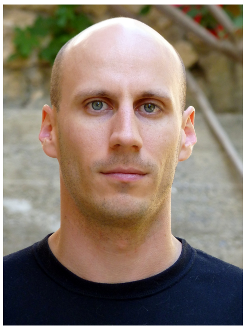

Rodrigo Castelan Carlson was born in Florianópolis, Brazil, in 1980. He received the Bel.Eng. degree in Control and Automation Engineering and the Me.Eng. degree in Electrical Engineering from the Federal University of Santa Catarina, Florianópolis, Brazil, in 2004 and 2006, respectively, and the Bel. degree in Business Administration from the University of the State of Santa Catarina, Florianópolis, Brazil, in 2006. From 2007, he worked toward the Ph.D. degree with the Dynamic Systems and Simulation Laboratory, Technical University of Crete, Chania, Greece.

From 2006 to 2007, he was a Research and Development Engineer with the Federal University of Santa Catarina. Since 2007, he has been a Research Assistant with the Dynamic Systems and Simulation Laboratory, Technical University of Crete, Chania, Greece. He is the author and coauthor of four technical papers in scientific journals and magazines and some 20 technical papers in scientific conference proceedings, and has been a reviewer for several journals and conferences. His main research interests include automatic control and optimisation theory and applications to traffic and transportation systems.

Mr. Carlson was the recipient of a scholarship for postgraduate studies abroad from The Capes Foundation, Ministry of Education of Brazil (during 2007-2011) and the Gold Medal of the Young European Arena of Research 2010 in the pillar "Mobility and Intermodality."

Abstract of the Thesis presented to the Technical University of Crete as a partial fulfillment of the requirements for the degree of Doctor of Philosophy.

MAINSTREAM TRAFFIC FLOW CONTROL ON MOTORWAYS

Rodrigo Castelan Carlson

September/2011

Supervisor: Professor Markos Papageorgiou
Co-Supervisor: Dr. Ioannis Papamichail
Keywords: mainstream traffic flow control, motorway traffic control, ramp metering, variable speed limits, fundamental diagram, optimal control, feedback control
Number of Pages: 164

The continuously increasing daily traffic congestions on motorway networks around the world call for innovative control measures that would drastically improve the current traffic conditions. Mainstream traffic flow control (MTFC) is proposed as a novel and efficient motorway traffic management tool, and its possible implementation and principal impact on traffic flow efficiency is analysed. Variable speed limits (VSLs), suitably operated and enforced, are considered as one (out of several possible) way(s) for MTFC realisation, either as a standalone measure or in combination with ramp metering.

A quantitative model of the VSL impact on aggregate traffic flow behaviour on motorways is proposed and allows for VSLs to be incorporated in a macroscopic second-order traffic flow model as an additional control component. The integrated motorway network traffic control problem involving ramp metering and VSLs is formulated as a constrained discrete-time optimal control problem and is solved efficiently even for large-scale networks by a suitable feasible direction algorithm.

An illustrative example of a hypothetical motorway stretch as well as a large-scale motorway ring-road are investigated under different control scenarios using the optimal control approach. It is shown that traffic flow efficiency can be substantially improved when MTFC via VSLs is used with or without integration with coordinated ramp metering actions.

Since sophisticated optimal control methods may face difficulties in practical field implementations, three simple controllers for local feedback MTFC on motorways, enabled via VSLs, are proposed in this thesis. All feedback controllers rely only on readily available real-time measurements (no on-line model usage and no demand predictions are needed), take into account a number of practical and safety restrictions, and are therefore robust and suitable for field implementations. The controllers are evaluated in simulation and compared with the optimal control results for a hypothetical motorway stretch. Despite their simplicity, the results show that the feedback controllers exhibit a satisfactory control behaviour and, indeed, approach the optimal control results for a number of investigated scenarios. Recommendations for the operation of the feedback controllers are given.

Περίληψη της Διατριβής που υπεβλήθη στο Πολυτεχνείο Κρήτης για τη μερική ικανοποίηση των απαιτήσεων για την απόκτηση Διδακτορικού Διπλώματος.

ΕΛΕΓΧΟΣ ΚΥΡΙΑΣ ΚΥΚΛΟΦΟΡΙΑΚΗΣ ΡΟΗΣ ΑΥΤΟΚΙΝΗΤΟΔΡΟΜΩΝ

Rodrigo Castelan Carlson

Σεπτέμβριος/2011

Επιβλέπων: Καθηγητής Μάρκος Παπαγεωργίου
Συν-Επιβλέπων: Δρ. Ιωάννης Παπαμιχαήλ
Λέξεις Κλειδιά: έλεγχος κύριας κυκλοφοριακής ροής, έλεγχος κυκλοφορίας αυτοκινητοδρόμων, έλεγχος ραμπών εισόδου, μεταβλητά όρια ταχύτητας, θεμελιώδες διάγραμμα, βέλτιστος έλεγχος, έλεγχος με ανατροφοδότηση
Αριθμός σελίδων: 164

Οι συνεχώς αυξανόμενες καθημερινές κυκλοφοριακές συμφορήσεις που λαμβάνουν χώρα σε δίκτυα αυτοκινητοδρόμων σε ολόκληρο τον κόσμο απαιτούν καινοτόμα μέτρα ελέγχου, τα οποία θα βελτιώσουν δραστικά τις τρέχουσες συνθήκες κυκλοφορίας. Ο έλεγχος κύριας κυκλοφοριακής ροής (ΕΚΚΡ) προτείνεται ως ένα νέο και αποτελεσματικό εργαλείο διαχείρισης της κυκλοφορίας των αυτοκινητοδρόμων, και αναλύεται η πιθανή εφαρμογή του και ο ουσιαστικός αντίκτυπός του στην αποτελεσματικότητα της ροής της κυκλοφορίας. Τα μεταβλητά όρια ταχύτητας (ΜΟΤ), όταν λειτουργούν και επιβάλλονται κατάλληλα, θεωρούνται ως ένας τρόπος (από τους πολλούς που είναι δυνατοί) υλοποίησης του ΕΚΚΡ, είτε ως αυτόνομο μέτρο ή σε συνδυασμό με τον έλεγχο ραμπών εισόδου.

Στην παρούσα διατριβή προτείνεται ένα ποσοτικό μοντέλο της επίδρασης των ΜΟΤ στη συνολική συμπεριφορά της ροής της κυκλοφορίας στους αυτοκινητοδρόμους, το οποίο επιτρέπει την ενσωμάτωση των ΜΟΤ σε ένα μακροσκοπικό μοντέλο κυκλοφοριακής ροής δεύτερης τάξης ως ένα πρόσθετο στοιχείο ελέγχου. Ο ολοκληρωμένος έλεγχος κυκλοφορίας δικτύων αυτοκινητοδρόμων, που περιλαμβάνει έλεγχο ραμπών εισόδου και έλεγχο με ΜΟΤ, διατυπώνεται ως ένα πρόβλημα βέλτιστου ελέγχου διακριτού χρόνου με περιορισμούς και επιλύεται αποτελεσματικά ακόμα και για δίκτυα μεγάλης κλίμακας μέσω ενός κατάλληλου αλγορίθμου εφικτής κατεύθυνσης.

Ένα επεξηγηματικό παράδειγμα ενός υποθετικού τμήματος αυτοκινητοδρόμου καθώς επίσης και ένας μεγάλης κλίμακας αυτοκινητόδρομος οδικού δακτυλίου διερευνώνται υπό διαφορετικά σενάρια ελέγχου χρησιμοποιώντας την προσέγγιση βέλτιστου ελέγχου, καταδεικνύοντας ότι η αποτελεσματικότητα της κυκλοφοριακής ροής μπορεί να βελτιωθεί σημαντικά όταν χρησιμοποιείται ΕΚΚΡ μέσω ΜΟΤ, με ή χωρίς την ενσωμάτωση του ελέγχου ραμπών εισόδου.

Οι αυξημένης πολυπλοκότητας μέθοδοι βέλτιστου ελέγχου μπορούν να αντιμετωπίσουν δυσκολίες στην πρακτική εφαρμογή τους στο πεδίο. Για το λόγο αυτό, στην παρούσα διατριβή προτείνονται τρεις απλοί ελεγκτές για τοπικό ΕΚΚΡ αυτοκινητοδρόμων με ανατροφοδότηση, οι οποίοι λειτουργούν μέσω ΜΟΤ. Όλοι οι ελεγκτές με ανατροφοδότηση βασίζονται μόνο σε άμεσα διαθέσιμες μετρήσεις πραγματικού χρόνου (χωρίς να κάνουν χρήση συνδεδεμένου μοντέλου και προβλέψεων της ζήτησης), λαμβάνουν υπόψη μια σειρά από πρακτικούς περιορισμούς και περιορισμούς ασφάλειας, και ως εκ τούτου είναι εύρωστοι και κατάλληλοι για πραγματικές εφαρμογές πεδίου. Οι ελεγκτές αξιολογούνται μέσω προσομοίωσης και συγκρίνονται με τα αποτελέσματα του βέλτιστου ελέγχου για ένα υποθετικό δίκτυο αυτοκινητοδρόμου. Παρά την απλότητά τους, τα αποτελέσματα δείχνουν ότι οι ελεγκτές ανάδρασης παρουσιάζουν ικανοποιητική συμπεριφορά ελέγχου και, πράγματι, προσεγγίζουν τα αποτελέσματα του βέλτιστου ελέγχου για μια σειρά από διερευνώμενα σενάρια. Επίσης, παρέχονται υποδείξεις για την εφαρμογή των ελεγκτών ανάδρασης.

Resumo da Tese apresentada à Universidade Técnica de Creta como parte dos requisitos necessários para obtenção do grau de Doutor.

CONTROLE DO FLUXO PRINCIPAL EM RODOVIAS

Rodrigo Castelan Carlson

Setembro/2011

Orientador: Prof. Markos Papageorgiou
Co-Orientador: Dr. Ioannis Papamichail
Palavras-chave: controle do fluxo principal, controle de tráfego em rodovias, controle de acesso, limites de velocidade variáveis, diagrama fundamental, controle ótimo, controle realimentado
Número de Páginas: 164

O aumento contínuo dos congestionamentos de tráfego observados diariamente em malhas rodoviárias em todo o mundo requer medidas inovadoras de controle que melhorem drasticamente as condições de tráfego atuais. Propõe-se o controle do fluxo principal (CFP) em rodovias como uma nova e eficiente ferramenta para o gerenciamento de tráfego rodoviário. A possível implantação e o principal efeito de CFP sobre a eficiência do fluxo de tráfego são analisados. Limites de velocidade variáveis (LVVs), adequadamente operados e aplicados, são considerados como uma (entre várias possíveis) maneira(s) de realização de CFP, seja como uma medida de controle independente ou em combinação com o controle de rampas de acesso.

Um modelo quantitativo do efeito de LVVs no comportamento agregado do fluxo de tráfego em rodovias é proposto e permite que LVVs sejam incorporados em um modelo de fluxo de tráfego macroscópico de segunda ordem como um componente adicional para controle. O problema de controle integrado de tráfego em malha rodoviária envolvendo controle de acesso e LVVs é formulado como um problema de controle ótimo sob restrições em tempo discreto, e é resolvido de forma eficiente mesmo para malhas rodoviárias de grandes dimensões por um algoritmo de direção factível.

Um exemplo ilustrativo de um trecho hipotético de malha rodoviária e também um anel rodoviário de grandes dimensões são investigados em diferentes cenários de controle, utilizando a abordagem de controle ótimo. Mostra-se que a eficiência do fluxo de tráfego pode ser substancialmente melhorada quando CFP via LVVs é usado com ou sem integração com controle coordenado de rampa de acesso.

Uma vez que métodos sofisticados de controle ótimo podem enfrentar dificuldades em implantações práticas em campo, três controladores simples para CFP realimentado de aplicação local em rodovias realizado via LVVs são propostos nesta tese. Todos os controladores realimentados dependem apenas de medições em tempo real de fácil obtenção (sem o uso de modelo em tempo de execução e sem a necessidade predições de demanda), consideram uma série de restrições práticas e de segurança, e são, portanto, robustos e adequados para implantações em campo. Os controladores realimentados são avaliados em simulação e tem seus resultados comparados com os resultados de controle ótimo para um trecho hipotético de malha rodoviária. Os resultados mostram que os controladores realimentados, apesar da sua simplicidade, apresentam um comportamento satisfatório de controle e se aproximam dos resultados obtidos com a abordagem de controle ótimo para uma série de cenários investigados. Recomendações para a operação dos controladores realimentados são fornecidas.

Contents

List of Figures

List of Tables

Chapter 1

Introduction

The major cause of congestion is the inefficient operation of highways during periods of high demand.

C. Chen, Z. Jia and P. Varaiya [7]

Motorways had been originally conceived to provide virtually unlimited mobility to road users. In the last decades, however, motorways have become notorious sites of extensive daily traffic congestion, particularly within and around metropolitan areas. The continuous increase of car ownership and demand has led to the daily appearance of recurrent and non-recurrent motorway congestions whose extent is steadily increasing in space and time.

Traffic congestion degrades the available infrastructure in the sense of reducing the motorway throughput (see, e.g., [53]). Thus, the expensive motorway infrastructure is underutilised ironically exactly at the only time (peak hour) it is actually needed. The consequences of this serious infrastructure degradation are enormous for economic and social life of the affected areas: excessive delays, increased fuel consumption and environmental pollution, and reduced traffic safety. In the USA, for example, the costs related to congestion in urban areas in 2009 reached US$ 115 billion [72]. In Europe by its turn, the European Commission estimates that, if drastic measures are not taken, the congestion related costs may increase by 50 percent in the next 40 years, reaching € 200 billion per year in 2050 [13].

In contrast to simple queuing systems, whose serving capacity is not affected by the existence of a waiting queue, a congestion forming on a motorway link affects the nominal motorway capacity and throughput due to two independent effects [53]: capacity drop at the head of forming congestions and blocking of off-ramps by the spreading congestion body. Both effects give rise to an escalation of infrastructure degradation, i.e., an accelerated increase of congestion that, by its turn, leads to further infrastructure degradation, further increase of congestion and so forth, until the formed congestions cover a significant part of the motorway network, often spilling over from one motorway to the other via the corresponding interconnections. At the stage of generalised congestion that is encountered daily in most metropolitan motorway networks, the total arriving demand is typically much lower than the nominal infrastructure capacity; but the seriously degraded congested infrastructure cannot serve the demand, hence the congestion persists until the demand falls to sufficiently low values (far below the infrastructure's nominal capacity) at the final phase of the peak period. The consequences of infrastructure degradation are even more accentuated in the case of neuralgic motorways, such as ring-roads, that act as a hub for dozens of urban on-ramps or merging motorways.

Under the outlined circumstances it is evident that the extended daily congestion on motorways cannot be attributed only to the excessive demand exceeding the nominal network capacity. Demand may indeed exceed temporarily and locally the motorway capacity, thus triggering local congestions; but the generalised congestion is the result of an unstable escalation caused by the degradation of the expensive infrastructure in absence of suitable traffic control measures that would counter and limit this devastating evolution.

The efficient, safe, and less-polluting transportation of persons and goods on motorways calls for an optimal utilisation of the available infrastructure via suitable application of a variety of traffic control measures such as ramp metering, driver information, route guidance, and variable speed limits (VSLs). A number of methodological approaches including optimal control, expert systems, fuzzy systems, neural networks, and feedback control have been developed in the past for the design of related control strategies. In fact, a couple of preliminary investigations have demonstrated that suitable traffic control measures may, under certain circumstances, provide significant improvements, see, e.g., [5, 7, 36].

On the other hand, various of those traffic control measures that have been proposed and partly implemented in motorway networks to alleviate traffic congestion are known to face limitations:

- Ramp metering is potentially valuable but its positive effect may be limited due to limited ramp storage space [67].
- Variable Speed Limits (VSLs) are valuable for traffic safety (reduction of accidents) but

their current usage has hardly any positive impact for the increase of throughput or for the decrease of average travel times as they are operated on the basis of very simple control strategies that cannot improve traffic flow efficiency [63]; moreover, the range of applied speed limits is usually limited [12].

- Route guidance and driver information systems are mostly helpful under non-recurrent, e.g., incident-induced congestion [84].
- Emerging vehicle-infrastructure integration (VII) systems provide a promising technological background for efficient traffic control, but specific efficiency-improving applications and corresponding control algorithms are still to be developed.

Among these control measures, the display of VSLs on appropriate variable message signs (VMSs) in response to the prevailing traffic conditions is of particular interest for this thesis because of the potential offered. A main targeted result of VSLs is enhanced traffic safety and indeed the selection of motorway stretches for VSL installation in several countries is guided by the frequency of registered accidents. The positive impact of VSLs on traffic safety is because of speed reduction and speed homogenisation that are correlated with a reduction of accident probability. Multi-year evaluations of the VSL impact on traffic safety indicate a reduction in accident numbers by as much as 20 to 30 percent after VSL installation. VSLs are also envisaged by some authorities as a means to reduce vehicle emissions and road noise. On the other hand, to the best of the author's knowledge, until recently there was no evaluation of the VSL impact of available installations that would demonstrate a consistent and measurable improvement of traffic flow efficiency, e.g., in the sense of reduced travel times. The single exception will be pointed out later in this thesis.

1.1 Problem Statement

The exposition up to this point may be summarised in the following statements:

- The current traffic situation in metropolitan motorways is characterised by heavy congestion during rush hours, and the related cost is very high for the economic and social life in metropolitan areas.
- The expensive motorway infrastructure is strongly underutilised due to congestion.

- The observed heavy congestions are only partly due to high demand. If vehicles are allowed to use the infrastructure at will (i.e., without control measures), the limited original congestions escalate and lead to extended breakdown areas and serious degradation of the expensive infrastructure. Like many other human-made systems and processes, motorways need to be controlled for maximum efficiency which is usually correlated with improved traffic safety and reduced environmental impact.

- Some traffic control measures are envisaged or applied in parts of some motorway networks, but the achievable improvements face limitations.

With respect to the latter statement, in what concerns VSLs, it should be noted that the ideal exploitation of the opportunities offered by VSLs would be to preserve the safety and environmental benefits offered by the current systems along with an increase of traffic flow efficiency. The fact that an efficiency increase could not be demonstrated in the conducted field assessments does not necessarily mean that VSLs per se are not an appropriate measure for the enhancement of traffic flow efficiency. As a matter of fact:

- The impact of VSLs on aggregate traffic behaviour, e.g., on the fundamental diagram, has not been sufficiently investigated with real data. As a consequence, the understanding of even qualitative (let alone quantitative) impacts of VSLs is limited to conjectures and assumptions; this lack of reliable understanding, by its turn, hinders the insightful development of VSL control strategies that would target an increase of traffic flow efficiency.

- Current VSL installations employ simple rule-based control strategies for VSL switching, which base their real-time decisions on preselected thresholds of traffic flow or occupancy or mean speed. The utilised thresholds are usually selected in an ad-hoc way that does not necessarily exploit the (anyhow unknown) potential impact of VSLs on traffic flow efficiency.

The design of pertinent control strategies that may increase traffic flow efficiency calls for a sufficiently accurate description of the VSL impact on the aggregate (macroscopic) traffic conditions. There were very few investigations in the past addressing the precise impact of VSLs on aggregate traffic flow behaviour, e.g., on the fundamental diagram. Recently, the effect of VSLs on the aggregate traffic flow behaviour (in form of the flow-occupancy diagram) was investigated by [62, 63] on the basis of traffic data from a VSL-equipped European motorway. This enhanced understanding of the VSL impact may eventually be exploited in order to assess and enhance the current VSL control strategies or to develop new control strategies that would target traffic flow efficiency while delivering similar benefits for traffic safety and environmental improvements as achieved by current systems.

1.2 Objectives and Approach

In view of the aforementioned difficulties, this thesis proposes and investigates an innovative motorway traffic control measure that improves drastically the current traffic conditions on motorways: mainstream traffic flow control (MTFC). MTFC aims at directly influencing the motorway mainstream flow via an appropriate actuator such as VSLs or specially operated traffic lights or emerging vehicle-infrastructure integration (VII) systems, and may complement existing control measures.

To this end, the following topics are addressed:

- The MTFC concept is proposed. Several MTFC-related issues are discussed and partially addressed. The application of MTFC to different types of bottlenecks is outlined.
- Because VSLs are used as an MTFC actuator, the impact of VSLs on aggregated traffic flow behaviour and the way VLSs can be used for control is analysed in the light of recent findings based on real field data. Then VSLs are incorporated in a general second-order traffic flow model as an additional control component, along with an accordingly extended optimal control formulation and its efficient solution.
- The optimal control approach is employed for MTFC via VSLs, and also for integrated MTFC via VSLs and ramp metering. A hypothetical motorway and a simulation model from a real infrastructure with realistic demands are used to investigate the operational impact and potential benefits of MTFC.
- Three simple, yet efficient MTFC local feedback controllers, based on the MTFC application concept proposed in this thesis, are developed using VSLs as an actuator. In contrast to the optimal control approach, the developed controllers are deemed practicable and directly applicable within a potential field implementation. The developed feedback control strategies exploit suitable methods of classical control theory that lead to high efficiency (comparable to the efficiency of optimal control) combined with

simplicity and robustness (as no traffic flow models are used on-line) that are deemed essential for easy, transparent and successful field operations. Several practical aspects of VSL operation are taken into account explicitly.

- The MTFC feedback controllers are evaluated by use of realistic simulation-based tests for a hypothetical motorway stretch using a second-order macroscopic traffic flow simulator in order to demonstrate their features, and have their efficiency compared against the sophisticated optimal control approach.
- Recommendations for the application of the developed feedback controllers are provided and possible extensions are outlined.

1.3 Delimitation

This thesis proposes the MTFC concept as a control measure for motorways. Although MTFC can be enabled, as mentioned earlier, by VSLs or by traffic lights or VII systems, only the use of VSLs as an MTFC actuator is investigated in this thesis. The other two actuators are only briefly discussed in Chapter 3.

All the simulations are performed by the use of the METANET macroscopic traffic simulator and AMOC optimal motorway control tool that are presented in Chapter 2. The limitations of the model related to the validation procedure with VSL field data are also discussed in Chapter 2. Details of the model parameters used are provided when appropriate. Further simulation results with microscopic traffic simulators such as AIMSUN [80] or VISSIM [1] are not presented without prejudice for the conclusions drawn in this thesis. Field implementations of MTFC have not occurred as yet.

MTFC can be applied to several different types of motorway bottlenecks and some examples are provided in Chapter 3. However, only the case of on-ramp merge bottlenecks are considered in the investigations of Chapters 5 and 6.

The investigations of integrated control, i.e., MTFC via VSLs integrated with ramp metering, are limited to the studies with optimal control. The integration for the feedback control case is only outlined, while related results will be presented in scientific publications in due time.

The field application of VSLs is subject to a number of constraints regarding the maximum admissible extent of VSL changes, both temporally and spatially (see also Section 4.7), that are not considered in AMOC. In addition, VSLs can only attain pre-specified discrete values in practice rather than the continuous (real-valued) speed limit values delivered by AMOC. Although the optimal speed limit values delivered by AMOC could be eventually treated appropriately to satisfy these constraints, it was preferred to leave them unaltered to assess the full possibilities provided by MTFC via VSLs. On the other hand, all these and other practical application requirements for MTFC via VSLs are taken into account when applying the feedback control approach.

1.4 Thesis Outline

Chapter 2 delivers a preliminary discussion of congestion causes and infrastructure degradation, followed by an overview of the main groups of motorway traffic control measures and their limitations. An overview of existing VSL strategies is also presented and some background issues related to VSLs are addressed, after which the resemblance of VSLs to ramp metering and the opportunities to avoid the detrimental capacity drop at active bottlenecks are highlighted. In the same chapter, VSLs are incorporated in a general second-order traffic flow model as an additional control component based on the results of a validation study. The augmented model leads to an accordingly extended optimal control formulation.

Chapter 3 begins with an historical overview of MTFC-like strategies followed by the elaboration of the MTFC Concept and impacts, and its potential ways of implementation. In addition, examples of the application of MTFC to different types of bottlenecks are presented, as well as a discussion of the use of VSLs as an MTFC actuator.

Chapter 4 expands on the use of MTFC via VSLs from a feedback control perspective. Three feedback controllers for MTFC via VSLs that are simple yet efficient and robust are designed, taking into account the practicality of the approach. Extensions of the proposed feedback controllers are outlined.

In Chapter 5 the MTFC concept and its integration with ramp metering are investigated by the use of the optimal control approach of Chapter 2. First, an illustrative example is discussed at local level for a hypothetical motorway stretch with a series of control scenarios. Then, a new set of simulations are performed for the evaluation of MTFC and ramp metering for a large-scale motorway ring-road with realistic demands.

In Chapter 6 the MTFC feedback controllers designed in Chapter 4 are evaluated and compared in simulation for a hypothetical motorway stretch, while considering several practical application aspects. The feedback strategies have their efficiency also compared against the optimal control approach.

Finally, Chapter 7 concludes this thesis and comments on further research.

1.5 Publications

The work presented in this thesis resulted in several scientific publications listed as follows:

1.5.1 Journals

- R. C. Carlson, I. Papamichail, M. Papageorgiou, and A. Messmer. Optimal Motorway Traffic Flow Control Involving Variable Speed Limits and Ramp Metering. *Transportation Science*, 44(2):238-253, 2010.
- R. C. Carlson, I. Papamichail, M. Papageorgiou, and A. Messmer. Optimal Mainstream Traffic Flow Control of Large-Scale Motorway Networks. *Transportation Research Part C: Emerging Technologies*, 18(2):193-212, 2010.
- R. C. Carlson, I. Papamichail, and M. Papageorgiou. Local Feedback-based Mainstream Traffic Flow Control on Freeways Using Variable Speed Limits. *IEEE Transactions on Intelligent Transportation Systems*. DOI:10.1109/TITS.2011.2156792
- R. C. Carlson, I. Papamichail, and M. Papageorgiou. Comparison of Local Feedback Controllers for the Mainstream Traffic Flow on Freeways Using Variable Speed Limits. *Journal of Intelligent Transportation Systems: Technology, Planning, and Operations*. Submitted.

1.5.2 Conferences, Symposia and Workshops

- R. C. Carlson, I. Papamichail, M. Papageorgiou, and A. Messmer. Optimal Mainstream Traffic Flow Control of Motorway Networks. In *12th IFAC Symposium on Control in Transportation Systems - CTS'09*, Redondo Beach, USA, 2009.
- M. Papageorgiou, R. C. Carlson, I. Papamichail, and A. Messmer. Optimal Mainstream Traffic Flow Control of Large-scale Motorway Networks. In *Models and Technologies for Intelligent Transportation Systems*, Rome, Italy, 2009.

- M. Papageorgiou, R. C. Carlson, I. Papamichail, and A. Messmer. Optimal Mainstream Traffic Flow Control of Motorway Networks. In *13th EURO Working Group on Transportation Meeting*, Padua, Italy, 2009.

- R. C. Carlson, I. Papamichail, M. Papageorgiou, and A. Messmer. Optimal Mainstream Traffic Flow Control of Motorway Networks. In *European Control Conference 2009 - ECC'09*, Budapest, Hungary, 2009.

- R. C. Carlson, I. Papamichail, M. Papageorgiou, and A. Messmer. Variable Speed Limits as a Mainline Metering Device for Freeways. In *89th Annual Meeting of the Transportation Research Board*, Washington, D.C., USA, 2010.

- M. Papageorgiou, I. Papamichail, R. C. Carlson, and A. Messmer. Nonlinear Optimal Control as a Source of Intelligent Traffic Control. In *5th IMA Conference on Mathematics in Transport*, London, UK, 2010.

- R. C. Carlson, I. Papamichail, and M. Papageorgiou. A Local Feedback Controller for Mainstream Traffic Flow Control Using Variable Speed Limits. In: Young European Arena of Research 2010, YEAR 2010 Abstracts, Brussels, Belgium, 2010.

- R. C. Carlson, I. Papamichail, and M. Papageorgiou. Local Feedback-based Mainstream Traffic Flow Control on Motorways Using Variable Speed Limits. In *NEARCTIS 3rd Workshop: towards new research area in co-operative traffic management*, Final Programme, Lausanne, Switzerland, 2010.

- R. C. Carlson, I. Papamichail, and M. Papageorgiou. Local Feedback-based Mainstream Traffic Flow Control on Freeways Using Variable Speed Limits. In *13th International IEEE Conference on Intelligent Transportation Systems*, Funchal, Madeira Island, Portugal, 2010.

- R. C. Carlson, I. Papamichail, M. Papageorgiou, and A. Messmer. Variable Speed Limits as a Mainline Metering Device for Freeways. In *5th International Congress on Transportation Research*, Volos, Greece, 2010.

- R. C. Carlson, I. Papamichail, and M. Papageorgiou. Controle Realimentado Local do Fluxo Principal em Rodovias com o Uso de Limites de Velocidade Variáveis. In *XXIV Congresso da ANPET*, Salvador, Brazil, 2010.

- R. C. Carlson, A. Ragias, I. Papamichail, and M. Papageorgiou. Mainstream Traffic

Flow Control of Merging Motorways Using Variable Speed Limits. In *19th Mediterranean Conference on Control and Automation*, Corfu, Greece, 2011.

- R. C. Carlson, I. Papamichail, and M. Papageorgiou. Local Feedback-based Mainstream Traffic Flow Control on Freeways Using Variable Speed Limits. In *Special International Conference on Complex Systems: Synergy of Control, Computing and Communications - COSY 2011*, Ohrid, Former Yugoslav Republic of Macedonia, 2011. Invited.

- R. C. Carlson, I. Papamichail, and M. Papageorgiou. Comparison of Local Feedback Controllers for the Mainstream Traffic Flow on Freeways Using Variable Speed Limits. In *14th International IEEE Conference on Intelligent Transportation Systems*, Washington, D.C., USA, 2011. Accepted.

- R. C. Carlson, I. Papamichail, and M. Papageorgiou. Comparação de Controladores para o Fluxo Principal em Rodovias com o Uso de Limites de Velocidade Variáveis. In *XXV Congresso da ANPET*, Belo Horizonte, Brazil, 2011. Submitted.

Chapter 2

Background

> *(...) lane control systems [VSL systems included] may prove much more useful than at present if their impact is studied more carefully and thoroughly so as to open the way to the design of efficient control strategies. This is perhaps one of the least studied areas within traffic control.*
>
> *M. Papageorgiou [52]*

This chapter covers some topics that served as a theoretical background for the development of the work in this thesis. Section 2.1 discusses the congestion causes and infrastructure degradation. In the same section, further details are provided about several motorway traffic control measures and their limitations. Variable speed limits play an important role in this thesis. Therefore, in Section 2.2 the state-of-the-practice and the knowledge on the impact of VSLs on aggregated traffic flow are reviewed. The VSL impact is then incorporated in a second-order validated macroscopic traffic flow model in Section 2.3. Finally, the integrated optimal control problem involving ramp metering and variable speed limits is presented in Section 2.4.

2.1 Motorway Traffic Flow Control

2.1.1 Congestion Causes and Infrastructure Degradation

A (latent) bottleneck on a motorway is a location where the flow capacity $q_{\mathrm{cap}}^{\mathrm{up}}$ upstream is higher than the flow capacity $q_{\mathrm{cap}}^{\mathrm{down}}$ downstream of the bottleneck location (Figure 2.1). Bottlenecks may be due to a number of reasons:

(i) Lateral inflow from on-ramps is the most common reason.

(ii) Infrastructure layout, such as lane drop, tunnel, strong grade or curvature; note that merging of on-ramps (mentioned under (i) above) may also be considered as a special case of lane drop.

(iii) Specific traffic conditions, e.g., strong weaving of traffic streams with different local origins or destinations.

(iv) Regulatory measures, e.g., speed limits at specific motorway stretches.

(v) External capacity-reducing events such as over-spilling off-ramps or incidents.

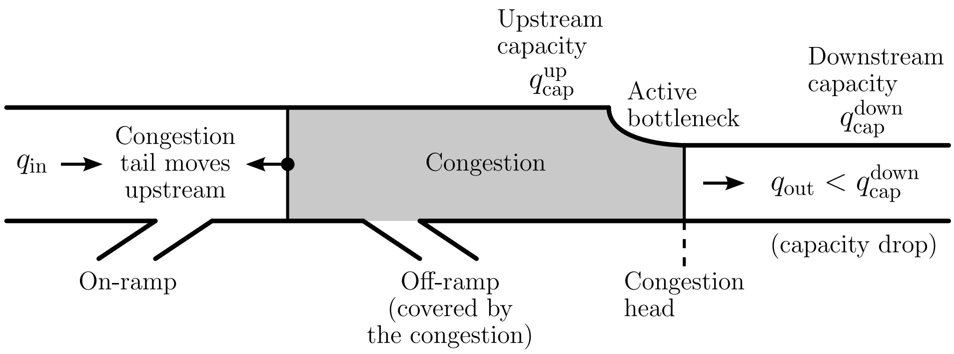

Figure 2.1: Active bottleneck notions.

The nominal bottleneck capacity $q_{\text{cap}}^{\text{down}}$, is the maximum traffic flow that can be maintained at the bottleneck location if the traffic flow q_{in} arriving from upstream happens (or is controlled) to be equal to $q_{\text{cap}}^{\text{down}}$. On the other hand, if the net arriving flow q_{in} upstream of the bottleneck (which naturally verifies $q_{\text{in}} \leq q_{\text{cap}}^{\text{up}}$) is higher than $q_{\text{cap}}^{\text{down}}$, the bottleneck is activated, i.e., a congestion is formed, whereby the congestion head is located at the bottleneck, while the congestion tail is moving upstream for as long as the upstream arriving flow is sufficiently high (Figure 2.1). Typically, multiple active bottlenecks are present simultaneously in a motorway network during the peak period, while the accumulated congestion length over the whole network may extend over several dozens of kilometres. The congestion forming at an active bottleneck has two kinds of detrimental effects on the motorway capacity and throughput [53]:

(1) *Capacity drop (CD) at the congestion head*: For most bottleneck types mentioned above, bottleneck activation leads to a speed breakdown upstream of the bottleneck location, in which case the passing vehicles have to accelerate from lower speeds (within the formed congestion) to higher speeds (downstream of the bottleneck); this is deemed to lead to

a CD, i.e., an active bottleneck outflow q_{out} that may be 5 to 20 percent lower than the nominal capacity $q_{\mathrm{cap}}^{\mathrm{down}}$ (Figure 2.1), see e.g., [11]. Several dedicated empirical investigations with real data (mostly from on-ramp merge bottlenecks) have confirmed the capacity drop phenomenon (e.g., [5]). The capacity drop leads to a corresponding serious degradation of the local motorway infrastructure. Avoiding the CD at active bottlenecks would increase the motorway throughput accordingly.

(2) *Blocking of off-ramps (BOR)*: In most cases, the tail of any formed congestion propagates upstream over several kilometres and covers several on-ramps and off-ramps upstream of the bottleneck (Figure 2.1). Because the traffic flow along the congested area is lower than the nominal capacity (due to the congestion and the additional on-ramp-entering traffic flows), the off-ramp flows drop accordingly; thus, vehicles that are bound for exits upstream of the active bottleneck, are also delayed due to the congestion and in fact contribute to an accelerated spatial increase of the congestion. This detrimental effect is magnified increasingly as the congestion grows longer and covers more and more off-ramps; in extreme cases, this may lead to genuine gridlocks around topological cycles of a motorway network [16, 51]. Note that the BOR effect is independent of the CD effect and leads to an accordingly additional reduction of the motorway throughput, i.e., it reflects an additional source of infrastructure degradation. Any reduction of the spatial or temporal extent of congestion would lead to corresponding throughput improvements.

2.1.2 Motorway Traffic Control Measures

Traffic control measures that have been considered and partly implemented in motorway networks to alleviate traffic congestion may be classified in four groups: ramp metering (RM), variable speed limits (VSLs), route guidance (RG) and emerging vehicle-infrastructure integration (VII) systems.

Ramp metering (RM) employs traffic lights at the on-ramps to control the traffic flow entering the motorway mainstream, e.g., in order to preserve capacity flow on the mainstream and avoid congestion [53]. Despite the ramp queue delays induced by ramp metering actions, the higher motorway throughput (and reduced mainstream delays) because of congestion reduction or avoidance may lead to shorter total travel times for most drivers. Indeed, RM may be used to establish highly-efficient traffic flow on the motorway mainstream but has a major limitation: the created ramp queues should not spill back to the adjacent upstream infrastructure. Because ramp storage space may be limited, RM is typically released when the ramp queue has covered the whole on-ramp. Since urban ramps are usually short, RM may delay the onset of congestion, accelerate its dissolution and reduce its space extent, but it may have to be de-activated for most of the peak period duration due to full ramps. Another drawback of RM is the preference of mainstream over the ramp-entering traffic, which may render it little popular with drivers encountering the ramp traffic lights, see [56] for details. Thus, the criterion of equity (i.e., similar delays to be encountered by the road users entering the motorway from different on-ramps) is also important for road user acceptance of the system. Coordinated ramp metering strategies make use of measurements from an entire region of the network to control all metered ramps included therein [53]. Hence, coordination of ramp metering actions at successive on-ramps may deliver improvements in terms of both efficiency and equity, compared to independent local actions, but even in this case sufficient storage space is essential for mainstream congestion avoidance [7, 67]. Coordinated ramp metering has been extensively studied in the past and involves sophisticated methods such as multivariable control strategies [17, 58] and optimal control strategies [9, 23, 36, 38, 55, 94].

Variable speed limits (VSLs) displayed on road-side variable message signs (VMSs) in response to prevailing traffic conditions is an increasingly popular motorway traffic control measure. The typical range of VSL variations is a subset of $[60, 120]$ km/h, but low VSL values (e.g., 60 km/h) are usually displayed only in exceptional cases (e.g., incident). A main targeted impact of VSLs is enhanced traffic safety as a result of the homogenisation of speeds of individual vehicles and of the mean speeds of different motorway lanes which reduce the accident risk. On the other hand, until recently there was no evaluation of the VSL impact of available installations that would demonstrate a measurable and consistent improvement of traffic flow efficiency (see Section 2.2.1), e.g., in the sense of reduced travel times. The only exception is the recent field test of the SPECIALIST approach [28, 30], which has been however deactivated after the field experiments (see also Section 3.1).

Route guidance (RG) is helpful mostly in cases of incidents or other events that render the traffic conditions unpredictable for commuting drivers [84]. However, the employment of RG calls for availability of alternative routes with sufficient capacity reserves.

Vehicle-infrastructure-integration (VII) systems have recently raised an enormous interest and significant research efforts around the world [81]. The basic principles of VII systems are:

- Vehicles act as mobile sensors for position (via satellite or cellular-phone based technologies), speed and inter-vehicle distance.

- Vehicles can communicate with each other and with the infrastructure (control centre) in a dual way, i.e., sending and receiving messages, via wireless communication technologies.

- The messages received by the vehicles include traffic information, warnings, alarms, but may also include commands, such as vehicle speed commands or speed limits that are automatically enforced.

Research on VII systems has mainly focused on development, testing and demonstration of the enabling advanced technologies, while first (mostly safety-related) applications start to emerge. The spectrum of potential applications exploiting the VII architecture and technologies is very widespread and includes safety-related, environmental-related and efficiency-related aspects. Of particular importance for this thesis is the possibility of imposing speed or speed limits to vehicles travelling in specific motorway areas. In this context, it is important to emphasise that, in order to implement a specific speed (limit) to the vehicles of a certain motorway area, it is not necessary to have access to each and every included vehicle. A small percentage of equipped (speed-controllable) vehicles, acting as factual platoon leaders in each lane, is usually sufficient because the non-equipped vehicles in the platoons will simply have to adjust their speeds to the speed of the respective leaders.

2.2 Variable Speed Limits

2.2.1 Existing VSL Strategies

The earliest applications of VSLs date from the 1960s. Today, numerous VSL installations are encountered in many European countries (e.g., a total of more than 800 km of VSL-equipped motorway stretches are currently in operation in Germany) and in North America and elsewhere, and their number is increasing at an accelerated pace. In this section, a summary of the state-of-the-practice is given without going into details of the several reported VSL field applications, but instead, focusing on the common characteristics of existing deployed VSL strategies. Countries where VSLs have been implemented in the field include: Australia, Canada, Denmark, England, Finland, France, Germany, Greece, The Netherlands, USA, Sweden, and Switzerland. For more details, see [12, 47, 71, 85, 86]

Variable speed limits are applied along motorway stretches, and the speed limits are changed appropriately according to current traffic or weather conditions. The speed limits are displayed on VMSs on overhead gantries or on roadside poles, typically spaced 0.5–2 km, with sign location and visibility being an important issue for a successful system deployment. In work zones, portable trailers equipped with a VMS are often used for the duration of the works. Variable speed limits systems may operate as a standalone system or as a part of a larger system, such as an incident management system or a congestion management system.

Most of the reported VSL systems share a common structure: data collection and processing, control algorithm or decision logic, and display. These three generic elements operate over a communication system for data exchange.

Data are collected by means of detectors or sensors of different types, and differ depending on each application. Traffic detectors are typically used for measuring speed, flow, and occupancy. In several applications weather conditions are used as inputs, therefore measurements of wind speed and direction, temperature, relative humidity, rain intensity, cumulative precipitation, ice and fog, as well as visibility may be of interest. Some applications also benefit from surface measurements, i.e., measurements of the pavement conditions (dry, wet, salted, snowy). After collection, the data are processed and forwarded to the system's control logic. Faulty or missing data should be handled at this stage. Depending on the application, a broad range of input data may be used, i.e., one or more types of measurements may be used in combination. The presence of crashes, congestion, or construction may also influence the operation of the system.

The control logic is the core of VSL systems operation and renders the system responsive to dynamic conditions. The main limitation of most of operational VSL systems is the control logic. In fact, these systems have simple threshold-based control logics and very often the adopted thresholds are sensitive to day-to-day stochastic variations, rendering the appropriate tuning of the parameters a difficult task. Furthermore, most of the strategies were designed without the proper knowledge on how traffic is affected by VSLs, and how the strategy should operate to accomplish a given objective. The control logic includes the application of coordination between displayed VSLs and the application of specific rules and restrictions. Most of the VSL systems are automated, but, despite of that, the possibility of manual operator override is usually considered along with a companion closed-circuit television system.

Displays are usually updated every one or two minutes, with some systems having the update period as large as six minutes. The speed limits are displayed in speed intervals of multiples of 5 when miles per hour are used, and of multiples of 10 when kilometres per hour are used. In some applications, not only the recommended speed limit is displayed, but also a minimum speed limit. The provision of real time information such as warning messages, advices or clarification about the reasons of the system operation on additional auxiliary signs or VMSs are sometimes available, and seem to improve operation and the perception of the users about the system. In most cases, VSLs are mandatory, i.e., legally equivalent to fixed speed limits, and may even be automatically enforced to increase driver compliance and hence impact.

The list of reported objectives is long and overlapping, but could be summarised as enhanced safety, efficient motorway operation and reduction of environmental impact. Some systems have their objectives in more than one of these groups. The target of most operational systems is enhanced safety and the intention is to display safe speed limits for different road conditions. In these cases specific objectives are, for example, increased driver compliance and reduction of infractions, reduction of driver error (e.g., because of speeding), and hazard and queue warning and consequent reduction of rear-end collision (e.g., because of an accident or congestion or fog). The stabilization of traffic flow and more uniform speeds along a lane and on different lanes are correlated with the reduction of overtaking manoeuvres and of crashes, and are, therefore, often targeted.

The aim of some VSL systems is an efficient use of motorway facilities. Ideally, these systems target a reduction of travel times by a stabilization of traffic flow due to more uniform speeds. However, the related results show that very few applications reported an improvement in traffic flow efficiency and, when reported, small improvements were obtained.

Regarding the reduction of environmental impact, very few systems considered this aspect. Minor reductions on the emissions of pollutants have been reported in a few cases. However, the increasing concerns with environment opens an avenue for further research, see, e.g., [32, 92, 93].

The results achieved by existing VSL strategies are mixed and the achievements of some applications were not observed in other applications. Several applications report up to 20-30 percent reduction in accident rates while others had a slight reduction in the number of accidents. Compliance has increased in some applications, even under advisory systems, along with a reduction in average speed, increased and more evenly distributed average time headways, better distribution of lane use and less lane change. Improvements in throughput level and reduction of travel times were most of the times minor.

2.2.2 The Fundamental Diagram

Under the assumption that traffic conditions do not change substantially in space (i.e., along a motorway stretch) and time (e.g., because of the arrival of shock waves from downstream), the traffic flow states may be approximated by the so-called fundamental diagram, which may be a flow-occupancy (or flow-density) diagram (inverse U shape) or a speed-flow diagram (left-turned U shape) (see Figure 2.2). Recall that the mean speed of a particular traffic state on the flow-occupancy diagram (Figure 2.2(a)) is proportional to the slope of the line that connects the particular traffic state point with the origin. A fundamental diagram may be (partially) obtained by collecting measurements of the related traffic variables (flow, occupancy, mean speed) at a specific motorway location and fitting an appropriate mathematical function. This procedure, however, may lead to flawed results if the underlying spatio-temporal traffic flow phenomena are not appropriately considered. In particular, the area around the critical occupancy (capacity flow) is properly visible in real data only at active bottleneck locations (see [62] for more details).

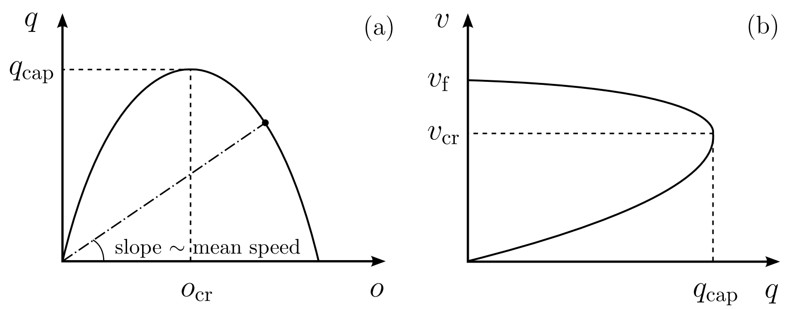

Figure 2.2: (a) Flow-occupancy and (b) speed-flow diagrams, where: q is flow (veh/h), o is occupancy (%), v is mean speed (km/h), q_{cap} is capacity flow (veh/h), o_{cr} is critical occupancy (%), v_f is free speed (km/h), and v_{cr} is critical mean speed (km/h).

2.2.3 The Impact of VSLs

2.2.3.1 Early Results

As mentioned earlier, there were very few investigations in the past addressing the precise impact of VSLs on aggregate traffic flow behaviour, e.g., on the fundamental diagram (flow-density curve). Some early investigations [90] based on traffic data from a two-lane German motorway with and without VSLs were summarised by [91]. The results indicate a speed homogenisation effect (less speed differences) for individual vehicles as well as for motorway lanes under the impact of VSLs. These results are useful for a better understanding of the VSL impact on individual vehicle speed distribution, but they do not reveal the impact of VSLs on aggregate traffic flow behaviour. The latter was also addressed in [91] (see Figure 2.3(a)) but in a rather qualitative way. Figure 2.3(a) illustrates that *"at lower or mean traffic volumes, the mean speed is lower due to the reduction effect whereas, at higher volumes, an increase is detected due to the stabilising effect. Thus, both capacity and speed rise by about 5 to 10 percent at the same time"* [91]. Zackor [91] did not comment on the possible increase of the critical occupancy (or critical density) under the influence of VSLs.

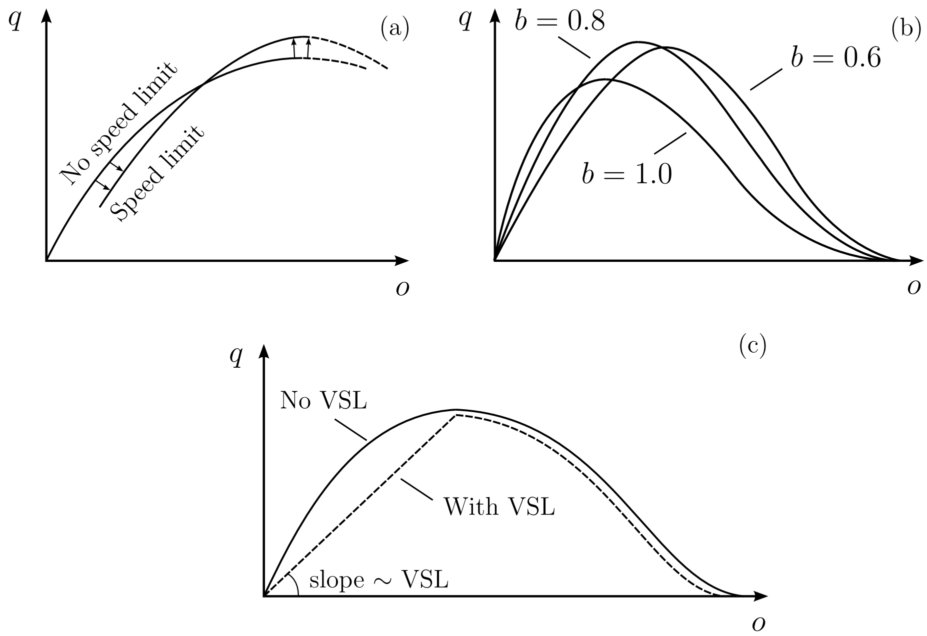

Figure 2.3: (a) Change of the fundamental diagram because of speed limits [91]; (b) Cremer model for VSL impact [14], in which $b = 1$ corresponds to no speed limit, $b = 0.8$ corresponds to $VSL = 0.8v_\mathrm{f}$, and 0.6 corresponds to $VSL = 0.6v_\mathrm{f}$; (c) Hegyi model for VSL impact [27].

The results reported in [90] were the basis for [14] to propose a quantitative model for the VSL-induced fundamental diagram change as displayed in Figure 2.3(b) where b is the ratio of the applied VSL divided by the free speed without VSLs and, by convention, $b = 1$ corresponds to the no-VSL case. It is quite likely that the displayed increase of flow capacity is rather exaggerated. In fact, later Dutch investigations could not identify any capacity increase that could be attributed to VSLs [77], albeit under advisory (not mandatory) VSLs.

In more recent research work regarding VSL control, the assumed VSL impact was to merely replace the left part of the flow-occupancy curve by a straight line with slope corresponding to the displayed VSL, (see Figure 2.3(c)) [27]. Other aspects of the impact of VSLs in modelling and control have also been investigated recently, see, e.g., [31, 35].

In conclusion, there seems to be very limited empirical evidence and indeed no factual consensus on the potential impact of VSLs on aggregate traffic flow behaviour, let alone quantitatively reliable results that could be used for efficient control strategy development. The expectations of the VSL impact along with their implications for potentially more efficient traffic flow are examined next, followed by a summary of the main findings by [63].

2.2.3.2 Reduction of Mean Speed at Under-critical Occupancies

It seems quite reasonable to assume that a VSL displayed at under-critical occupancies will reduce (with reasonable driver compliance) the (otherwise higher) mean speed (Figure 2.4(a)). The magnitude of this effect is likely to depend on the displayed VSL as well as on driver compliance. The new VSL-affected states serve the same flow at lower speed and higher occupancy than the original states, which implies that the travel time increases accordingly. Thus, applying VSLs at under-critical traffic states is likely to increase travel times and hence deteriorate traffic flow efficiency.

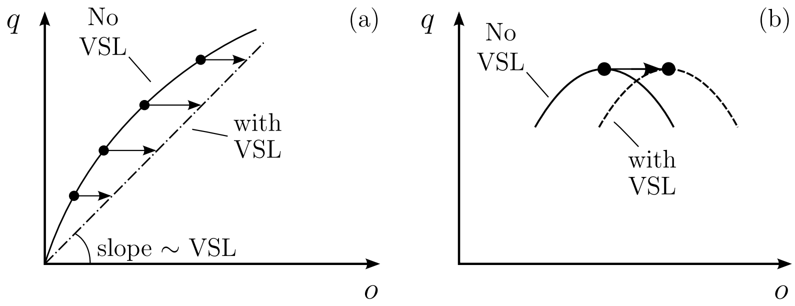

Figure 2.4: (a) Potential VSL impact on undercritical mean speeds; (b) cross-point of diagrams with and without VSLs.

The described state transition when applying VSLs at under-critical occupancies could, however, be exploited in a different context. The application of VSLs upstream of a bottleneck that is close to becoming active will temporarily (for the duration of the traffic state transition triggered by the VSL) decrease the mainstream flow arriving in the bottleneck area, thus retarding the bottleneck activation and the resulting congestion. Note that the temporary flow decrease during the VSL-triggered traffic state transition is because of the fact that occupancy (and density) in the VSL state is higher than in the original non-VSL state; thus, during the transition the flow is temporarily reduced to “create” the higher traffic density of the VSL state. It should be noted that this is the main VSL impact exploited by [27].

It is quite important to emphasise that the impact of VSL activation upstream of a potential bottleneck (e.g., an on-ramp merge area) in under-critical traffic conditions as illustrated in the state transition of Figure 2.4(a), bears great similarities to the impact of local ramp metering in the case of limited ramp storage space. More particularly:

- During the state transition of Figure 2.4(a), the mainstream flow toward the bottleneck is reduced similarly to ramp metering where instead it is the ramp flow that is reduced to avoid or delay the onset of a merge area congestion.
- During the state transition of Figure 2.4(a), the mainstream density is increased similarly to ramp metering where instead vehicles are stored in the ramp rather than in the mainstream.
- After the state transition, the mainstream flow returns to its pre-transition values (essentially equal to the upstream arriving mainstream demand) similarly to ramp metering being released when the ramp queue covers the whole ramp to avoid interference with the adjacent street traffic. More precisely, when the free ramp storage is about to be exhausted, ramp metering switches to queue control mode, attempting to maintain a maximum admissible ramp queue (see [76, 88, 89]), in which case the ramp outflow becomes essentially equal to the arriving ramp demand.
- After the state transition, the mainstream density remains at its increased value, similarly to ramp metering where the on-ramp queue remains full until the arriving demand drops to sufficiently low values. This way, the activation of VSLs upstream of a mainstream bottleneck in under-critical conditions induces some delays to the concerned vehicles because of lower speed similarly to ramp metering inducing delays to the vehicles queuing on the ramp, but this may be more than counterbalanced by the avoidance or retarding of the bottleneck congestion and its associated vehicle delays.

Some interesting aspects and theoretical analysis of VSLs and ramp metering application, and their similarities, are discussed by [40, 41].

2.2.3.3 Increase of Throughput and Retarding of Congestion at Overcritical Occupancies

According to the Hegyi model [27] (Figure 2.3(c)), both flow-density curves (for VSL and non-VSL) meet but do not actually cross while Zackor [91] suggests that there is actually a genuine cross-point of both curves somewhere near the critical occupancy (Figure 2.3(a)). The cross-points (if any) are likely to lie at increasing occupancy values for decreasing VSLs because of the accordingly decreasing slope of the under-critical VSL-affected curves. In fact, there may be no cross-point for very low VSLs. As the VSL impact is evaluated at occupancies near or higher than the cross point, the following (partly overlapping) questions are of interest (see also Figure 2.4(b)):

- Where is the cross-point (if any) located with respect to the non-VSL critical occupancy?
- Are VSL-induced critical occupancies higher than their non-VSL counterparts?
- Are VSL-induced flows higher at overcritical occupancies than their non-VSL counterparts?
- Is there a flow capacity increase for some VSLs?

These issues were partly studied by [62, 63], and the related results are summarised in the next section.

2.2.4 The Effect of VSLs on Aggregate Traffic Flow Behaviour

The effect of VSLs on aggregate traffic flow behaviour (in the form of the flow-occupancy diagram) was investigated [62, 63] on the basis of traffic data from a European motorway where a flow/speed threshold-based VSL control algorithm is currently used. A main focus of the reported work was on verifying some long-held conjectures (Section 2.2.3) regarding the VSL impact on the shape of the flow-occupancy diagram.

Some findings of the reported investigations are summarised as follows (Figure 2.6, which will be explained in more detail later, may be useful for illustration of the following aspects):

(i) Speed limits—when applied at undercritical occupancies—have the effect of decreasing the slope of the flow-occupancy diagram. Moreover, the smaller the imposed speed limit, the larger the decrease in the slope of the flow-occupancy diagram. This impact may be exploited to hold back traffic flow to retard the onset of congestion at downstream bottlenecks, as explained in Section 2.2.3.2 and practiced, e.g., by [27].

(ii) The VSL-affected flow-occupancy curve crosses (at least for some VSLs) the non-VSL curve, shifting the critical occupancy to higher values in the flow-occupancy diagram.

The major cross-points were found to lie around or beyond the non-VSL critical occupancy. This impact may be exploited to hold more vehicles in the motorway without falling into congestion. It may sound paradoxical but these cross-points imply that the mean speed at overcritical densities is higher when a speed limit is imposed than in no-VSL cases; this may happen because of the homogenisation effects mentioned earlier.

(iii) Regarding the potential increase of flow capacity, the data analysis was rather inconclusive because a slight increase is indeed visible at some locations for some VSL values while at other locations no capacity increase can be observed for any VSL value. In locations where VSLs indeed yield a capacity increase, this may be exploited by a suitably designed control strategy for throughput increase, as practiced, e.g., by [66], and further discussed in Section 4.7.7 and investigated in Section 6.2.4.

(iv) Independently of whether flow capacity is actually increased for some VSL values or not, sufficiently low VSLs lead to accordingly lower flow capacity in the fundamental diagram than in non-VSL cases.

Finding (iv) implies that a controllable mainstream congestion may be deliberately created via VSLs with benefit upstream of an uncontrolled potential bottleneck (e.g., an on-ramp merge area) to avoid its activation and the related reduction of throughput because of the capacity drop. This idea forms the base for the application of MTFC via VSLs which will be introduced and detailed in the next chapter.

2.3 Traffic Flow Modelling

A macroscopic second-order traffic flow model is used in this thesis. The model was validated against real traffic data at several instances [37, 59] and was found to reproduce the whole range of real traffic conditions (free flow, critical, congested) with remarkable accuracy. The model is included in the METANET motorway traffic flow simulator [46] and is extended here to incorporate VSL control measures.

2.3.1 Preliminaries

The motorway network is represented by a directed graph whereby the links of the graph represent motorway stretches. Each motorway stretch has uniform characteristics, i.e., no on- or off-ramps and no major changes in geometry. The nodes of the graph are placed at locations where major changes in road geometry occur as well as at junctions, on-ramps, and off-ramps.

The macroscopic description of traffic flow implies the definition of adequate variables expressing the aggregate behaviour of traffic at certain times and locations. The time and space arguments are discretised. The discrete-time step is denoted by T (typically, $T = 10$ s). A motorway link m is divided into N_m segments of equal length L_m (typically, $L_m = 500$ m) (Figure 2.5). The traffic in each segment i of link m at discrete-time $t = kT$, $k = 0, 1, \dots, K$, where K is the time horizon, is macroscopically characterised via the following variables: the *traffic density* $\rho_{m,i}(k)$ (veh/km/lane) is the number of vehicles in segment i of link m at time $t = kT$ divided by L_m and by the number of lanes λ_m; the *mean speed* $v_{m,i}(k)$ (km/h) is the mean speed of the vehicles included in segment i of link m at time $t = kT$; and the *traffic volume* or *flow* $q_{m,i}(k)$ (veh/h) is the number of vehicles leaving segment i of link m during the time period $[kT, (k + 1)T)$ divided by T.

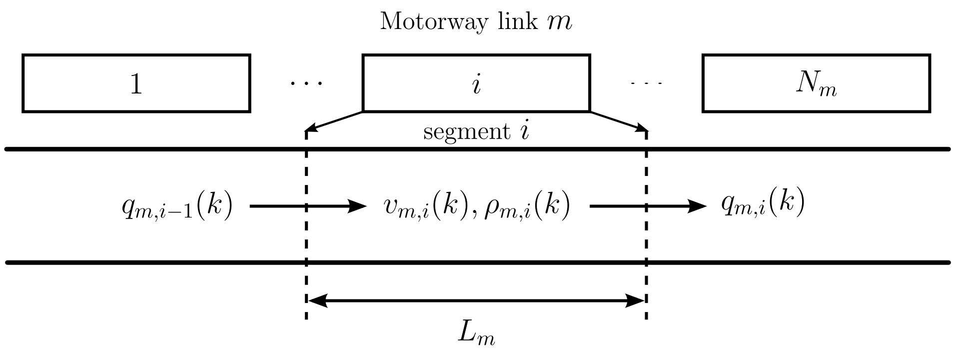

Figure 2.5: Discretised motorway link.

2.3.2 The Motorway Link Model

The previously defined traffic variables are calculated for each segment i of link m at each time step k by the following equations:

$$\rho_{m,i}(k+1) = \rho_{m,i}(k) + \frac{T}{L_m \lambda_m} [q_{m,i-1}(k) - q_{m,i}(k)] \tag{2.1}$$

$$q_{m,i}(k) = \rho_{m,i}(k) v_{m,i}(k) \lambda_m \tag{2.2}$$

$$
\begin{aligned}
v_{m,i}(k+1) = v_{m,i}(k) &+ \frac{T}{\tau}\{V[\rho_{m,i}(k)] - v_{m,i}(k)\} \\
&+ \frac{T}{L_m}[v_{m,i-1}(k) - v_{m,i}(k)]v_{m,i}(k) \\
&- \frac{\nu T}{\tau L_m}\frac{\rho_{m,i+1}(k) - \rho_{m,i}(k)}{\rho_{m,i}(k) + \kappa}
\end{aligned} \tag{2.3}
$$

$$
V[\rho_{m,i}(k)] = v_{\mathrm{f},m} \exp\left[-\frac{1}{\alpha_m}\left(\frac{\rho_{m,i}(k)}{\rho_{\mathrm{cr},m}}\right)^{\alpha_m}\right], \tag{2.4}
$$

where (2.1) is the conservation equation; (2.2) is the transport equation to be replaced in (2.1); (2.3) is an empirical dynamic mean speed equation where (2.4), the static speed-density relationship corresponding to the fundamental diagram, must be replaced; and τ (a time constant), ν (an anticipation constant), and κ are model parameters that are equal for all the network links. Two further terms may be added to (2.3) for higher accuracy under certain conditions [59].

The original (non-VSL) model includes three link-specific constant parameters in the speed-density curve (2.4): the free speed $v_{\mathrm{f},m}$ encountered at zero density ($\rho_{m,i} = 0$), the critical density $\rho_{\mathrm{cr},m}$ at which traffic flow is close to capacity $q_{\mathrm{cap},m}$, and α_m. Combining (2.2)–(2.4) under stationary (i.e., $v_{m,i}(k+1) = v_{m,i}(k)$) and spatially homogeneous (i.e., $v_{m,i-1} = v_{m,i}$ and $\rho_{m,i+1} = \rho_{m,i}$) conditions for $\rho_{m,i} = \rho_{\mathrm{cr},m}$ (i.e., the critical density) yields the capacity of the fundamental diagram (flow-density curve):

$$
q_{\mathrm{cap},m} = v_{\mathrm{f},m} \cdot \rho_{\mathrm{cr},m} \exp(-1/\alpha_m). \tag{2.5}
$$

2.3.3 Incorporating the VSL Impact

The described link model may be extended to incorporate the impact of displayed VSL values on the traffic flow behaviour under the assumption that a single VSL value (if any) is displayed in each link (using, in real implementations, as many VMS gantries as necessary, depending on the link length). It should be noted that this assumption is not really restrictive because:

- If a higher spatial granularity (resolution) of VSL values is desired, links may be selected accordingly short.
- If a lower spatial granularity (resolution) of VSL values is desired, there is a possibility for the user of the related software tools METANET (simulator) and AMOC (optimal

control; see Section 2.4) to create clusters of links, each cluster having a common VSL value.

To start with, particular VSL values are reflected in the link-specific VSL rates $b_m(k)$ that prevail, by definition, during $[kT,(k+1)T)$. The VSL rates are naturally control variables with an admissible value range $b_m(k) \in [b_{\min,m}, 1]$, where $b_{\min} \in (0,1)$ is a lower admissible bound for VSL rates (see further below for a physical interpretation of b_m).

Using the defined VSL rates, the appropriate inclusion of these control variables into the link model (2.1)–(2.4) are performed next. Pursuing the lines of previous works [3, 14, 27], this is materialised by rendering the static speed-density relationship (2.4) b_m-dependent. Based on available real data evidence from [34, 62, 63], this is enabled by actually rendering the three parameters included in (2.4) b_m-dependent by use of the following linear function:

$$v^*_{\mathrm{f},m}[b_m(k)] = v_{\mathrm{f},m} b_m(k), \tag{2.6}$$

and by the use of the following affine functions:

$$\rho^*_{\mathrm{cr},m}[b_m(k)] = \rho_{\mathrm{cr},m}\{1 + A_m[1 - b_m(k)]\} \tag{2.7}$$

$$\alpha^*_m[b_m(k)] = \alpha_m[E_m - (E_m - 1)b_m(k)], \tag{2.8}$$

where $v_{\mathrm{f},m}$, $\rho_{\mathrm{cr},m}$, α_m denote the specific non-VSL values for these parameters as in (2.4), while A_m and E_m are constant parameters to be estimated based on real data.

As (2.6) reveals, b_m is equal to the VSL-induced $v^*_{\mathrm{f},m}$ divided by the non-VSL $v_{\mathrm{f},m}$ or approximately equal to the displayed VSL divided by the legal speed limit without VSL. Thus, if $b_m(k) = 1$, no VSL is applied, else $b_m(k) < 1$ and, in fact, for $b_m(k) = 1$, all parameters are seen in (2.6)–(2.8) to attain their respective non-VSL values. Equations (2.7) and (2.8) suggest that for $A_m > 0$ and $E_m > 1$, $\rho^*_{\mathrm{cr},m}$ and α^*_m are affine increasing functions for decreasing b_m starting with their usual non-VSL values for $b_m(k) = 1$.

For the extended model, (2.4) is then replaced by:

$$V[\rho_{m,i}(k), b_m(k)] = v^*_{\mathrm{f},m}[b_m(k)] \exp\left[-\frac{1}{\alpha^*_m[b_m(k)]}\left(\frac{\rho_{m,i}(k)}{\rho^*_{\mathrm{cr},m}[b_m(k)]}\right)^{\alpha^*_m[b_m(k)]}\right], \tag{2.9}$$

and $V[\rho_{m,i}(k)]$ in (2.3) now reads $V[\rho_{m,i}(k), b_m(k)]$ while the VSL-induced capacity flow is given by:

$$q^*_{\mathrm{cap},m}[b_m(k)] = v^*_{\mathrm{f},m}[b_m(k)] \cdot \rho^*_{\mathrm{cr},m}[b_m(k)] \cdot \exp\left(-\frac{1}{\alpha^*_m[b_m(k)]}\right). \tag{2.10}$$

The extended speed-density curve (2.9) encompassing (2.6)–(2.8) was validated by use of traffic data taken from a European VSL-equipped motorway location [34], where the legal speed limit is 70 mph and the applied VSL values are 60 mph, 50 mph, and 40 mph. These values correspond to VSL rates $b_m \in \{1, 0.86, 0.71, 0.57\}$. The validation furnished different parameter values for different motorway locations; more specifically, at some locations the real data and resulting values of A and E indicated an increase of the VSL-induced capacity $q^*_{\mathrm{cap},m}(b_m)$ compared to the non-VSL capacity $q_{\mathrm{cap},m}$ for some VSL values; while at other locations no capacity increase was observed for any VSL, i.e., $q^*_{\mathrm{cap},m}(b_m) \le q_{\mathrm{cap},m}$ for all b_m. For one of the locations, the validation exercise furnished the following estimated parameter values, which will be used, except where otherwise stated, in the simulations of Chapters 5 and 6: $v_{\mathrm{f},m} = 115$ km/h, $\rho_{\mathrm{cr},m} = 28.2$ veh/km/lane, and $\alpha_m = 2.15$ (leading via (2.5) to a non-VSL capacity value $q_{\mathrm{cap},m} = 2{,}036$ veh/h/lane) while the estimated VSL-related parameters were $A_m = 0.7$ and $E_m = 1.9$ for (2.7) and (2.8), respectively.

Figure 2.6 displays the corresponding flow-density curves using the above estimated parameters, generalised for a broader range $b_m \in [0.2, 1.0]$. In accordance with Section 2.2.3, the following may be observed in Figure 2.6:

(i) Free speeds are decreasing with decreasing VSLs.

(ii) Cross-points of VSL affected curves with the non-VSL curve appear near or beyond the non-VSL critical density; critical densities are increasing with decreasing VSLs.

(iii) No capacity increase (for any VSL value) was observed at this location. Note that data from a different location of the same motorway yielded capacity increases for $b_m \in (0.6, 1)$ with a maximum increase of 8 percent at $b_m = 0.82$ [34].

(iv) For $b_m = 0.9$, capacity is virtually equal as in the non-VSL case but is seen to monotonically decrease with (further) decreasing b_m values.

All the other model parameter values used in this study (Chapters 5 and 6) are taken from a previous model calibration for a real motorway [37], namely, $\tau = 18$ s, $\nu = 60$ km^2/h, $\kappa = 40$ veh/km/lane. It should be noted that the isolated validation of the fundamental

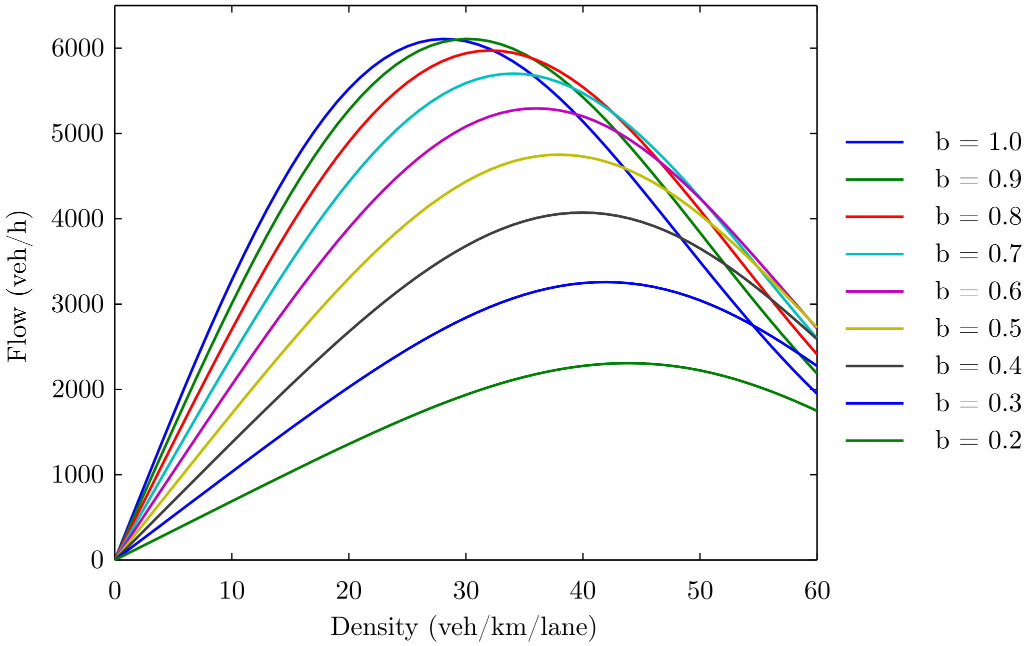

Figure 2.6: Fundamental diagrams for different VSL rates, without increase of capacity: $b = 1.0$ means no VSL applied, decreasing b-values correspond to decreasing VSLs.

diagram before incorporating it within the more comprehensive dynamic model (2.1)–(2.3) and (2.9) may have a quantitative impact on the accuracy of the VSL-extended dynamic model. Nevertheless, because the static speed-density relationship (2.9) (or, in the non-VSL case, (2.4)) is known to dominate within the dynamic speed-density relationship (2.3), the overall dynamic model is deemed to reflect the impact of VSLs sufficiently accurately for the requirements of the present study. As a matter of fact, the validation results by [34] were derived with traffic data collected at one single motorway. Hence, more validation work, using data from different motorways and countries, is necessary before arriving at a quantitatively accurate and reliable description of the VSL impact on traffic flow. However, the control results obtained in simulation in Chapters 5 and 6 exploit two particular impacts of VSLs that are quite certain to occur (at least qualitatively) in reality as well (with appropriate enforcement measures) because of physical reasons (see Section 2.2.4): the decrease of free speeds with decreasing VSLs (aspect (i)) and the decrease of capacity with (sufficiently) decreasing VSLs (aspect (iv)).

It is also noted that the maximum mainstream flow created by the dynamic model (e.g., at on-ramp merge areas) may be higher than the fundamental diagram's $q_{\text{cap},m}$ (and $q^*_{\text{cap},m}$) because of the impact of other terms in (2.3). Thus, the "factual capacity" of merge areas (without VSLs) in the simulations of Chapters 5 (Section 5.1) and 6 is about 2,080 veh/h/lane, which is higher than $q_{\text{cap},m} = 2,036$ veh/h/lane. Finally, as observed in numerous previous simulation studies with the METANET simulator, the overall dynamic model (2.1)–(2.3) (with or without VSL-related extensions) automatically creates a (factual) capacity drop (of typically 8 to 10 percent) at active bottlenecks.

2.3.4 The Origin Link Model

For origin links, i.e., links that receive traffic demand d_o and forward it into the motorway network, a simple queue model is used (Figure 2.7). The outflow q_o of an origin link o depends on the arriving demand, on the traffic conditions of the corresponding mainstream segment $(\mu, 1)$, and on the existence of ramp metering control measures. If ramp metering is applied, then the outflow $q_o(k)$ that leaves origin o during period k is a portion $r_o(k)$ of the outflow $\hat{q}_o(k)$ that would leave in absence of ramp metering. Thus, $r_o(k) \in [r_{\mathrm{min},o}, 1]$ is the metering rate for the origin link o, i.e., a control variable where $r_{\mathrm{min},o}$ is a minimum admissible value. If $r_o(k) = 1$, no ramp metering is applied; else, $r_o(k) < 1$. The queuing model is described by the following conservation equation:

$$w_o(k+1) = w_o(k) + T[d_o(k) - q_o(k)], \tag{2.11}$$

where $w_o(k)$ (veh) is the queue length in origin o at time kT, and $d_o(k)$ (veh/h) is the demand flow at o. The outflow $q_o(k)$ is determined as follows:

$$q_o(k) = r_o(k)\hat{q}_o(k) \tag{2.12}$$

with

$$\hat{q}_o(k) = \min\{\hat{q}_{o,1}(k), \hat{q}_{o,2}(k)\} \tag{2.13}$$

and

$$\hat{q}_{o,1}(k) = d_o(k) + w_o(k)/T \tag{2.14}$$

$$\hat{q}_{o,2}(k) = Q_o \min\left\{1, \frac{\rho_{\mathrm{max}} - \rho_{\mu,1}(k)}{\rho_{\mathrm{max}} - \rho_{\mathrm{cr},\mu}}\right\}, \tag{2.15}$$

where Q_o (veh/h) is the on-ramp's capacity flow, i.e., the on-ramp's maximum possible outflow under free-flow traffic conditions in the mainstream, and ρ_{max} (veh/km/lane) is the maximum density in the network, which is $\rho_{\mathrm{max}} = 180$ veh/km/lane for the simulations in Chapters 5 and 6. According to (2.13)–(2.15), the uncontrolled outflow $\hat{q}_o(k)$ is determined by the current origin demand if $\hat{q}_{o,1}(k) < \hat{q}_{o,2}(k)$; else it is determined by the geometrical

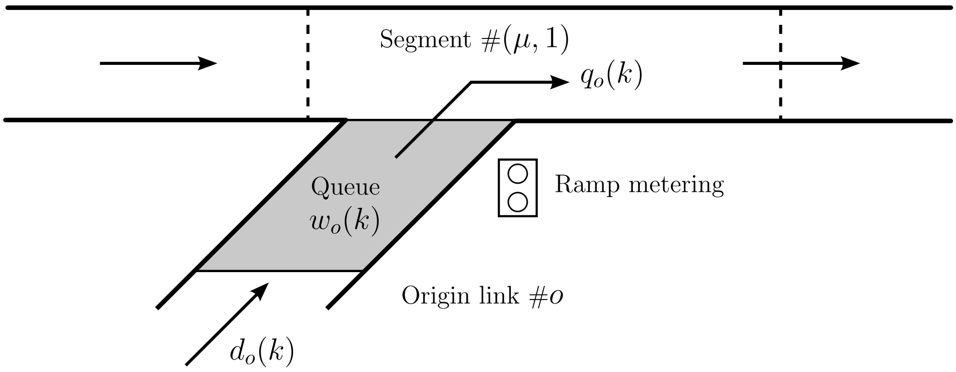

Figure 2.7: The origin link queue model.

capacity Q_o (if the mainstream density is undercritical, i.e., $\rho_{\mu,1}(k) < \rho_{\mathrm{cr},\mu}$) or by the reduced capacity because of congestion of the mainstream (if $\rho_{\mu,1}(k) > \rho_{\mathrm{cr},\mu}$).

2.3.5 The Node Model

Motorway bifurcations and junctions (including on-ramps and off-ramps) and, more generally, link bounds are represented by nodes. Traffic enters a node n through a number of input links and is distributed to the output links according to the following equations:

$$Q_n(k) = \sum_{\mu \in I_n} q_{\mu,N_\mu}(k) \tag{2.16}$$

$$q_{m,0}(k) = \beta_n^m(k) Q_n(k) \quad \forall m \in O_n, \tag{2.17}$$

where I_n is the set of links entering node n, O_n is the set of links leaving n, $Q_n(k)$ is the total traffic volume entering n at period k, $q_{m,0}(k)$ is the traffic volume that leaves n via out-link m, and $\beta_n^m(k) \in [0, 1]$ is the portion of $Q_n(k)$ that leaves n through link m (turning rates).

At a network node n, the upstream influence of the downstream link density (e.g., in case of congestion spill-back) has to be taken into account in the last segment of the incoming links (see (2.3) for $i = N_m$). This is provided via

$$\rho_{m,N_m+1}(k) = \frac{\sum\limits_{\mu \in O_n} \rho_{\mu,1}^2(k)}{\sum\limits_{\mu \in O_n} \rho_{\mu,1}(k)}, \tag{2.18}$$

where $\rho_{m,N_m+1}(k)$ is the virtual density downstream of any entering link m to be used in (2.3) for $i = N_m$ and $\rho_{\mu,1}(k)$ is the density of the first segment of the leaving link μ. The quadratic form is used to account for the fact that congestion on one leaving link may spill back into the entering link even if there is free flow in the other leaving links.

Similarly, at a network node n, the downstream influence of the upstream-link speed has to be taken into account according to (2.3) for $i = 1$. The required upstream mean speed value is calculated from the flow-weighted average

$$v_{m,0}(k) = \frac{\sum\limits_{\mu \in I_n} v_{\mu,N_\mu}(k) q_{\mu,N_\mu}(k)}{\sum\limits_{\mu \in I_n} q_{\mu,N_\mu}(k)}, \tag{2.19}$$

where $v_{m,0}(k)$ is the virtual speed upstream of any leaving link m that is needed in (2.3) for $i = 1$.

2.3.6 The Overall Dynamic Model

Combining the equations developed above, a non-linear macroscopic discrete-time state-space model

$$\mathbf{x}(k+1) = \mathbf{f}[\mathbf{x}(k), \mathbf{u}(k), \mathbf{d}(k)], \quad \mathbf{x}(0) = \mathbf{x}_0 \tag{2.20}$$

is obtained for the entire motorway network, where $\mathbf{x}$ is the state vector, $\mathbf{u}$ is the control vector, and $\mathbf{d}$ is the disturbance (external variable) vector. The state vector consists of the densities $\rho_{m,i}$ and the mean speeds $v_{m,i}$ of every segment i of every link m and the queues w_o of every origin o. The control vector consists of the VSL rates b_m of every link m where VSLs are applied and of the ramp metering rates r_o of every origin o that is metered. The disturbance vector consists of the demand d_o at every origin o and the turning rates β_n^m at every bifurcation node n.

2.4 The Integrated Optimal Control Problem

The integrated motorway network traffic control problem is formulated as a discrete-time dynamic optimal control problem with constrained control variables over a given optimisation horizon K_{P}, which is solved very efficiently even for large-scale networks by a suitable feasible direction algorithm [50, 54]. This extended formulation (to incorporate the VSL impact) and the numerical solution algorithm are incorporated in an accordingly extended version of the open-loop optimal control tool AMOC [38] which is able to consider coordinated ramp metering, system optimum route guidance, and variable speed limits (using the introduced extension via (2.6)–(2.9)) as well as integrated control combining all control measures simultaneously.

If only ramp metering and VSLs are considered, the general discrete-time formulation of the optimal control problem is the following:

> Given disturbance predictions $\mathbf{d}(k)$, $k = 0, 1, \ldots, K_\mathrm{P} - 1$ and the initial state $\mathbf{x}_0 = \mathbf{x}(0)$, minimise
>
> $$J = \vartheta[\mathbf{x}(K_\mathrm{P})] + \sum_{k=0}^{K_\mathrm{P}-1} \varphi[\mathbf{x}(k), \mathbf{u}(k), \mathbf{d}(k)] \tag{2.21}$$
>
> subject to (2.20) and the inequality constraints imposed on the ramp metering rates $r_{\mathrm{min},o} \leq r_o(k) \leq 1$ and the VSL rates $b_{\mathrm{min},m} \leq b_m(k) \leq 1$.

The chosen cost criterion is the total time spent (TTS) by all vehicles in the network (including the waiting time experienced in the ramp queues), which is a natural objective for the traffic systems considered. The maximum ramp queue constraints may be taken into account via the introduction of penalty terms in the cost criterion penalising queue lengths larger than $w_{\mathrm{max},o}$, which is a predetermined maximum admissible queue for origin o. Another penalty term may be added to suppress high-frequency oscillations of the optimal control trajectories. More precisely, the cost criterion used as (2.21) is the following:

$$\begin{aligned}
J = {} & T \sum_{k=1}^{K_\mathrm{P}-1} \sum_{m} \sum_{i} \rho_{m,i}(k) L_m \lambda_m + T \sum_{k=1}^{K_\mathrm{P}-1} \sum_{o} w_o(k) \\
& + T \sum_{k=1}^{K_\mathrm{P}-1} \sum_{o} \alpha_\mathrm{r} [r_o(k) - r_o(k-1)]^2 \\
& + T \sum_{k=1}^{K_\mathrm{P}-1} \sum_{m} \alpha_\mathrm{b} [b_m(k) - b_m(k-1)]^2 \\
& + T \sum_{k=1}^{K_\mathrm{P}-1} \sum_{o} \alpha_\mathrm{w} [\max\{0, w_o(k) - w_{\mathrm{max},o}\}]^2,
\end{aligned} \tag{2.22}$$

where α_r , α_b, and α_w are weighting factors for the corresponding penalty terms.

The solution determined by AMOC may reflect a local minimum, because the problem is non-convex, but the experience with the tool shows that an excellent solution (from the application point of view) has always been found. The AMOC solution consists of the optimal ramp metering and VSL rate trajectories as well as the corresponding optimal state trajectory. It is interesting to note that the solution algorithm can account for control variables that change their value less frequently than the state variables. Moreover, for the VSL rates, common control variables can be considered for clusters of links.

It should be stressed that the extension of AMOC to also consider VSL rates necessitated the specialised and rigorous incorporation of accordingly extended generic necessary optimality conditions along with the corresponding Jacobian matrices, etc. This has led to a universal optimal control tool that is readily applicable to any, (even large-scale) motorway network to deliver optimal control results with quite low computational effort that would even allow for real-time application of the tools. This marks a clear progress compared to most previous works involving optimal VSL control. More details on the integrated traffic control problem (without VSLs) and the numerical solution algorithm may be found in [38].

It must be emphasised that optimisation and optimal control methods applied adequately to specific application problems are distinguished by an inherent intelligence. More specifically, while searching for the mathematical optimum, optimal control methods (based on adequate modelling) may "discover" the particular application ways, measures, and combinations of control variables that lead to optimal performance. Thus, an engineering application-specific interpretation of the optimal results may lead to new general insights regarding the specific application. In the case here, some of the insights for the development of the MTFC Concept (Chapter 3) were, in fact, revealed upon interpretation of the obtained optimal AMOC results. In the simulation investigations of Chapters 5 and 6, AMOC is seen to automatically behave as if it were aware of all the particularities of MTFC.

In summary, the optimal control problem delivers ideal solutions in a simulation environment due to the "perfect" model, the exact knowledge of (future) disturbances (demands and turning rates) and the lack of some VSL constraints. Clearly, these solutions cannot be outperformed (in simulation) by any other control strategy but may be used to assess the efficiency of other (simpler) strategies under different scenarios.

Chapter 3

The MTFC Concept

The control of traffic flow to increase flow.

H. Greenberg and A. Daou [24]

Mainstream traffic flow control (MTFC) is proposed in this chapter as a new avenue for efficient motorway traffic management. The intended effect of MTFC may be summarised by the title of an early paper by Greenberg and Daou [24]: *"The control of traffic flow to increase flow"*. Several previous works had, in some way or another, similar intentions. Therefore, this chapter begins, in Section 3.1, with a historical overview of the traffic flow control approaches that were applied to the mainstream of motorways and that have similarities with MTFC. Then, in Section 3.2 the motivation and the basic idea of MTFC are presented, followed by examples of how MTFC can be applied to different types of bottlenecks in Section 3.3. Afterwards, several MTFC related issues are discussed in Section 3.4. Finally, Section 3.5 presents ways of how VSLs can be used as an actuator for MTFC.

3.1 MTFC-like Strategies

In a research effort over the late 1950s and 1960s to increase the throughput of the tunnels under the Hudson River, connecting New York City with New Jersey, the involved traffic scientists revealed that *"congestion inside the tunnel reduces its throughput (...) due to the fact that most cars do not accelerate very efficiently once they have to stop, or even just slow down"* [22], which corresponds, in more recent terminology, to the "capacity drop" at the head of congestion [5, 64]. To address the problem, the Port Authority of New York introduced an inflow traffic control system (using traffic lights but also other signs) which was one of the very first (initially fixed-logic, then computer-based) traffic-responsive control systems ever. The system was using real-time traffic measurements from the bottleneck location to decide on the inflow control actions so as to neither overload nor starve-for-flow the tunnel, since both of these effects would reduce the throughput. A first feedback control strategy was of the bang-bang type (similar to the one employed, e.g., in electric irons) and led to a mere 2 percent of throughput increase due to the (expected) oscillations [15, 20]. Eventually, a more sophisticated (albeit heuristic) feedback algorithm increased the throughput by 9 percent [19, 22].

Another remarkable traffic control system within the same class, that has been in operation for over 35 years, is the traffic-light based entrance control system of the San Francisco-Oakland Bay Bridge [45] that was found to increase the westbound Bay Bridge throughput by 5 percent. The employed feedback algorithm (as described in [8]) is based on heuristics, but seems to have remarkable similarities with the ALINEA-like (I-type feedback) algorithm proposed in [78]. These early successes motivated other researchers [25, 33] to propose "mainline metering" (by use of traffic lights) as a promising new traffic management tool for motorways, without, however, developing this idea in more technical detail.

Since the usage of traffic lights on the motorway mainstream may be quite controversial, more recent works have considered MTFC-like strategies enabled by use of VSLs with different control approaches and traffic application settings. An early VSL control initiative [3] incorporated the model proposed by Cremer [14] (Section 2.2.3.1) in a general dynamic model leading to an optimal control formulation. However, a heuristically fixed control law was eventually used because of the size of the problem, and its parameters were optimised based on particular scenarios.

The thesis [27] was the first recent work attempting to use VSLs to regulate the mainstream traffic flow. Despite of the good results achieved even in microscopic simulation [29], the proposed control strategy is based on an optimal control approach that may be not sufficiently practicable (similarly to the optimal control approach presented in Section 2.4). In addition, the proposed numerical solution procedure (making use of available non-linear programming codes) does not allow for consideration of large-scale applications. An ALINEA-like feedback controller for the mainstream using VSLs was proposed in [95] and tested via microscopic simulation. However, the lack of an acceleration area (see Section 3.2) is the likely reason for obtaining only marginal improvements. Two VSL control algorithms were designed in

[42] for work zones. The obtained results were satisfactory, but the algorithms do not seem applicable for a wider range of bottleneck types. The distributed feedback controller against moving shock waves, as proposed in [69], seems quite complex and difficult to fine-tune for the general case. Another approach against moving shock waves was tested in microscopic simulations by the use of a series of local ALINEA controllers, one for each VSL equipped section, activated based on switching logics [6]. The improvements achieved were moderate, but the approach lacks of theoretical foundation for its design. On the other hand, the recent SPECIALIST effort [28, 30] is particularly valuable because it demonstrated that mainstream traffic flow regulation via VSLs actually works in practice; however the SPECIALIST setting also addresses moving shock waves (rather than bottlenecks) and is a feed forward (rather than feedback) scheme. Feedback motorway traffic control using VSLs was also proposed in [10] by use of H-infinity control theory but without explicitly addressing throughput maximisation at bottleneck locations. Finally, [44] employed the basic MTFC concept proposed in this thesis (via already published papers, see Section 1.5), including an acceleration area, but the proposed feedback switching I-type regulator does not seem suitable to deliver stable or sufficiently damped control actions.

3.2 The Basic Idea of MTFC

The basic idea of MTFC is to enable the mainstream traffic flow at selected locations (e.g., upstream of bottlenecks) to take values ordered by an appropriate control strategy in order to establish optimal traffic conditions (maximum efficiency) for any appearing demand. A local aspect of this basic idea is illustrated in Figure 3.1 for better appreciation of the potential MTFC impact. The bottleneck of Figure 3.1 is not activated (and no MTFC is needed) as long as $q_{\mathrm{in}} < q_{\mathrm{cap}}^{\mathrm{down}}$, in which case $q_{\mathrm{out}} \approx q_{\mathrm{in}}$. If q_{in} grows bigger than the bottleneck capacity $q_{\mathrm{cap}}^{\mathrm{down}}$, the bottleneck would be activated in absence of control as in Figure 2.1 and q_{out} would be reduced due to capacity drop; whereas MTFC can implement a controlled outflow q_{c} such that q_{out} is equal to the bottleneck capacity. Clearly, the mainstream congestion cannot be avoided via MTFC because $q_{\mathrm{in}} > q_{\mathrm{cap}}^{\mathrm{down}}$ (otherwise MTFC would not intervene), but:

- The congestion outflow in the MTFC case is higher than in the no-control case because the capacity drop is avoided; this eliminates the detrimental effects of capacity drop on the infrastructure degradation.
- For the same reason (higher outflow with MTFC), the created congestion in the MTFC

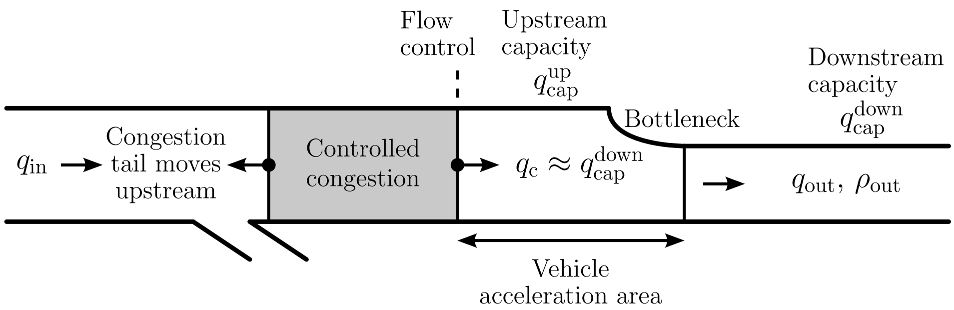

Figure 3.1: A local aspect of MTFC.

case (a) has a higher internal speed and (b) is shorter than in the no-control case. Thus MTFC leads to a shorter and lighter mainstream congestion and hence to less blocking of less off-ramps, which marks a potential improvement for the detrimental effects of BOR on the infrastructure capacity.

Nevertheless, the fact that MTFC leads to the formation of (limited) mainstream congestion implies that BOR effects may be reduced but not fully avoided. Hence, MTFC is less efficient than ideal RM (with sufficient on-ramp storage space) which leads to complete congestion avoidance on the mainstream; but the simulation results reported in Section 5.2 indicate that the efficiency difference may be small. In other words, MTFC is a control measure against CD in the first place, while any improvements related to BOR effects are due to shorter and lighter mainstream congestion.

The advantage of MTFC, compared to ramp metering, is that its action is not compromised by the limited ramp storage space. A combination of MTFC and ramp metering, whereby, e.g., MTFC is only activated when the on-ramp storage is about to be exhausted, is addressed in Chapter 5 based on optimal control. A similar approach, albeit based on simple feedback concepts, is outlined in Chapter 4.

It should be noted that the capacity drop phenomenon, the occurrence of which has been repeatedly confirmed with traffic data (see, e.g., [5]), is deemed to occur because of the need for vehicles to accelerate from low speeds within the bottleneck congestion to higher speeds as they reach the congestion head [64]. Since a mainstream controlled congestion will be formed upstream of the flow control location, as indicated in Figure 3.1, vehicles exiting this controlled congestion area will have a relatively low speed (depending on the controlled mainstream flow q_{c}), which is likely to be lower than the critical speed v_{cr} leading to bottleneck capacity flow $q_{\text{cap}}^{\text{down}}$ (Figure 2.2(b)). Thus, in order to enable capacity flow $q_{\text{cap}}^{\text{down}}$ at the downstream bottleneck area Figure 3.1 (i.e., to actually avoid the capacity drop), vehicles must be allowed to accelerate to the critical speed $v_{\rm cr}$ (around 70 km/h), i.e., the speed at which capacity flow occurs, and enter the downstream bottleneck area with a roughly critical speed $v_{\rm cr}$. To this end, the head of the deliberately created mainstream congestion (i.e., the mainstream flow control location) should be placed sufficiently upstream of the addressed bottleneck. According to Figure 2.7 of [26], a distance of some 700 m should be sufficient for vehicles to accelerate from low speeds to 70 km/h. In lack of an acceleration area, the capacity drop may not be avoided (as demonstrated in Section 5.2) and this is the likely reason for obtaining only marginal improvements in [95].

The proposed length of the acceleration area should be understood as an upper limit which should suffice even if the necessary controlled mainstream flow $q_{\rm c}$ is very low. On the other hand, if $q_{\rm c}$ is (lower but) close to $q_{\rm cap}^{\rm down}$, the vehicles exiting the controlled congestion area will have a relatively high speed, and hence they may not need to accelerate substantially. Thus, to facilitate an efficient traffic flow through the bottleneck for any $q_{\rm c}$, i.e., for any vehicle speed, it is advisable to post an appropriate speed limit for vehicles entering the acceleration area as well as for the vehicles in the downstream bottleneck area. In fact, these speed limits can also be explored for increased efficiency by taking advantage of increased critical density (see Section 2.2.4 and also Section 4.7) or increased capacity as demonstrated in [66] and further investigated in Section 6.2.4.

Clearly, this implementation concept for MTFC has not yet been tested in the field; but it is interesting to note that an accidental (unintended) MTFC action (due to a disabled vehicle in the median lane) upstream of a lane-drop bottleneck, as reported and analysed by [11], may have enabled avoidance of the capacity drop and restoring of capacity in real traffic conditions.

3.3 MTFC Applied to Different Types of Bottlenecks

In the previous section, the MTFC concept was applied to an abstract motorway bottleneck shown in Figure 3.1. To further clarify the MTFC concept, in this section the MTFC concept is applied to some typical motorway bottlenecks. For each type of bottleneck a new figure equivalent to Figure 3.1 is presented. Similar to Section 2.1.1 (Figure 2.1), $q_{\rm in} > q_{\rm cap}^{\rm down}$, and the bottleneck would be activated in absence of control, i.e., a congestion would occur. Additionally, the special case of off-ramp spill-back into the motorway, where MTFC can hardly help, is also presented.

3.3.1 Merging On-ramp

On-ramp merge bottleneck is one of the most common types of bottlenecks. Figure 3.2 depicts a three-lane motorway stretch with a merging on-ramp. The motorway traffic flow q_{in} arriving upstream of the bottleneck is the sum of the mainstream arriving traffic flow $q_{\mathrm{in}}^{\mathrm{m}}$ and the on-ramp inflow $q_{\mathrm{in}}^{\mathrm{r}}$. Likewise, the upstream capacity $q_{\mathrm{cap}}^{\mathrm{up}} > q_{\mathrm{cap}}^{\mathrm{down}}$ is the sum of the mainstream and on-ramp capacities, $q_{\mathrm{cap}}^{\mathrm{m}}$ and $q_{\mathrm{cap}}^{\mathrm{r}}$, respectively. For this type of bottleneck, the controlled outflow q_{c} implemented by MTFC should be, approximately, the difference between the bottleneck capacity $q_{\mathrm{cap}}^{\mathrm{down}}$ and the on-ramp inflow $q_{\mathrm{in}}^{\mathrm{r}}$. In the case of the existence of other on-/off-ramps within the acceleration area, the value of the controlled outflow will be equivalently smaller/larger. In the investigations in Chapters 5 and 6 this type of bottleneck will be addressed.

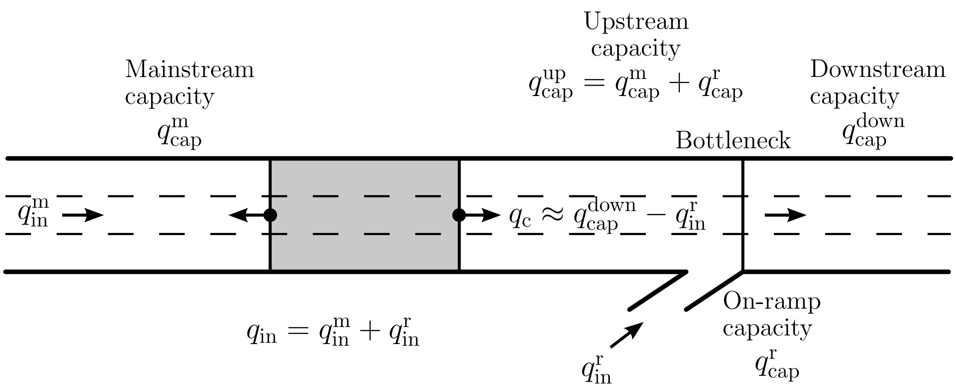

Figure 3.2: The MTFC concept applied to an on-ramp merge bottleneck.

On-ramp merge bottlenecks are of particular interest because of the opportunity of integrating MTFC with ramp metering, whereby the control load would be shared between the MTFC controlled outflow and the metered on-ramp outflow. This aspect is further discussed in Sections 3.4.1 and 4.8.2.

3.3.2 Merging Motorways

Motorway-to-motorway (mtm) control by the use of traffic lights has been shown to provide significant benefits to the management of traffic flow on motorways [25, 67]. This can be achieved by the use of MTFC via VSLs as well, without the controversies raised by the use of metering traffic lights. The use of MTFC for mtm control is straightforward and if MTFC is to be applied to a single motorway, i.e., only at one of the merging motorways, the analysis is similar the on-ramp merge case (Section 3.3.1) and the second motorway takes the role of the on-ramp. Additionally, MTFC may be applied simultaneously to both motorways, as shown in Figure 3.3, in the aim of a more equitable distribution of the metering delays. In the figure, a two-lane motorway is merging into a three lane motorway.

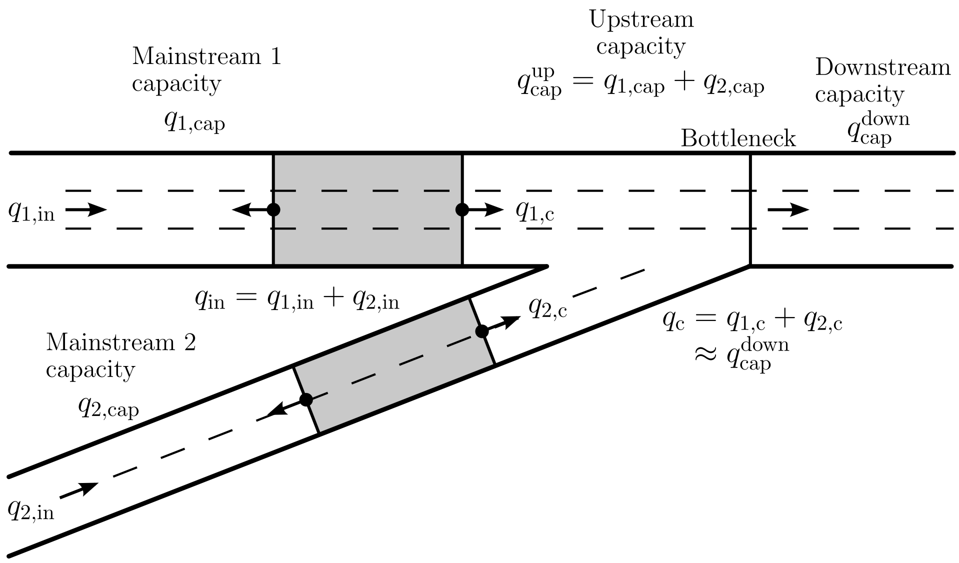

Figure 3.3: The MTFC concept applied to a bottleneck due to merging motorways.

The motorway traffic flow q_{in} arriving upstream of the bottleneck is the sum of the mainstreams arriving traffic flows $q_{1,\text{in}}$ and $q_{2,\text{in}}$. Likewise, the upstream capacity $q_{\text{cap}}^{\text{up}} > q_{\text{cap}}^{\text{down}}$ is the sum of the mainstreams capacities, $q_{1,\text{cap}}$ and $q_{2,\text{cap}}$. For this type of bottleneck the controlled outflow q_{c} implemented by MTFC is given by the sum of the controlled outflow for each mainstream $q_{1,\text{c}}$ and $q_{2,\text{c}}$, and is approximately equal to the bottleneck capacity (when there are no on-/off-ramps in the acceleration area). MTFC applied to merging motorways is further discussed in Section 4.8.1.

3.3.3 Lane Drop and Work Zones

Another type of bottleneck is a lane drop. In this type of bottleneck, the number of lanes in the motorway mainstream is reduced by one or more lanes. Lane closures in work zones are in effect lane drops and dedicated control measures for work zone operation have been investigated at several instances [42, 64, 87]. If MTFC is to be applied to a lane drop bottleneck or to a work zone the approach is rather similar. In Figure 3.4 one lane is dropped from a three-lane motorway. The interpretation for this type of bottleneck is identical to the one in Section 3 (Figure 3.1).

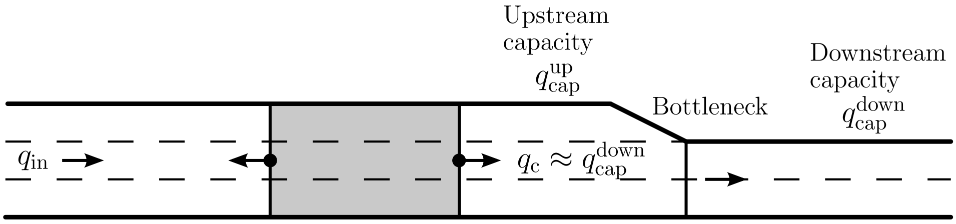

Figure 3.4: The MTFC concept applied to a lane drop bottleneck.

3.3.4 Strong Curvatures, Tunnels, Bridges, Strong Grades and Strong Weaving Sections

The three types of bottlenecks presented so far have as a common characteristic the fact that the number of lanes upstream of the bottleneck is bigger than the number of lanes downstream of the bottleneck. Assuming that all lanes have the same capacity, it is clear that the downstream capacity is smaller than the upstream capacity by the ratio of the number of lanes downstream and upstream of the bottleneck location. Very often, however, bottlenecks arise even if there is no apparent physical reduction of motorway capacity. Changes in infrastructure such as strong curvatures, tunnels, bridges, strong grades as well as strong weaving sections are all examples of locations of potential bottlenecks. In Japan, for example, 13 percent of congestion in 1997, measured as the product of congestion extension by congestion duration, was located at tunnel entrances [49]. Also, some of the early works on MTFC-like strategies (Section 3.1) were applied at bottlenecks in tunnels that also involved strong grades. Although the San Francisco-Oakland bay bridge control system does not fit in this category, because the number of downstream lanes is reduced, it also features an 1.2 miles incline of 3.5 percent grade at its entrance. McCalden [45] reported that *"the metering system (...) allowed heavy trucks to get up to normal speed before reaching the incline"*, while under stop-and-go traffic (without metering) heavy trucks would cover the same section at a speed of less than 20 mph. This experience also highlights the importance of the acceleration area.

Figure 3.5 depicts a three-lane motorway where the dotted section corresponds to any one of the infrastructures described above, a strong curvature or a tunnel or a bridge or a strong grade, or a section with strong weaving (origin and destinations not shown). The bottleneck, marked by a dashed line, may be at any point of the given section, i.e., not necessarily at its beginning. The interpretation of this figure is identical to the one in Section 3.2 (Figure 3.1).

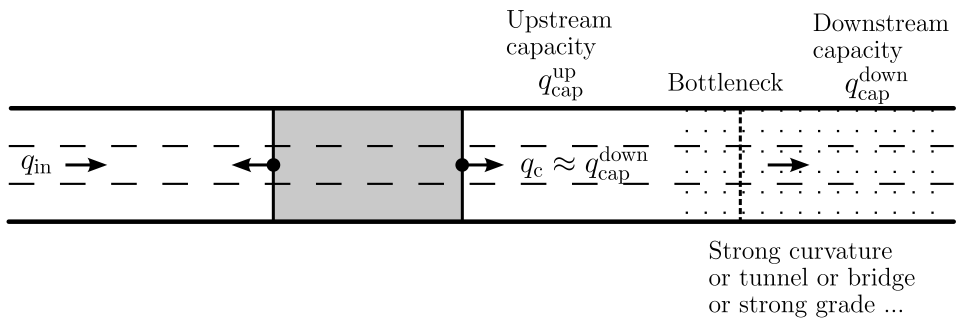

Figure 3.5: The MTFC concept applied to a bottleneck due to specific infrastructure change.

3.3.5 Off-ramp Spillback

Off-ramp spillback, i.e., a queue forming at a motorway off-ramp that spills back into the mainstream is another common type of bottleneck (Figure 3.6). MTFC has a limited effect on this type of bottleneck because the capacity-reducing events affecting the off-ramp usually do not have their production influenced by the upstream traffic flow.

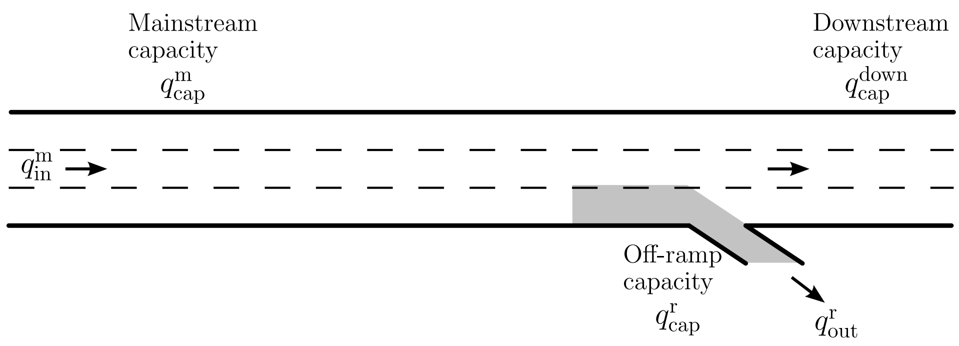

Figure 3.6: The MTFC concept may not be suitable for a bottleneck caused by off-ramp spill-back.

3.4 MTFC-related Issues

The outlined basic idea of MTFC brings along a number of questions, issues and problems that are only partly addressed in this thesis and are considered in corresponding on-going research.

3.4.1 Integration of MTFC with RM

MTFC may be appropriately developed either as a stand-alone control measure or in combination with available or new RM. For the latter case, the developed integrated control strategy should be able to:

- Combine MTFC with any other available control measures for best synergy in terms of achievable efficiency and equity.

- Allow for easy implementation of various operational policies or specifications; for example, MTFC may only be activated if RM is about to become inactive due to full on-ramps; or MTFC may only be activated if the on-ramp waiting time due to RM exceeds a pre-specified threshold; or MTFC and RM may enable a pre-specified share of capacity for mainstream versus on-ramp vehicles; or a pre-specified distribution of unavoidable delays between mainstream and on-ramps vehicles (see also [64]).

This issue is partly addressed in Chapters 4 and 5.

3.4.2 Network-wide MTFC

The local aspects discussed with Figure 3.1 reveal only a portion of the MTFC impact. In fact, the increased bottleneck outflow in the MTFC case corresponds to an increased inflow for the next downstream bottleneck and may activate a (latent) bottleneck that was not active in the no-control case. Moreover, an MTFC controlled active bottleneck queue propagating upstream, may reach the next upstream active bottleneck and de-activate it, as both related congestions will be integrated in a single bigger congestion. In other words, the motorway network is a unique entity and should therefore be addressed by a unique network-wide integrated MTFC strategy for maximum benefits. Although an utterly decentralised control strategy would improve the no-control traffic conditions thanks to the avoidance of the capacity drop, it may be non-optimal in the network-wide sense under certain circumstances. More specifically, holding back traffic at some controlled bottlenecks (i.e., $q_\mathrm{c} < q_\mathrm{cap}^\mathrm{down}$) may provide more benefits for the traffic flow further downstream than the local losses (as, e.g., gating actions in urban traffic networks). These issues are partly addressed in Chapters 4 and 5.

3.4.3 Uncertain Flow Capacities

For the sake of simplicity, flow capacities have been considered so far as having infrastructure-dependent constant values. In reality, motorway flow capacities may vary due to the prevailing environmental conditions (lighting, visibility, pavement condition); but even under comparable environmental conditions, the flow value at which the first traffic breakdown (bottleneck activation) occurs, may vary by even 10 percent from day to day [43]. This problem may be tackled locally via introduction of a local feedback loop that employs traffic occupancy measurements (details are omitted for the sake of brevity) and guarantees maximum bottleneck outflow (equal to capacity), whatever value today's flow capacity happens to have similarly to [64]. Nevertheless, uncertain bottleneck capacities remain a problem to be adequately addressed at the network-wide MTFC level. Research work is in progress with respect to these issues.

3.4.4 MTFC Implementation

Figure 3.1 illustrates the local effect of MTFC without any reference on how to impose the controlled flow q_c on the motorway mainstream. Three alternative actuators may be envisaged to this end:

- Special green-red traffic signals, one for each mainstream lane, placed on appropriate gantries above the motorway and operated with asynchronous phasing as proposed and tested in [64]. Unlike the traffic lights of urban junctions, the signals operate very short traffic cycles with green phases that allow only 1–2 vehicles at a time to pass. Under these conditions, vehicles upstream of the traffic lights may not really have to stop (as in front of urban traffic lights) but merely to slow down as appropriate to create the ordered controlled mainstream flow q_c. It should be noted that traffic lights are the most direct and immediate actuator for MTFC, and related research work is ongoing. On the other hand, the introduction of traffic lights on the motorway mainstream may call for appropriate campaigns (until the road users are accustomed with the new control measure) and perhaps also for change of some related traffic regulations. It should be noted that similar difficulties were encountered in some countries prior to the introduction of ramp metering at on-ramps, but also several decades ago, when traffic signals were first introduced in urban road junctions.

- Variable speed limits may be used to slow down the motorway traffic flow sufficiently in order to create the ordered controlled mainstream flow q_c. As mentioned earlier, the range of utilised VSLs in most current installations does not exceed $[60, 120]$ km/h (see, e.g., [12]) which is not sufficient for the implementation of low-valued controlled flows q_c. Therefore, the lower bound of the currently usual range of practiced VSLs should be lowered to 40 km/h or less for MTFC, while appropriately designed user campaigns should inform the road users on the rationale and utility of the system in order to increase compliance to the displayed VSL; currently practiced (automatic) enforcement procedures are known to lead to high compliance as well. VSLs are considered as an MTFC actuator in the investigations of this thesis.

- Emerging vehicle-infrastructure integration systems may be used to slow down equipped vehicles in order to create the ordered controlled mainstream flow q_c in a similar way as with VSLs above. The required penetration level of equipped vehicles for appropriate operation must be investigated for this particular actuator.

The aforementioned actuators should remain switched off for as long as MTFC is not needed (e.g., in the off-peak period). A "warm-up" period with appropriate pre-signals and messages (on variable message signs) upstream of the MTFC area should be applied before the actual activation of the actuator (e.g., at the start of the peak period) in order to warn arriving drivers about the imminent activation. But also during MTFC operation, the same pre-signals and VMS should continue to warn arriving drivers about the applied mainstream traffic control further downstream.

MTFC, by its nature, creates areas of slower moving vehicles upstream of the mainstream control point which may be deemed a safety risk for faster vehicles approaching the tail of the lower-speed area. Of course, the speed level in these areas under MTFC will be higher than in uncontrolled traffic congestions (due to higher flow), and the above mentioned VMS will timely warn the approaching drivers. Nevertheless, in order to minimise the risk for arriving vehicles, VSLs (or VII control) may also be used between flow-controlled bottlenecks to gradually reduce the speed of arriving vehicles to the level required at each particular bottleneck (see Section 4.7).

3.4.5 User and Road Authority Acceptance

Motorways are still considered by some road users and responsible authorities as transportation facilities that should be bare of any restrictive regulation measures. This conception belongs definitely to the past. To start with, Germany is the only country in the world where unlimited vehicle speed can indeed be legally applied in parts of the country's motorways, but these are usually not within metropolitan areas. In addition, available VSL installations may order speeds as low as 60 km/h, and existing RM systems have introduced traffic lights at the borders of the motorway mainstream. Last not least, the average speed on metropolitan motorways during the peak period are very low within the extended congestions, while stop-and go traffic conditions are a daily experience for most commuters. Thus, the original view of the motorway infrastructure as a terrain of fast and unlimited mobility cannot be retained any further. What is needed is the optimal utilisation of the limited capacity infrastructure in a way that will benefit all roads users (equity) in terms of reduced travel times, improved traffic safety and reduced environmental pollution via all appropriate traffic control measures that can protect it from the detrimental effects of "spontaneously" (without control) forming congestions. In view of the mentioned limitations of current control measures (RM, VSLs), the proposed innovative MTFC concept is a natural step towards orderly, efficient, safer and less polluting traffic conditions on metropolitan motorways. Clearly, MTFC may still sound unconventional or even unacceptable for some road users or authorities. Similar feelings and viewpoints were possibly encountered when traffic lights were first introduced in most urban junctions; however, it is known today that, in the rare event of a general failure of the urban traffic lights in an urban road network during the peak period, traffic conditions deteriorate substantially, leading to driver complaints (rather than to a relief due to de-activation of the annoying red lights).

3.5 MTFC via VSLs

The investigations in this thesis are carried out using VSLs as an MTFC actuator. In view of this, the MTFC concept is revisited in this section with focus on its implementation via VSLs. Figure 3.7 is a modified version of Figure 3.1 according to the technical aspects imposed by the use of VSLs. In the figure, a VMS gantry labelled 'VSL 3' and, possibly, other VMS gantries within the application area, display the appropriate VSL (corresponding to a VSL rate b) that will determine the controlled outflow q_{c} that leaves the application area. The gantries 'VSL 1' and 'VSL 2' and, possibly, other gantries within the bottleneck and acceleration areas, display an appropriate VSL that leads the vehicles to a a safe and efficient speed while crossing the bottleneck area. The gantries 'VSL N' to 'VSL 4' display gradually decreasing speed limits for a safe approach of the vehicles reaching the congested area. Additional gantries are added as the congestion moves upstream.

When VSLs are used as an MTFC actuator, if the mainstream demand q_{in} (Figure 3.7) arriving from upstream is higher than the VSL-induced capacity $q^*_{\mathrm{cap}}(b)$, then the VSL application area becomes an active mainstream bottleneck that limits the area's outflow q_{c} to values corresponding to the (lower) VSL-induced capacity. Recall that the state transition

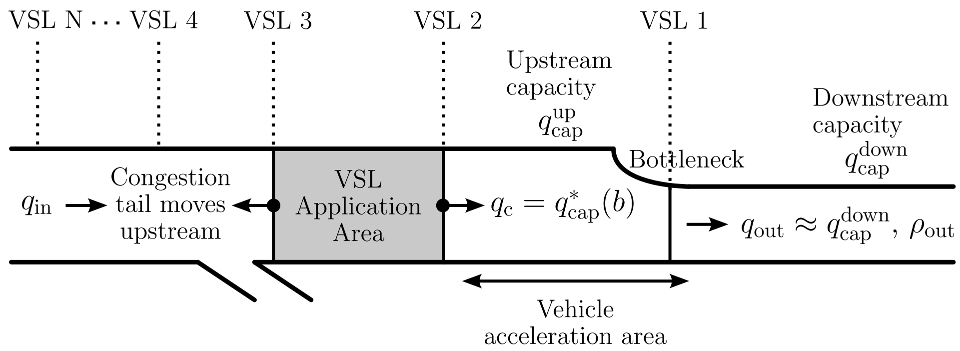

Figure 3.7: A local aspect of MTFC via VSLs.

discussed in Section 2.2.3.2 yields a *temporary* VSL-induced mainstream flow decrease, after which the outflow from the VSL application area returns essentially to values equal to the upstream arriving demand q_{in}. In contrast, in the case discussed here, the arriving demand q_{in} is higher than the VSL-induced capacity $q_{\text{cap}}^{*}(b)$; hence, there is the possibility of applying a more durable mainstream flow control that persists even after the transition period, with mainstream flow values q_{c} depending on the applied VSL values. More specifically, if the outflow of the upstream VSL-controlled bottleneck is regulated such that capacity flow can be established at the downstream bottleneck ($q_{\text{out}} \approx q_{cap}^{down}$), then the final mainstream outflow is maximised, leading to a corresponding decrease of the total time spent in the system.

For the use of VSLs as an actuator, some restrictions apply to the posted speed limits. First, the speed limits cannot assume arbitrary real values, since only discrete speed limits values within the range of permitted VSL scan be used (e.g., at intervals of 10 km/h). Second, VSLs are usually subject to constraints regarding the maximum admissible temporal and spatial changes of displayed VSL values to avoid driver confusion and increase compliance. Therefore, the speed limit difference between two consecutive posted VSLs at the same gantry cannot be bigger than a pre-specified value (e.g., 20 km/h). Similarly, a difference limit between two VSLs posted at consecutive gantries must be observed. This is particularly sensible upstream of the VSL application area to improve traffic safety conditions in view of the related, deliberately created shock wave (Figure 3.7). Note, however, that in absence of VSL control, a more serious and more durable shock wave would result from the activation of the downstream bottleneck. Hence, the VSL-induced mainstream bottleneck is likely to improve traffic safety conditions as well (see Section 6.1.7). Finally, speed limits cannot be allowed to change more frequently than at a predefined time interval (e.g., 1 min), which corresponds to the control period of the control strategies to be designed in Chapter 4. Further details on these issues are provided in Section 4.7.

Chapter 4

Feedback MTFC Design

To some extent, in most of our behaviour, we act in order to receive feedback and most of our actions are initiated by feedback. Life without feedback would be rather boring.

P. Albertos and I. Mareels [2]

The relevance and efficiency of the control strategy largely determines the efficiency of the overall control system. Therefore, whenever possible, control strategies should be designed with care, via application of powerful and systematic methods of optimization and automatic control, rather than via questionable heuristics.

M. Papageorgiou [52]

In this chapter, three feedback controllers are elaborated based on the MTFC concept introduced in Chapter 3. Variable speed limits are used as an MTFC actuator for the feedback controllers. The MTFC feedback control problem is introduced in Section 4.1. Then, based on the analysis of the VSL impact and on the traffic flow modelling of Chapter 2, a control design model is developed in Section 4.2. The control design model is used in Sections 4.3, 4.4, and 4.5 as the basis for the design of each of the three feedback controllers. In Section 4.6 some important characteristics of the designed controllers are highlighted. The application of MTFC via VSLs brings along several practical aspects that are discussed in Section 4.7. Finally, two possible extensions of the proposed feedback controllers are outlined in Section 4.8.

4.1 Control Setting and Control Goal

A single-input-single-output (SISO) control design model has one input, in this thesis the VSL rates $b(k)$ applied upstream of a bottleneck according to Figure 3.7; and one output, in this thesis the traffic conditions at the location where the congestion is formed. The resulting feedback control law uses real-time measurements of the output (and possibly of other internal process variables) to calculate in real time, within a closed loop, appropriate values for the input, so as to maintain the output close to a pre-specified reference or set value.

In the process of Figure 3.7, the control goal is to operate the VSLs appropriately, so as to maintain the flow q_{out} through the bottleneck close to capacity. However, similarly to the well-known feedback ramp metering strategy ALINEA [60, 61], it is preferable to consider as an output the bottleneck density ρ_{out} (or the corresponding occupancy), in which case the related set value, that leads to throughput maximisation, is the critical density ρ_{cr}. The usage of the flow q_{out} as a system output is discarded for two reasons; first, due to the non-linearity of the fundamental diagram (Figure 2.2(a)), the flow q_{out} may take the same value under undercritical or overcritical conditions, which would clearly require different control actions; second, the usage of a fixed flow capacity set value is not appropriate, since the actual flow capacity may vary from day to day by as much as 10 percent (which is in the order of the capacity drop that exploitation is being attempted) (see Section 3.4.3); in contrast, the critical density is more stable, even under different lighting or weather conditions [63].

In conclusion, the objective is to find a SISO control design model for the process of Figure 3.7, with input $b(k)$ (the VSL rates applied at the VSL application area) and output $\rho_{\text{out}}(k)$ (the bottleneck density) or, in practice, the corresponding occupancy as in ALINEA.

4.2 Control Design Model

Traffic flow systems are highly non-linear, and feedback control design based on non-linear models, like the one presented in Section 2.3, may be difficult and lead to complex feedback laws. In fact, it is quite typical in control engineering to develop a simple "control design model" of the process under control, which leads to an accordingly simple feedback law. Due to their intrinsic robustness properties, appropriately designed feedback control strategies are then suitable, even when applied (in simulation) to more elaborate process models and, most importantly, when actually applied to the real process. Following this line of development, a simple linear model of the VSL impact on traffic flow is derived in this section via linearisation around an operation point, i.e., a high-flow but uncongested traffic state upstream of the bottleneck.

Section 2.2.4 listed four aspects of the effect of VSLs on aggregate traffic flow behaviour. Aspects (i) and (iv) play a major role in the specification of the desired control design model, and are discussed next, while aspects (ii) and (iii) are further discussed in Section 4.7.

Recall that aspect (i) induces a temporary flow reduction and can be exploited to hold back traffic flow to retard the onset of congestion at downstream bottlenecks. Aspect (iv), by its turn, yields a more durable flow reduction that can be used to specify a controlled flow upstream of a potential bottleneck so as to avoid its activation.

The aspects (i) and (iv) cannot be associated to a specific VSL range in a motorway, since they depend also on the arriving demand q_{in}. Aspect (i) will be observed more often for higher VSL rates and lower arriving demands, while aspect (iv) will show up for lower VSL rates and higher arriving demands. However, as long as the arriving demand is sufficient for (iv) to occur, the VSL-induced capacity (and hence the controlled outflow q_{c}) will be the same for the same VSL rate.

The two aspects mentioned above can be observed in the input-output behaviour of the system, i.e., in the flow responses (output) to a step variation of the VSL rate b (input)[1]. More specifically, a motorway stretch as in Figure 3.7 is simulated by use of METANET with appropriate constant arriving demand q_{in}, and an input step change $\Delta b < 0$ of the VSL rate is applied at time 0, i.e., a switch from $b = 1$ to $b = 1 + \Delta b$ (Figure 4.1(a)). Figure 4.1(a) also includes the corresponding "step responses", i.e., the related flows q_{c} and q_{out} calculated by METANET, whereby q_{c} is measured immediately downstream of the VSL application area, while q_{out} corresponds to the flow measured in the downstream bottleneck area. In the middle case of Figure 4.1(a), the arriving demand q_{in} was chosen lower than the VSL-affected capacity (aspect (i)), and hence q_{c} is seen to be initially reduced (due to the transition of Figure 2.4(a)) but to eventually recover fully. On the other hand, q_{in} was chosen higher than the VSL-affected capacity for the right case of Figure 4.1(a) (aspect (iv)), and hence q_{c} is seen to recover only partially after the state transition.

The dynamic behaviour of flow q_{c} (with partial or total recovery) can be modelled approxi-

[1]Input step response is a typical procedure in Control Engineering to deduce the main characteristics of the process under control so as to design an appropriate controller.

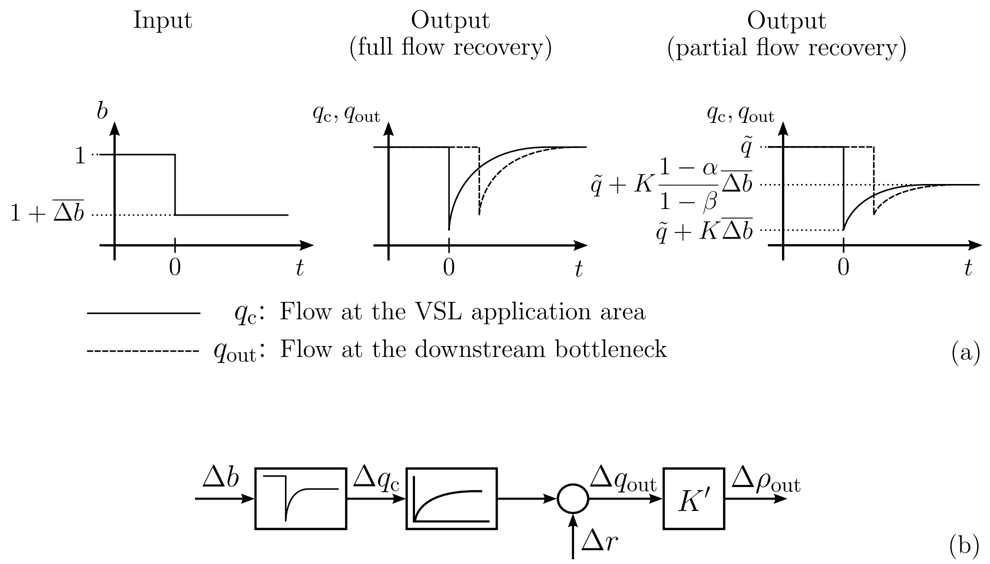

Figure 4.1: Simplified system modelling: (a) step response with temporary (aspect (i)) and lasting (aspect (iv)) flow reduction; (b) system block diagram.

mately via a linear discrete-time z-transfer function (input-output relation):

$$\frac{\Delta q_c(z)}{\Delta b(z)} = K\frac{z-\alpha}{z-\beta} \tag{4.1}$$

where α, β, $K > 0$ are model parameters to be specified appropriately; z the discrete-time complex variable [21]. After proper transformation from the frequency domain to the time domain (inverse z-transform), (4.1) yields the following difference equation:

$$\Delta q_c(k+1) - \beta\Delta q_c(k) = K\Delta b(k+1) - \alpha K\Delta b(k). \tag{4.2}$$

Since $\Delta q_c(k) = \Delta b(k) = 0$ for $k < 0$, and $\Delta b(k) = \overline{\Delta b}$ for $k \geq 0$, the final value theorem [21] applied to (4.2) (or (4.1)), yields for the stationary flow value $\overline{\Delta q}_c = \Delta q_c(\infty)$:

$$\Delta q_c(\infty) - \beta\Delta q_c(\infty) = K(1-\alpha)\overline{\Delta b} \Rightarrow \overline{\Delta q}_c = \Delta q_c(\infty) = K\frac{1-\alpha}{1-\beta}\overline{\Delta b}. \tag{4.3}$$

Since the system is non-oscillating (Figure 4.1(a)), (4.1) must have $0 \leq \beta \leq 1$. In the case of full flow recovery, $\overline{\Delta q}_c = 0$, hence, from (4.3), $\alpha = 1$. In the case of partial flow recovery, it can be deduced from Figure 4.1(a) that $K\overline{\Delta b} < K\overline{\Delta b}(1-\alpha)/(1-\beta) < 0$, which implies $\alpha > \beta$ and $\alpha < 1$. Thus, the linearised model parameters are, in summary, $K > 0$ and $0 < \beta < \alpha \leq 1$.

Now, consider the q_{out}-response at the bottleneck area. Clearly, in absence of congestion mounting from downstream, q_{out} is a smoothed and delayed version of q_{c}. This behaviour can be modelled as a simple first-order system with a time-constant roughly equal to the time necessary for the related kinematic wave that leaves the controlled link to reach the downstream bottleneck location, i.e.,

$$\frac{\Delta q_{\text{out}}(z)}{\Delta q_{\text{c}}(z)} = \frac{\tau}{z+\tau-1}. \tag{4.4}$$

The desired final output at the bottleneck area, however, is the density (or occupancy). The transition from flow Δq_{out} to density ρ_{out} is enabled by a linearisation of the fundamental (flow-density) diagram around the critical density, as also done in the design of the ramp-metering feedback control strategy ALINEA [60], i.e.:

$$\frac{\Delta \rho_{\text{out}}}{\Delta q_{\text{out}}} = K'. \tag{4.5}$$

The final system transfer function is given by multiplying (4.1), (4.4) and (4.5):

$$\frac{\Delta \rho_{\text{out}}(z)}{\Delta b(z)} = KK'\frac{\tau}{z+\tau-1} \cdot \frac{z-\alpha}{z-\beta}. \tag{4.6}$$

The complete system is depicted in Figure 4.1(b), the first block corresponding to (4.1), the second to (4.4), and the third to (4.5), while Δr represents a possible external disturbance to the system, such as the ramp inflow in case of merge bottlenecks, or an off-ramp outflow, or both.

In principle, specific values of the model parameters α, β, τ, K and K' could be easily derived, e.g., via graphical methods, for a specific simulated input step response. However, since the system is intended to operate for the whole admissible VSL range and under different traffic conditions, it is rather pointless to specify precise parameter values. Instead, realizing that the values of α, β, τ, K and K', may vary in dependence of the application conditions (e.g., the length of the application area, the length of the acceleration area) of each installation and of the traffic conditions, a feedback controller that is robust enough to achieve the control goal efficiently under any realistic conditions must be designed. This is a feasible endeavour in view of the intrinsic robustness properties of appropriately designed feedback controllers.

4.3 Cascade Feedback Controller Design

The mentioned parameter variations of the linear control design model, which stem from the non-linear characteristics of the traffic flow model (and actual traffic flow process), call for a careful and appropriate feedback control design. Otherwise, the resulting closed-loop system may not be sufficiently damped and may even become unstable [44]. Although a simple dead-beat feedback controller could be immediately designed for (4.6), at an initial stage the parameter variations imposed difficulties in the tuning of appropriate controller gains, and the resulting control loop could be, depending on the prevailing conditions, too slow or oscillating or even unstable. Therefore, a less direct controller design approach is pursued in this section and two potentially simpler approaches are developed in the sections that follow.

Cascade control, widely used in the control of chemical processes [73, 79], makes use of a second (or more) feedback measurement(s) and divides the process by the use of nested control loops, one for each measurement, that have their references determined by the respective outer loops. Figure 4.2 depicts a typical two-loop cascade control structure for a SISO system with input u, output y_1, intermediate output y_2, and respective reference values r_1 and r_2 and control errors e_1 and e_2. Cascade control is suitable when the secondary process G2 in the figure is subject to non-linearities or gain variations, which are then isolated from the primary loop; while the primary process G1 presents non-minimum phase behaviour or delay. Closing the loop around G2 also allows for disturbance rejections in G2 before they affect G1. From the previous section it is clear that the system at hand matches several of these characteristics. Furthermore, the adoption of cascade control is rather intuitive given the similarity, as will be shown next, of the present system with chemical processes where, very often, flow control loops are cascaded with other control loops [74, 79]. Finally, a well-tuned cascade controller will respond faster, compared to a single monolithic controller, and provides for better damping and increased robustness to uncertainties, e.g., process parametric variations [48, 73].

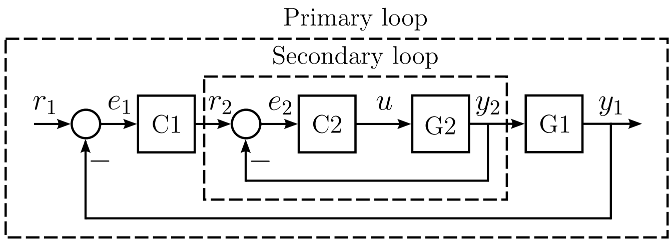

Figure 4.2: Two-loop feedback cascade control structure.

From the MTFC concept with the use of VSLs described in Section 3.5 and the resulting linear model of the system in Section 4.2, it can be seen that the system can be divided in a VSL-versus-flow dynamics part (first block in Figure 4.1(b)), followed by a flow propagation part (second block in Figure 4.1(b)), that also affects the density in the bottleneck area (third block in Figure 4.1(b)), similarly to some controlled chemical processes. Considering the first block as the secondary process and the second and third blocks as the primary process, the appropriate process division for applying cascade control is obtained.

The cascade control structure in Figure 4.2 is reproduced in Figure 4.3 with transfer function blocks and variables corresponding to the MTFC feedback cascade controller structure designed in this section. In Figure 4.3, the secondary loop is affected by the VSL rate b delivered by the secondary controller that will determine the outflow q_c of Figure 3.7. This flow is measured immediately downstream of the application area and is fed back and compared to the desired (reference) flow $\hat{q}_c$ delivered by the primary controller. The primary loop uses the measured density ρ_{out} (or occupancy) at the bottleneck area and compares it with the set-point density $\hat{\rho}_{out}$ defined by the operator (which should be set equal to ρ_{cr} for throughput maximisation).

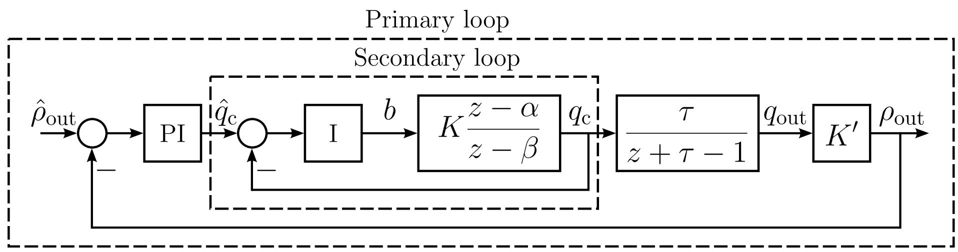

Figure 4.3: MTFC feedback cascade controller structure using VSLs as an actuator.

The usual procedure for controller design and tuning in cascade controllers is to start from the most internal loop and move, one by one, to the most external loop. In what follows, first the controllers will be designed appropriately before proceeding with the tuning of the involved controller parameters.

The secondary controller of Figure 4.3 is designed as an integral (I) controller with transfer function:

$$\frac{b(z)}{e_q(z)} = \frac{K_I}{z-1}, \tag{4.7}$$

or, in the time domain,

$$b(k) = b(k-1) + K_I e_q(k) \tag{4.8}$$

where K_I is the integral gain of the controller and $e_q(\cdot) = \hat{q}_c(\cdot) - q_c(\cdot)$ is the flow control error, given per lane. Note that, for increasing values of the controller gain K_{I}, the closed-loop pole originating from the controller pole at 1.0 moves along the real axis of the z-plane root locus towards the system zero at α; while the closed-loop pole originating from the open-loop pole β moves along the real axis in the direction of $-\infty$. Thus, a sufficiently large controller gain K_{I} can be obtained so that the open-loop system zero at α is neutralised or cancelled by the closed-loop pole moving towards it, while the other closed-loop pole, which will dominate the closed-loop response, remains in the right-half plane, i.e., the closed-loop system is stable and damped. This yields a first-order dominant closed-loop response that is faster than the open-loop system. Obviously, when the zero at α equals 1.0 (flow recovers fully), the secondary controller cannot guarantee zero stationary error. However, this is deemed of minor importance, since full flow recoveries will usually occur in the early stage of the control action, i.e., at a transient period, while the primary controller is updating its output (the reference of the secondary controller) so as to drive the system closer to the reference value of the main output.

According to the outlined controller design of the secondary loop, the resulting dynamics of the internal loop and primary process can be approximated by a second-order system. Hence, the primary loop controller is specified to be a Proportional-Integral (PI) controller (Figure 4.3), which provides for a desired zero steady-state error, while keeping a satisfactory transient response and disturbance rejection. The PI-type controller reads:

$$\frac{\hat{q}_{\mathrm{c}}(z)}{e_{\rho}(z)} = \frac{(K'_{\mathrm{P}} + K'_{\mathrm{I}})z - K'_{\mathrm{P}}}{z-1} \tag{4.9}$$

or, alternatively:

$$\hat{q}_{\mathrm{c}}(k) = \hat{q}_{\mathrm{c}}(k-1) + (K'_{\mathrm{P}} + K'_{\mathrm{I}})e_{\rho}(k) - K'_{\mathrm{P}}e_{\rho}(k-1) \tag{4.10}$$

where K'_{I} and K'_{P} are the integral and proportional gains of the controller, respectively, and $e_{\rho}(\cdot) = \hat{\rho}_{\mathrm{out}} - \rho_{\mathrm{out}}(\cdot)$ is the density control error.

Tuning of the controllers was performed with the aid of the METANET simulator described in Section 2.3, using different traffic flow conditions and for the whole operating range of VSLs. The methodology adopted was the zone-based procedure, as described in [18]. The idea behind this methodology is to decouple the controller gain tuning so that each gain can be adjusted individually. This is rendered possible by assuming that each gain is dominant over a certain frequency zone. Higher frequency zones are adjusted first. For the PI case, the proportional gain K'_{P} is tuned first, while the integral gain K'_{I} is set to zero. The starting value for K'_{P} is a low value that guarantees stability; then K'_{P} is increased and the step response evaluated until a (first) acceptable overshoot is obtained. Next, after K'_{P} is obtained, K'_{I} is increased from zero until the response exhibits a (second and final) overshoot value.

For the cascade structure, the secondary controller is tuned first, with the primary controller disconnected. Since the real system is non-linear and subject to parameter variations, it must be tuned for the worst case. After tuning the secondary controller, the primary controller is connected and tuned. The tuning procedure furnished the following gains for the cascade controller, which are used in the simulations of Chapter 6: $K_{\mathrm{I}} = 0.0007$ h/veh/lane for the secondary controller; and $K'_{\mathrm{I}} = 3.0$ km/h/lane and $K'_{\mathrm{P}} = 50.0$ km/h/lane for the primary controller. The gain values obtained for the primary controller were confirmed by the use of the SIMC PID tuning method [75]. It is expected that these regulator parameter values are quite representative and robust for several real situations; nevertheless, modern automatic fine-tuning tools [39] could prove useful in field implementations.

Whenever the secondary controller furnishes a VSL rate $b(k)$ in (4.8) that exceeds one of its bounds $b(k) \in [b_{\min}, 1]$, i.e., saturates, the value of $b(k)$ must be truncated to the respective bound and used as $b(k-1)$ in (4.8) for the next control period to avoid the wind-up effect. The same applies for $\hat{q}_{\mathrm{c}}(k)$ in (4.10) with $\hat{q}_{\mathrm{c}}(k) \in [\hat{q}_{\min}, \hat{q}_{\max}]$ with appropriately fixed bounds $\hat{q}_{\min}$, $\hat{q}_{\max}$. In addition, when the secondary controller has reached its limits, it is unable to respond to commands $\hat{q}_{\mathrm{c}}(k)$ from the primary controller, while the primary controller would, nevertheless, keep moving the command attempting to correct the output error. This behaviour would configure a wind-up for the primary controller, although its own limits are not reached [74]. Therefore, whenever the secondary controller is not able to respond to the primary controller, because it is saturated, the primary controller's output is only allowed to change if it de-saturates the secondary controller.

4.4 Lookup Feedback Controller Design

An alternative design for the controller presented in the previous section is to drop its secondary loop and replace the secondary controller by use of a non-linear lookup table as depicted in Figure 4.4. The lookup table reflects, roughly, the (stationary) relationship of flow capacity versus VSL rates. The solid line in Figure 4.5 corresponds to the VSL-induced capacity obtained from (2.10) with the parameter values used in Figure 2.6 (Section 2.3.3), when there is no increase of capacity. Thus, the lookup table is a static non-linearity that is

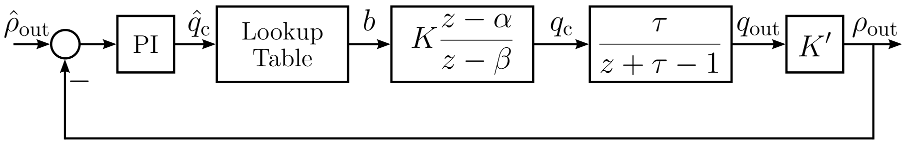

Figure 4.4: MTFC feedback lookup controller structure using VSLs as an actuator.

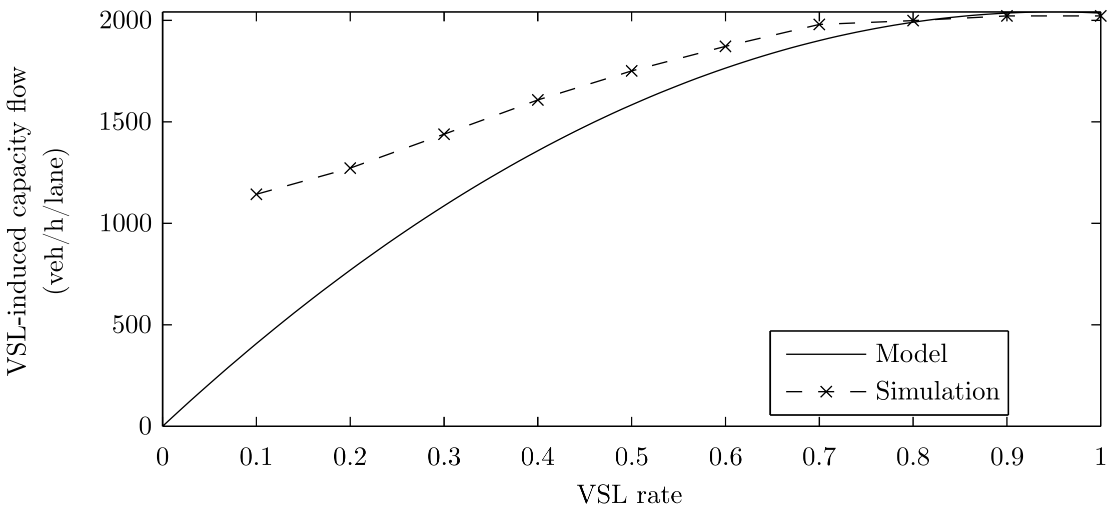

Figure 4.5: Modeled and simulated VSL-induced capacity flow.

fed with the PI controller output $\hat{q}_{\text{c}}$ to deliver the desired VSL rate b that will determine the flow q_{c} leaving the application area. Such a structure can be viewed as a special case of gain scheduling [70].

A similar approach was adopted in [95] by deriving a non-linear function that maps the flow delivered by an ALINEA (I-type) controller into a corresponding speed limit. However, as mentioned before, the lack of an acceleration area is the likely reason for obtaining only marginal improvements.

The design of the lookup table within a simulation environment such as METANET (Section 2.3) is quite straightforward. A simple motorway stretch with no on-/off-ramps and with a VSL application area is simulated, with an upstream demand equal to the (factual) capacity flow of the stretch. Under these conditions, any applied VSL rate acts according to aspect (iv) of Section 2.2.4 and leads (in the steady state) to a corresponding VSL-induced capacity outflow. Thus, a set of admissible VSL rates is considered, and each of them is applied to the application area, allowing sufficient time for the system to reach steady-state conditions, before the corresponding stretch outflow is recorded. The dotted line in Figure 4.5 corresponds to the VSL-induced capacity obtained from this simulation-based exercise (along with linear interpolation of points corresponding to specific VSL rate values). Note that the difference of both curves in Figure 4.5 is due to the dynamic terms included in the simulator (2.20), but not included in (2.10).

Taking into account discrete admissible VSL values, the lookup table may then be constructed from Figure 4.5 via appropriate discretisation, as in Figure 4.6, to be used in the Lookup Controller for the investigations of Section 6.2.

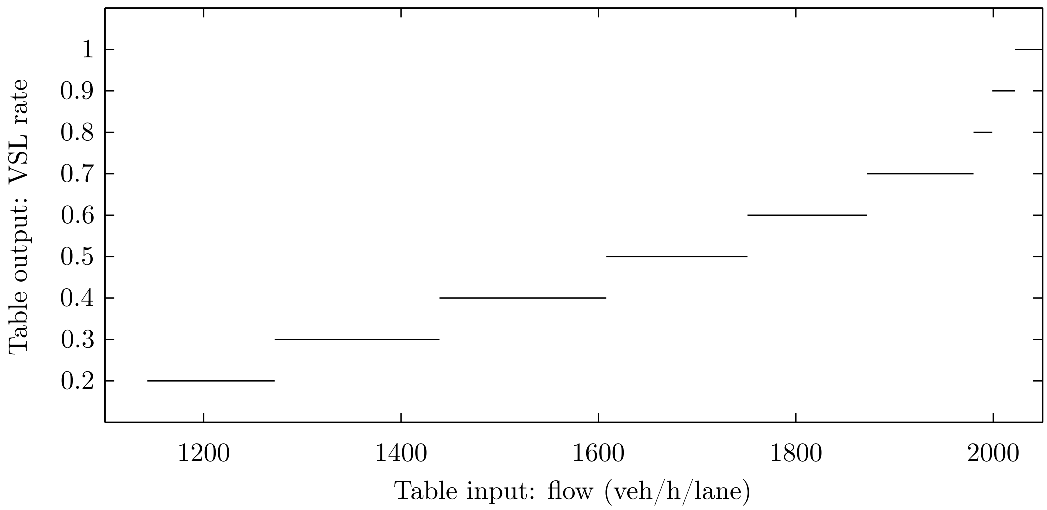

Figure 4.6: Lookup table.

In practice, the design of the lookup table may be more challenging, since the aforementioned experiments can hardly be effectuated; hence, one may have to rely on more or less accurate estimations, based on simulation and/or any available data with specific VSLs. When the system starts operating, a fine-tuning of the lookup table may be performed as new data become available. It should be emphasised that the (practically inevitable) errors resulting from the ignored dynamics between b and q_c, from ignoring of aspect (i) of Section 2.2.4, from the open-loop nature of the lookup table and from any other error sources may be handled by the feedback controller if it proves sufficiently robust; the robustness of the Lookup Controller to mismatches in the lookup table is discussed in Section 4.7.8 and investigated in Section 6.2.5.

The closed-loop reference-output behaviour of the secondary loop in the Cascade Controller case is reasonably fast, as is the non-linear compensation provided by the lookup table; therefore, the PI controller in use in the Cascade Controller is deemed suitable for the Lookup Controller as well. Surprisingly, any effort of re-tuning the PI controller in the lookup case resulted in only marginal improvements or undesired (non-smooth) outputs from a traffic operation point of view; hence the same gains of the cascade primary controller are used for the Lookup Controller in Section 6.2.

Similarly to the Cascade Controller, whenever the PI controller furnishes an ordered flow $\hat{q}_c(k)$ in (4.10) that exceeds one of its bounds $\hat{q}_c(k) \in [\hat{q}_{\min}, \hat{q}_{\max}]$, i.e. saturates, the value of $\hat{q}_c(k)$ must be truncated to the respective bound and used as $\hat{q}_c(k-1)$ in (4.10) for the next control period to avoid the wind-up effect.

4.5 PI Feedback Controller Design

Field implementations call for simple and efficient systems that would expedite their application. Realizing that the simulated capacity flow curve (dotted line) in Figure 4.5 is quite flat and could be, to some extent, approximated by a straight line (particularly for low VSL rates), an even simpler linear PI Controller may be envisaged for local MTFC via VSLs. In this case, the controller structure is similar to the one in Figure 4.4, albeit with the lookup table block dropped, i.e., the PI controller, with appropriate gains, delivers directly the VSL rate b:

$$b(k) = b(k-1) + (\hat{K}_\mathrm{P} + \hat{K}_\mathrm{I})e_\rho(k) - \hat{K}_\mathrm{P} e_\rho(k-1) \tag{4.11}$$

where the variables are as defined previously, and $\hat{K}_\mathrm{P}$ and $\hat{K}_\mathrm{I}$ are the proportional and integral gains of the controller, respectively. The controller gains in this case should be roughly the same gains used for the Lookup Controller, scaled by the slope of the line used to approximate the VSL-induced capacity curve (dotted curve in Figure 4.5) which is, approximately, 0.0007. Some minor fine-tuning was nevertheless performed around the scaled values via trial-and-error, and the final gains obtained are $\hat{K}_\mathrm{I} = 0.003$ km/veh/lane and $\hat{K}_\mathrm{P} = 0.04$ km/veh/lane.

Similarly to the Cascade and Lookup Controllers, whenever the PI controller furnishes a VSL rate $b(k)$ in (4.11) that exceeds one of its bounds $b(k) \in [b_{\min}, 1]$, i.e. saturates, the value of $b(k)$ must be truncated to the respective bound and used as $b(k-1)$ in (4.11) for the next control period to avoid the wind-up effect.

4.6 Some Characteristics of the Designed Controllers

Some significant characteristics of the designed controllers should be emphasised at this point:

- The Cascade Controller makes use of two real-time measurements of flow q_c and density ρ_{out} (or occupancy) according to Figure 4.3 to execute (4.8) and (4.10). The Lookup and PI Controllers make use of one real-time measurement of density ρ_{out} (or occupancy) according to Figure 4.4 to execute (4.8) and (4.11), respectively. There are no other requirements, in particular no measurements of the arriving demand q_{in} or of any on-ramp or off-ramp flows that may exist between the VSL application area and the downstream bottleneck. All these disturbances are automatically rejected by the feedback loops. Note that stochastic measurement errors have a minor impact on the feedback control efficiency (as, e.g., witnessed in many field applications of ALINEA [61]).

- The feedback controllers do not make use of any model. The only quantity needed for their application is the density set value $\hat{\rho}_{\text{out}} = \rho_{\text{cr}}$ (for throughput maximisation) which can be pre-specified, as frequently done for the ALINEA ramp metering regulator, albeit taking into account that the application of a VSL at the downstream bottleneck may increase its value according to Figure 2.4(b).

- The designed feedback regulators deliver VSL rates $b \in [b_{\min}, 1]$ which are convenient for use in the simulation investigations of Chapter 6. For field application, the controllers can be readily modified (i.e., multiplied with v_{f} according to (2.6)) to deliver VSLs in km/h for direct display.

- In case of limited driver compliance to the displayed VSL, the corresponding q_{c} will be higher than at full compliance. However, thanks to the integral term in the controllers, this would lead automatically to even lower VSLs, until the required level of q_{c} is actually reached. Thus, limited compliance would have a minor impact on the feedback dynamics (as red-light violations have a minor impact on ALINEA), but could lead earlier to a controller saturation, i.e., to earlier reaching of the lower bound $b_{\min}$ (where applicable).

- Parts of the designed controllers may be used also for different actuators that would enable MTFC (with appropriate retuning). For example, if mainstream traffic lights would be used for MTFC instead of VSLs (mainline metering), $\hat{q}_{\text{c}}$ could be directly and promptly implemented, similarly to ramp metering installations [57]. In this case a lookup table or a mathematical function could be used to translate the ordered flow into green times, similarly to the Lookup Controller. In fact, the outer PI-controllers of Figures 4.3 and 4.4 are identical to the one proposed in [82] for ramp metering with a distant downstream bottleneck, which controls essentially the same flow propagation process as in the outer loop of Figure 4.3. Remarkably, the controller parameters tuning in this thesis led to very similar values with those in [82] despite using different tuning procedures. Moreover, it is very encouraging for the present control design, that the distant-bottleneck PI ramp metering controller was successfully field-implemented, see [68].

4.7 Practical Application Aspects

The field application of MTFC via VSLs calls for the consideration of the practical implementation aspects mentioned in Section 3.5, along with an additional issue of interest, the control period for VSL switching.

4.7.1 Discrete VSLs

The designed feedback regulator delivers real-valued VSL rates while only discrete VSL values, out of a pre-specified set of such values, can be displayed in practice. For example, a possible set of allowed speed limits could be $VSL \in \{40, 50, \ldots, 120\}$ km/h, but, for convenience, a set of allowed discrete VSL rates $b \in \{0.2, 0.3, \ldots, 1.0\}$ is defined for use in the simulation investigations. Thus, the VSL rate to be applied is obtained by rounding the VSL rate $b(k)$ given by the control strategy (4.8) in the Cascade Controller case or by the control strategy (4.11) in the PI Controller case to the closest allowed discrete VSL rate, while the Lookup Controller has discrete VSL rates naturally defined in the design of the corresponding lookup table. It is important to note that the rounded value of $b(k)$ is used only for display, not as $b(k-1)$ in (4.8) or (4.11).

4.7.2 Limited VSL Time-Variation

The difference between two consecutive speed limits at the same VSL sign can be limited to a pre-specified value, e.g. 20 km/h. Again, the VSL rate variation is limited instead, by disallowing a difference of more than 0.2. Similarly to when discrete VSL values are used, the limited value of $b(k)$ is used for display only.

4.7.3 Limited VSL Space-Variation

The designed feedback controllers deliver appropriate VSLs to be displayed sufficiently upstream of the bottleneck area, so as to create an appropriate mainstream flow q_c according to Figure 3.7. This creates a controlled congestion (Figure 3.7) whose tail may propagate upstream. Thus, vehicles arriving to the congestion tail will have to decelerate to join the congestion, which may be deemed a safety risk. Although (for reasons mentioned in Chapter 3) the related speed gradient (and hence the safety risk) is lower in the MTFC case compared to the "natural" congestion without control, it is advisable to further reduce the safety risk by appropriate activation of VSLs upstream of the controlled congestion. Clearly, this calls for availability of VSL gantries at reasonable spacing (e.g., every 1–2 km) on the upstream part of the motorway, i.e., upstream of the gantries that implement the regulator's VSL decisions. The basic idea of operation of these upstream VSLs is to limit the space/time gradients of vehicle speeds along and upstream of the controlled congestion to reduce the safety risk (see also Section 6.1.7). The following rules may be applied to the upstream VSLs via a corresponding algorithm:

(i) No gantry displays a lower VSL than the next downstream gantry. The difference between the VSLs displayed at two consecutive gantries is limited to, e.g., 20 km/h, as discussed in Section 4.7.2.

(ii) The displayed VSL should not be much higher than the (measured) mean speed around the corresponding gantry. This is in order to avoid situations where drivers are forced (due to the controlled congestion) to drive at a relatively low speed while facing much higher speed limits displayed.

(iii) Starting from the regulator's VSL and proceeding in upstream direction, the VSL of each gantry is increased, compared to the VSL of the next downstream gantry, by, e.g., 20 km/h, unless the limits (i) or (ii) apply.

These rules lead to equal VSL displays along the motorway stretch occupied by the controlled congestion; while vehicles driving towards the congestion tail will encounter gradually decreasing VSLs that will "guide" them to a safe joining of the controlled congestion.

4.7.4 Downstream VSLs

Vehicles exiting the controlled congestion should accelerate (if necessary) and cross the downstream bottleneck at a stationary speed. To "guide" drivers accordingly, a VSL could be activated at the acceleration and bottleneck areas. For example, a constant VSL rate of 0.9 may be applied in these areas, whenever MTFC via VSLs is active. This action might even improve the system's performance in cases where the motorway capacity can be increased by the display of moderate speed limits, see Section 4.7.7. Independent of the possibility of capacity increase or not, a VSL applied at the bottleneck area will shift the location's critical density to higher values according to aspect (ii) of Section 2.2.4. Therefore, this should be taken into account when determining the set-point for the feedback control strategies.

4.7.5 Downstream Congestion

For the beneficial MTFC effect of increasing the bottleneck throughput it is necessary to have free-flow conditions downstream of the bottleneck. If there is another congestion (controlled or not) mounting from downstream and reaching the bottleneck, then the throughput is dictated by the mounting congestion and MTFC actions become obsolete. Thus, if appropriately placed speed detectors indicate a congestion mounting from downstream, then the MTFC area becomes essentially part of a downstream congestion and, hence, all included VSL gantries should operate as described in Section 4.7.3.

4.7.6 VSL Control Period

Some directions for the choice of the control time step of discrete-time feedback controllers have been established in Control Engineering since long. For the feedback MTFC via VSLs, this choice determines the frequency of posted VSL changes which should be limited. In this thesis, except where otherwise stated, the control period is chosen as $T_\mathrm{c} = 60$ s. This control period seems to be suitable for practical purposes as it is quite widespread in current VSL installations in various countries. In fact, even if a VSL panel is visible from few hundred meters upstream, it is very unlikely that a driver will see the same panel changing the speed limit more than once, something that could be deemed as confusing. Note, however, that longer control periods may be desired or required by traffic operators and policy makers. Therefore, the choice of the control period and its effect on the controllers' performance is specifically investigated and discussed in Section 6.2.3.

4.7.7 Increase of Capacity

Another practical issue is related to aspect (iii) of Section 2.2.4 with respect to the possibility of capacity increase due to the application of VSLs (as, e.g., in Figure 4.7 with parameters of Section 6.2.4), since capacity increases were indeed observed in some occasions and locations [63]. As a matter of fact, additional benefits can be achieved by the use of MTFC via VSLs in the case of actual capacity increase for some VSL values, and the designed controllers should, preferably, be able to take advantage of this possibility. A preliminary study has demonstrated the application of MTFC via VSLs with capacity increase via an optimal control approach [66] and this issue is further investigated in Section 6.2.4 for the three feedback controllers.

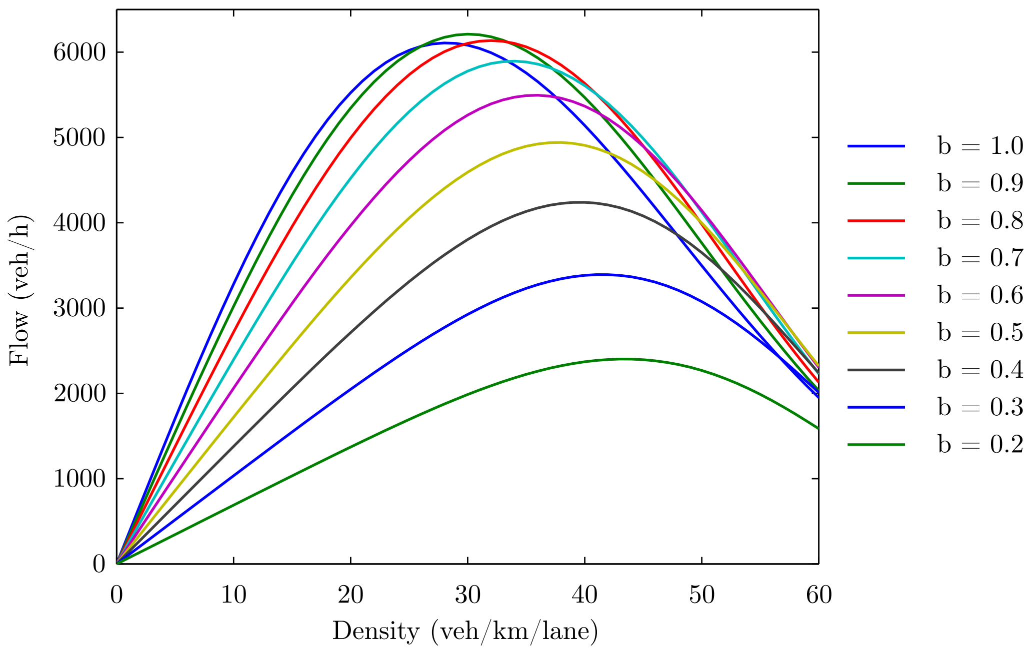

Figure 4.7: Fundamental diagram for different VSL rates, with increase of capacity: $b = 1.0$ means no VSL applied, decreasing b-values correspond to decreasing VSLs.

4.7.8 Robustness of the Lookup Controller

It was seen earlier that the design of the lookup table must be performed empirically based on data sets and operator experience. This leads, unavoidably, to design inaccuracies, particularly in the initial stage of the table design. Thus, the Lookup Controller is also evaluated in Section 6.2.5 with respect to its robustness to mismatches in the lookup table.

4.8 Further Extensions

In this section, further extensions of the feedback controllers designed in this chapter are outlined. These extensions address some of the MTFC-related issues discussed in Section 3.4.

First, the MTFC application concept of Section 3.5 is applied to two merging motorways in Section 4.8.1. To this end, the MTFC feedback controllers developed in Section 4.3 could be extended such that the VSL control action is introduced to both motorways so as to balance the respective experienced delays while maintaining capacity flow at the merge area. An outline of the extension of the MTFC feedback cascade controller for two merging motorways is presented.

Second, the local integrated control problem, involving MTFC via VSLs and ramp metering is addressed in Section 4.8.2. In this case, any of the feedback controllers developed in Section 4.3 could be extended such that the control action is shared by applying VSLs at the mainstream while traffic lights are applied at the merging on-ramp. An outline of the extension of the MTFC feedback cascade controller for the integrated case is presented.

4.8.1 Feedback MTFC via VSLs for Two Merging Motorways

The case of two merging motorways, as in Figure 3.3, is considered. A merge congestion (and hence a capacity drop) will appear in absence of control if the sum of the arriving flows exceeds the bottleneck capacity as described in Section 3.3.2. If the MTFC feedback concept of Section 3.5 is applied to one motorway only, maximum bottleneck throughput may be achieved, but a corresponding controlled congestion may be created only on the controlled motorway, while vehicles on the other motorway may have free access to the merge area, which may be deemed unfair. A more balanced approach can be achieved if MTFC is applied to both merging motorways, via separate VSL for each of them and corresponding controllable mainstream flows $q_{1,\mathrm{c}}$ and $q_{2,\mathrm{c}}$ (Figure 3.3). This creates an additional degree of freedom that may be exploited to enable a predefined ratio of experienced delays for vehicles arriving from the two motorways.

As for a single motorway, the idea is to specify flow values $q_{1,\mathrm{c}}$ and $q_{2,\mathrm{c}}$ upstream of the bottleneck location in order to keep the bottleneck density ρ_{out} around the critical density, i.e., maximise the bottleneck throughput. To this end, the feedback cascade control structure of Figure 4.3 is extended to consider two VSL rates and a split-range-like control scheme [79] as depicted in Figure 4.8. The primary loop is almost identical as in Figure 4.3 but delivers a reference $\hat{q}_c$ for the total bottleneck inflow that is split to $\hat{q}_{1,c}$ and $\hat{q}_{2,c}$, which are handled (as in Figure 4.3) by two respective secondary loops to produce the real respective outflows that enter the bottleneck area.

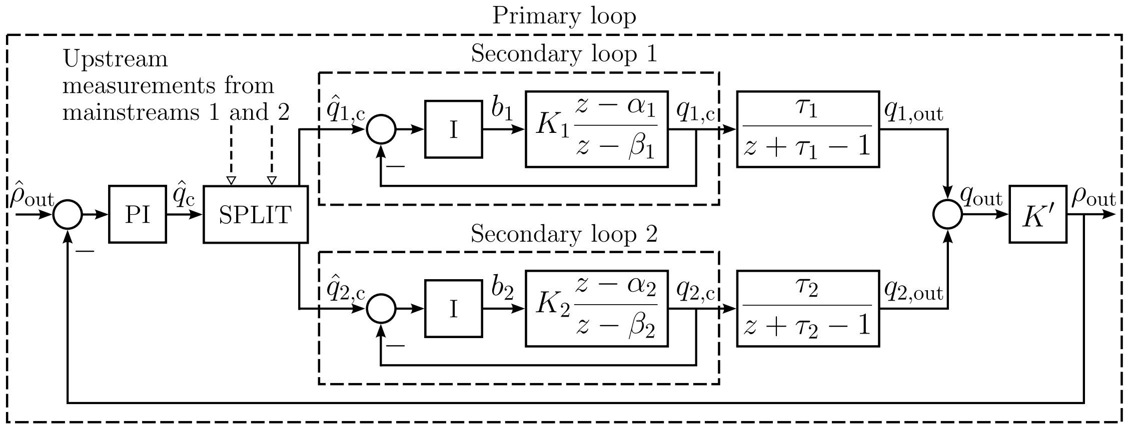

Figure 4.8: Two merging motorways MTFC feedback cascade controller structure using VSLs as an actuator.

The splitting of $\hat{q}_c$ may be effectuated in a fixed way (e.g. according to the merging motorway capacities); or in a data-dependent way (e.g. according to both arriving demands); or in other possible ways that materialise a specific operational policy, e.g. delay balancing (or any other prescribed delay ratio) for vehicles crossing the two respective controlled congestion areas of Figure 3.3. Delay balancing is the locally most equitable splitting policy and more elaborate to implement compared to other mentioned possibilities. Delay is defined as the actual travel time minus the travel time under free-flow conditions (the latter having a fixed value for a specific motorway stretch). Delay balancing calls for availability of real-time estimates of delay of the vehicles exiting the controlled congestions of each merging motorway. The delay experienced by exiting vehicles can be readily calculated if mean speed detectors are available upstream of the flow control point at a sufficient resolution (e.g., 500 m) and suitable methods of travel time or delay calculation [65] may be used, otherwise a suitable estimation scheme may be employed [83], see dashed lines entering the SPLIT box in Figure 4.8.

The split control is designed to achieve the balancing of experienced delays by drivers on both motorways by the use of a PI controller. To reduce the burden of the PI controller and achieve smoother control reactions a feed forward controller [73] is added to the control scheme. More details about the system and preliminary results can be found in [4].

4.8.2 Integrated MTFC via VSLs and Ramp Metering

The case of integrated MTFC via VSLs and ramp metering for on-ramp merge bottlenecks, as in Figure 3.2, is considered. A merge congestion (and hence a capacity drop) will appear in absence of control if the sum of the arriving flows exceeds the bottleneck capacity as described in Section 3.3.1. The equity problem is also relevant for this case, as it was for the case of merging motorways and an analogous interpretation is applicable here albeit by the use of VSLs in the mainstream or by the use of traffic light at the on-ramp. However, ramp metering may be preferable over MTFC via VSLs but, as discussed earlier, ramp storage capacity is a major limitation of ramp metering and congestion may appear after the ramp is full. An integrated approach allows to keep operating the motorway at maximum efficiency if MTFC via VSLs is applied to the motorway mainstream and ramp metering by the use of traffic lights is applied at the on-ramp.

The idea is to specify flow values $q_{\mathrm{m,c}}$ upstream of the bottleneck location and $q_{\mathrm{r,c}}$ at the on-ramp in order to keep the bottleneck density ρ_{out} around the critical density. To this end, the feedback cascade control structure of Figure 4.3 is extended to consider a split-range-like control scheme [79] as depicted in Figure 4.9. The primary loop is almost identical as in Figure 4.3 but delivers a reference $\hat{q}_{\mathrm{c}}$ for the total bottleneck inflow that is split to $\hat{q}_{\mathrm{m,c}}$ which is handled by the respective secondary loop (as in Figure 4.3) and to $\hat{q}_{\mathrm{r,c}}$ applied via an appropriate metering police [56, 57] so as to produce the real respective outflows that enter the bottleneck area.

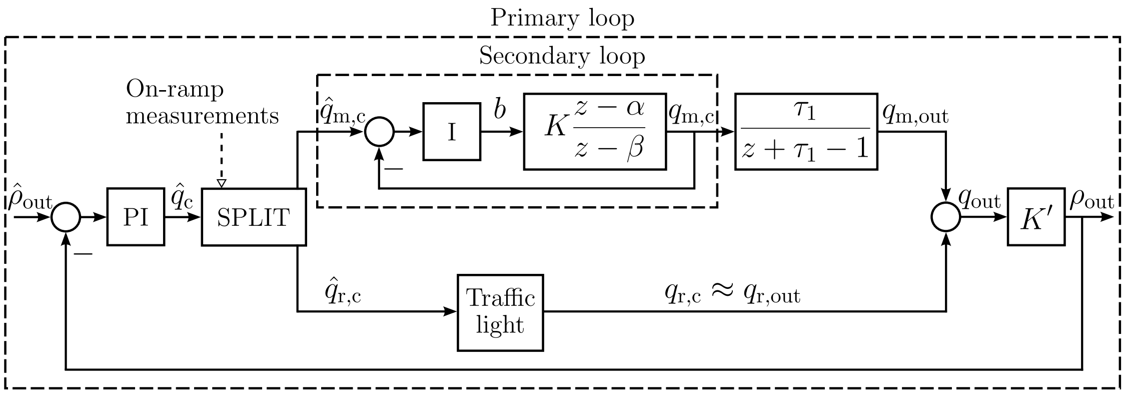

Figure 4.9: Integrated ramp metering and MTFC feedback cascade controller structure using VSLs as an actuator.

The splitting of $\hat{q}_{\mathrm{c}}$ may be performed by different policies, as already discussed for the merging of motorways case in the previous section. A possible policy is to apply ramp metering until the capacity of the on-ramp is exhausted, then the ramp begins to operate in queue management mode and MTFC is applied at the mainstream. This splitting is actually implicitly applied by optimal control in Chapter 5. This application is straightforward and, initially, all the flow reduction ordered by the primary loop is performed by the ramp metering. Meanwhile a queue management controller operates in an override control scheme [74]. Every time that the ordered flow reduction by the primary loop is bigger than what can be provided by the ramp-metering, MTFC starts operating. The lower bound of ramp metering is defined by two values, the minimum allowed ramp metering rate (maximum ramp closure) or by the ramp queue management. The development of this integrated control scheme is ongoing.

Chapter 5

Optimal Control Results

The optimal decisions resulting from the solution of the formulated optimal control problem may in many cases surprise the designer and may even call for an a posteriori interpretation, thus challenging his/her technical judgement and extending or correcting his/her presumed expertise.

A. Kotsialos, M. Papageorgiou, M. Mangeas and H. Haj-Salem [38]

In this chapter the optimal control approach presented in Section 2.4 is applied to two different motorway networks. In Section 5.1 a hypothetical motorway stretch is investigated, while a large scale network with realistic demands is investigated in Section 5.2. The interpretations of the content of this chapter assisted in the development of the MTFC concept introduced in the Chapter 3. Indeed, the results of this chapter show that optimal control behaves according to the MTFC concept despite the fact that the concept is not explicitly implemented in the optimal controller. Optimal control is applied using VSLs as an actuator. The integration of VSLs and ramp metering is also investigated.

5.1 Local Control

In this section a hypothetical motorway stretch is studied under all possible traffic states (free flow, critical, and congested). The investigation is carried out for a localized bottleneck using VSLs and ramp metering. The sensitivity of the controller to lower bounds on the VSL rates is investigated.

5.1.1 Network Model and Demand

For the purposes of this study, a hypothetical three-lane motorway stretch of 6.5 km, depicted in Figure 5.1, is considered. The mainstream is divided into five links (L0 to L4). There are two on-ramps (O1 and O2) on this motorway and one off-ramp (D1) in between. The demand profiles shown in Figure 5.2 are used for the motorway input (U1) and for the two on-ramps, whereby the last 30 min is a cool-down period with zero inflows in the on-ramps and only 1,000 veh/h in the mainstream. This was introduced to have equal traffic conditions on the stretch at the end of the simulation and hence comparable TTS values for all investigated scenarios. The exit rate, i.e., the percentage of the mainstream flow that leaves the motorway at the off-ramp D1 is set to five percent; the model time step used is $T = 10$ s. A number of different control scenarios are examined in the following, each for a time horizon of 2.5 hours. The scenarios and respective TTS results calculated over the 2.5 hours of simulation are summarised in Table 5.1.

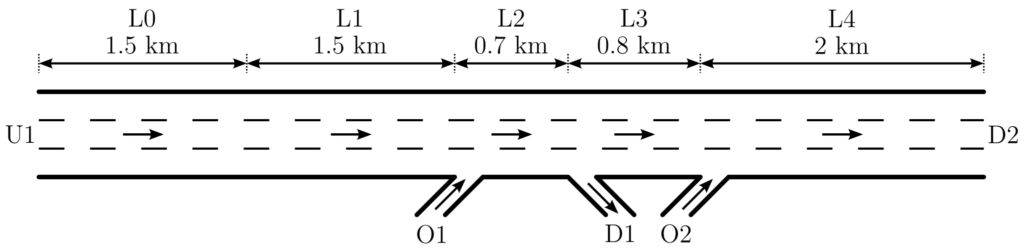

Figure 5.1: Hypothetical motorway stretch.

5.1.2 No-control Case

Figure 5.3 shows the resulting ramp queue, density, speed, and flow profiles for both merge areas, when no control measures are applied. The flow in the merge area of O2 is seen to reach the factual capacity (6,240 veh/h) at $t = 1$ h. As arriving flows continue to increase, a mainstream congestion appears after 1 h in the merge area of the O2 on-ramp; this leads to a visible gradual mainstream flow decrease (capacity drop). The created congestion (shock wave) travels upstream and reaches the merge area of the O1 on-ramp at around $t = 1.2$ h, leading to a visible speed drop and flow decrease there as well. In this scenario, the short queue (18 veh) that forms at the O2 on-ramp is because of the reduction of the on-ramp's flow capacity caused by the mainstream congestion (see (2.15)). The resulting TTS is equal to 1,167 veh·h.

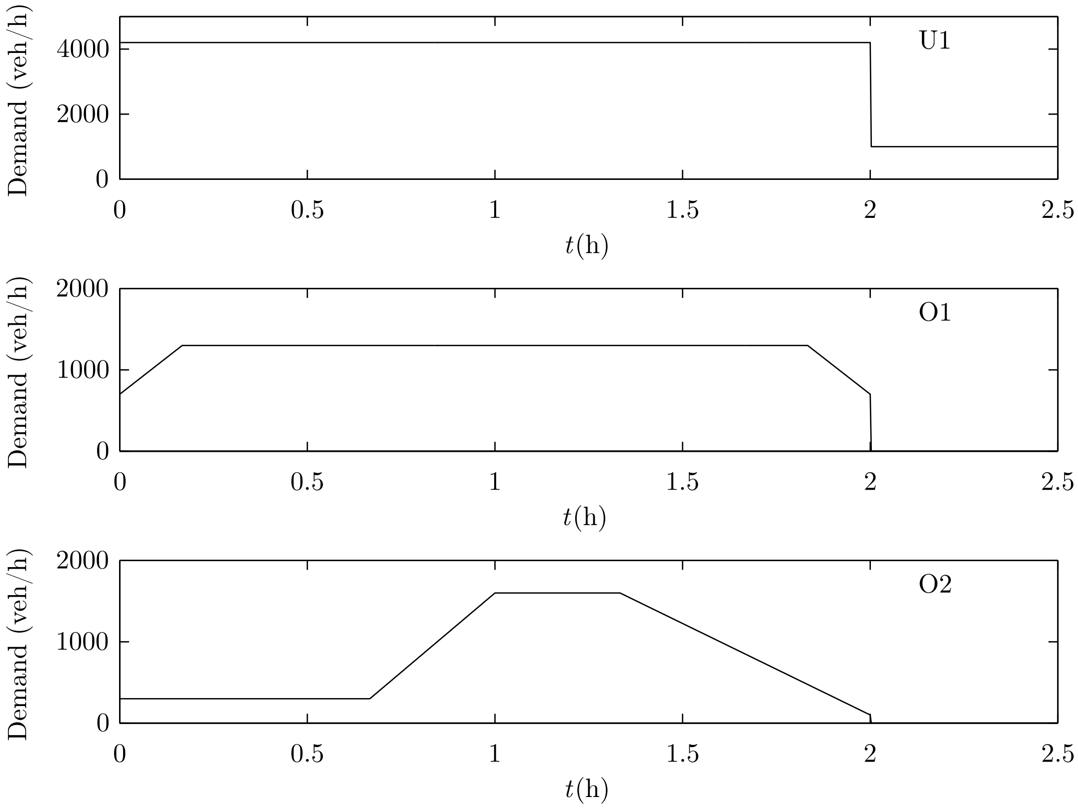

Figure 5.2: Demands at the network origins.

Table 5.1: Summary of simulated control scenarios.

Strategy	Description	TTS (veh·h)	%
No-control	-	1,167	-
Coordinated RM	Optimal coordinated ramp metering (AMOC) applied at O1 and O2 with maximum admissible queues of 50 veh for each on-ramp.	1,060	−9.2
MTFC via VSLs ($b_{\min,m} = 0.5$)	Optimal MTFC with VSLs (AMOC) applied at L11, L12–L13 and L14 with $b_{\min,m} = 0.5$.	1,078	−7.6
MTFC via VSLs ($b_{\min,m} = 0.2$)	Optimal MTFC with VSLs (AMOC) applied at L11, L12–L13 and L14 with $b_{\min,m} = 0.2$.	988	−15.3
Integrated Control ($b_{\min,m} = 0.5$)	Coordinated RM and MTFC via VSLs with $b_{\min,m} = 0.5$	992	−15.0
Integrated Control ($b_{\min,m} = 0.2$)	Coordinated RM and MTFC via VSLs with $b_{\min,m} = 0.2$	939	−19.5

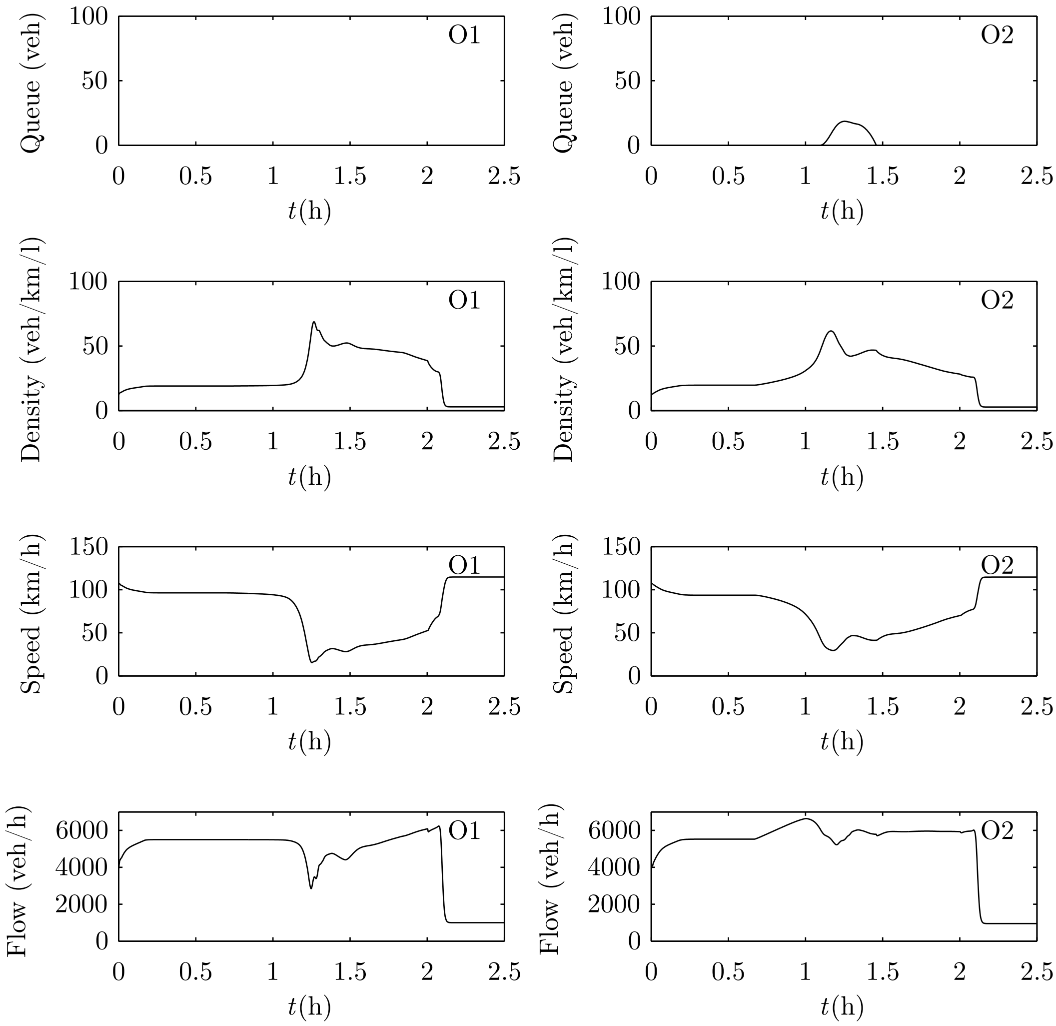

Figure 5.3: No-control: conditions at the merge-areas.

5.1.3 Coordinated Ramp Metering

AMOC is now applied for coordinated ramp metering with maximum admissible queue equal to 50 veh for each on-ramp. The ramp metering rates are allowed to change every 30 s with a minimum admissible value equal to 0.05 (to avoid ramp closure). The resulting TTS value is equal to 1,060 veh·h, which is a 9.2 percent improvement compared to the no-control case. The related ramp queue, density, speed, and flow profiles for both merge areas are shown in Figure 5.4. The dotted curves appearing in the queue plots correspond to the utilised maximum admissible ramp queues.

The situation is identical to the no-control case until short before $t = 1$ h, but eventually the optimal solution maintains the density and the flow at the O2 merge area close to the critical density and factual capacity values, respectively, as long as possible, to maximise the

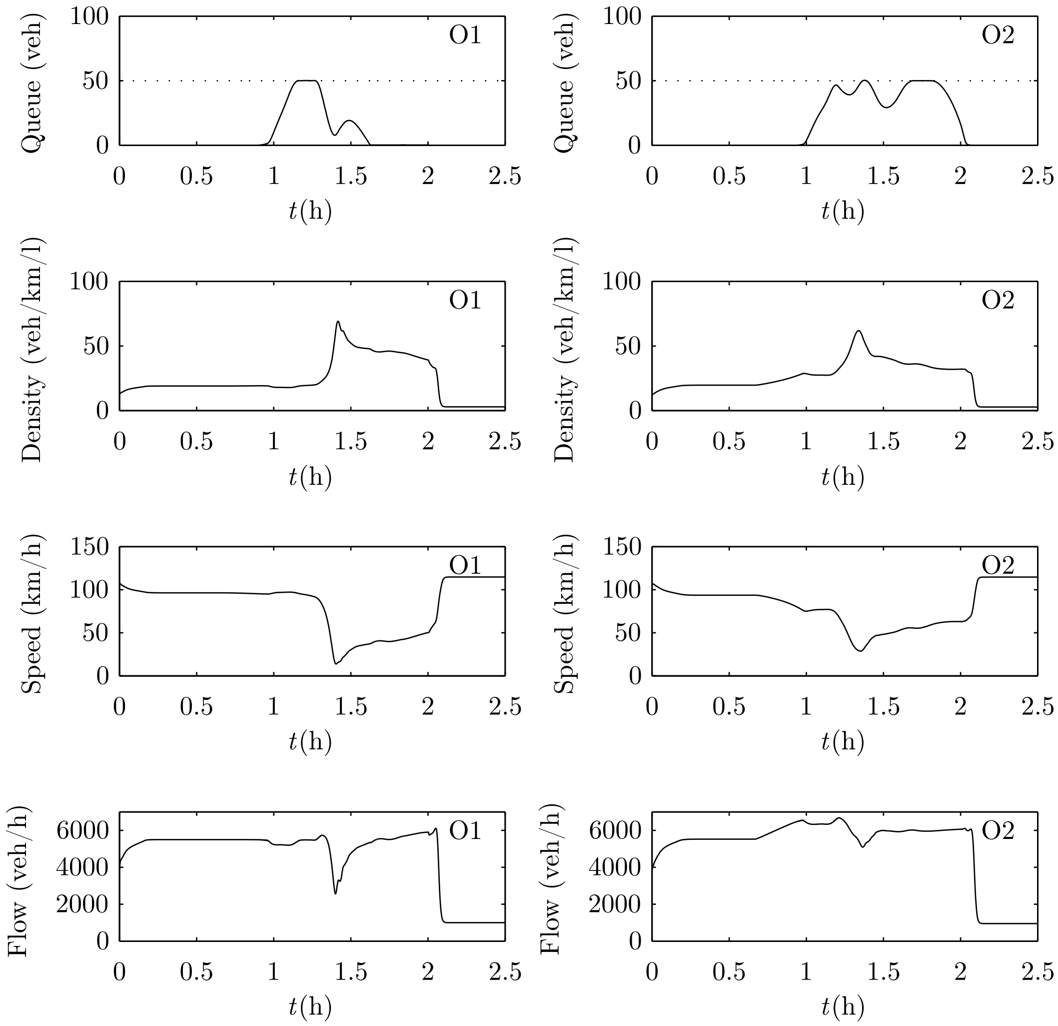

Figure 5.4: Coordinated ramp metering: conditions at the merge-areas.

motorway exit flow (which leads to minimisation of TTS). To achieve this, ramp queues are created quasi-simultaneously in both ramps. The congestion appearing at the O2 merge area at around $t = 1.2$ h is unavoidable in view of the high involved demands and the exhausted limited ramp storage.

5.1.4 MTFC via VSLs

For the application of MTFC via VSLs, the mainstream is divided into four clusters of links, each with its own VSL rate. The first cluster comprises L0 where no VSL control is applied, i.e., $b_{\mathrm{L0}}(k) = 1$, $k = 0, 1, \ldots, K_{\mathrm{P}} - 1$; the second cluster comprises L1; the third cluster comprises L2 and L3, i.e., one single VSL rate is used for both L2 and L3 ($b_{L2} = b_{L3}$); and the fourth cluster comprises L4. The VSL rates are allowed to change every 300 s and

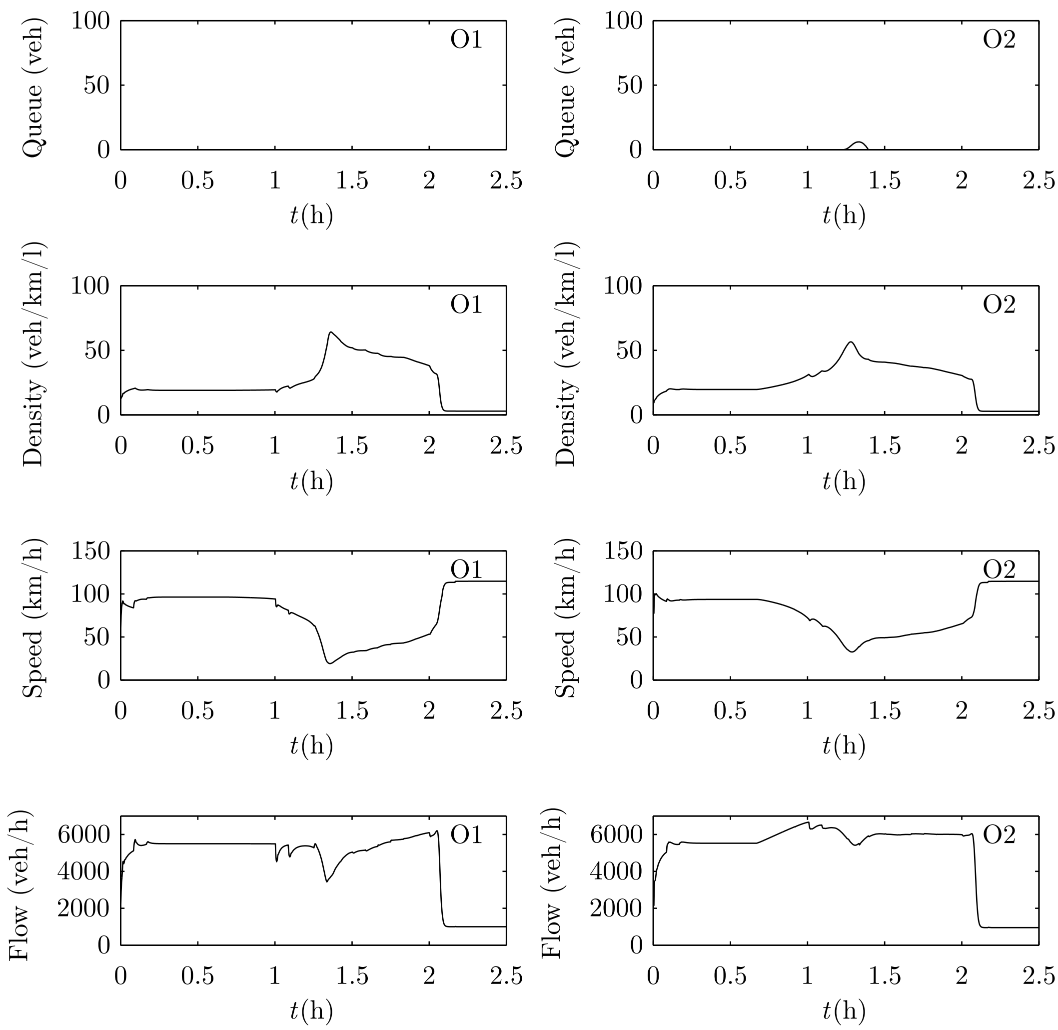

Figure 5.5: MTFC via VSLs ($b_{\min,m} = 0.5$): conditions at the merge-areas.

two cases are examined for the value of the minimum admissible VSL. In the first case, $b_{\min,m} = 0.5$ for all controlled link clusters, and in the second case, $b_{\min,m} = 0.2$. Maximum ramp queue constraints are not taken into account when only MTFC via VSLs is applied.

When $b_{\min,m} = 0.5$ is adopted, the resulting TTS value is equal to 1,078 veh·h, which is a 7.6 percent improvement compared to the no-control case. The related ramp queue, density, speed, and flow profiles for both merge areas are shown in Figure 5.5 and the optimal VSL rate trajectories are shown in Figure 5.6.

The situation is here also virtually identical to the no-control case until $t = 1$ h, because no congestion appears yet. At $t = 1$ h, the VSL rate of L4 is seen to switch gradually to values around 0.85; this allows the O2 merge area to accommodate a higher number of vehicles (because of higher critical density) without any real loss in flow capacity (Figure 2.6). The next issue is the need to keep the O2 merge area density close to its (increased) critical density

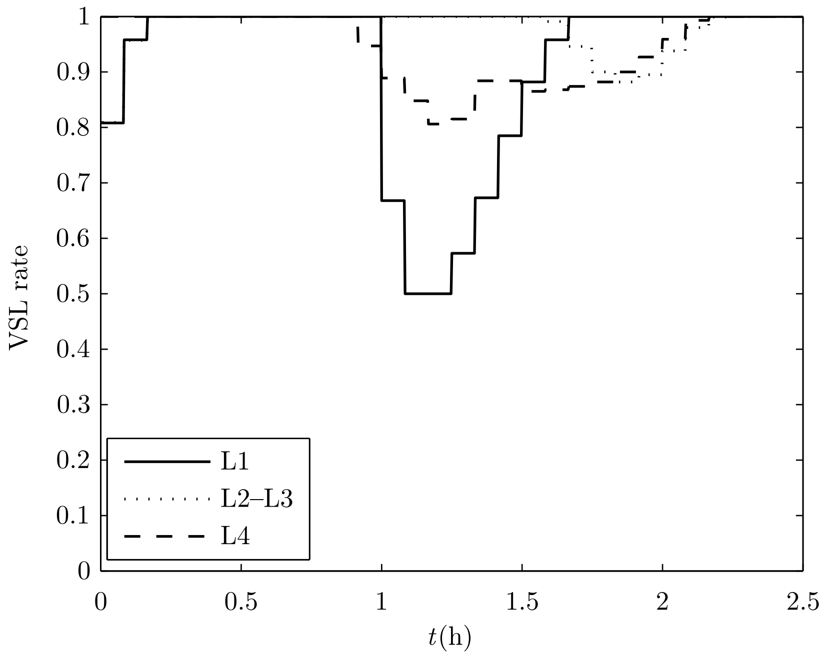

Figure 5.6: Optimal VSL rates for MTFC via VSLs ($b_{\mathrm{min},m} = 0.5$).

for as long as possible to avoid the congestion appearing there after $t = 1$ h in the no-control case scenario and enable maximum motorway exit flow (which leads to TTS minimisation). Indeed, the VSL rate for L1 is seen to switch from one to (the lower admissible bound) 0.5 in essentially two steps (Figure 5.6) shortly after $t = 1$ h. According to Section 2.2.3.2, the corresponding state transitions create temporary mainstream flow reductions that are clearly visible in the flow curve of merge area O1 (Figure 5.5) as short negative pulses. Because the (factual) mainstream capacity for a VSL rate of 0.5 is still higher than the upstream arriving demand, the mainstream flow is seen to fully recover after the state transition. These temporary flow reductions are effectuated to keep the O2 merge area density close to its critical value for as long as possible, but after reaching the lower bound of 0.5, no further flow decrease is possible and the O2 merge area congestion (and corresponding flow reduction) after $t = 1.2$ h becomes unavoidable similarly to the ramp metering case.

Remarkably, AMOC decides to create a mainstream bottleneck by use of the VSL of L1 rather than of L2–L3. The reason for this may be found in Chapter 3: the VSL application area of L2–L3 is used as an acceleration area for vehicles exiting the low-VSL link L1 to avoid capacity drop at the O2 merge area. In fact, if AMOC is rerun with uncontrolled L1 (not shown here), it refuses to create a VSL-induced mainstream bottleneck at L2–L3, because this would not bring real benefits (capacity drop is not avoided). Further interpretation details (e.g., regarding the VSL switch-off period after $t = 1.5$ h) are deemed less significant and are omitted here for the sake of brevity.

Allowing MTFC via VSLs to go to even lower values ($b_{\min,m} = 0.2$) results in a TTS value equal to 988 veh·h, which is a 15.3 percent improvement compared to the no-control case. The related ramp queue, density, speed and flow profiles for both merge areas are shown in Figure 5.7 and the optimal VSL rate trajectories are shown in Figure 5.8.

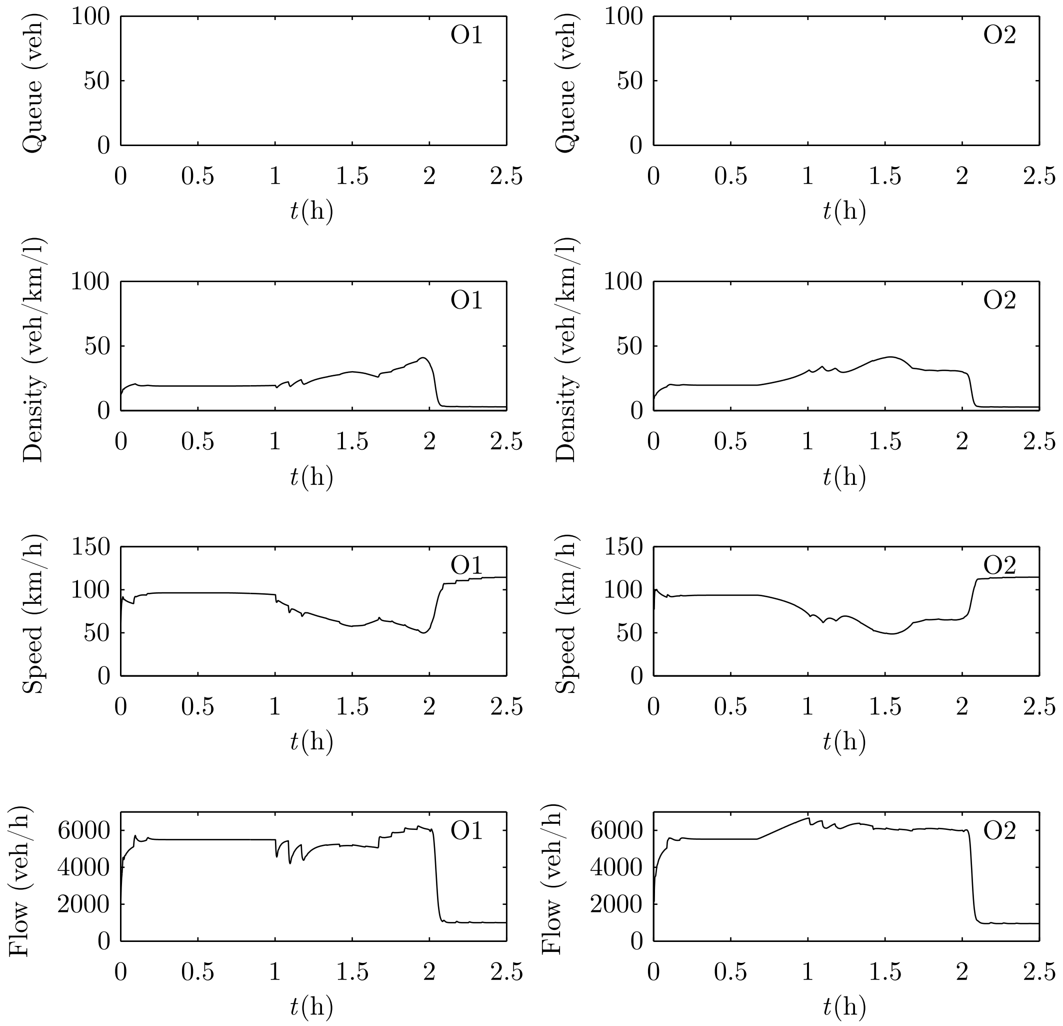

Figure 5.7: MTFC via VSLs ($b_{\min,m} = 0.2$): conditions at the merge-areas.

The interpretation of these results is similar to the previous case with one notable difference. The (factual) mainstream capacity for the new (lower) admissible limit of 0.2 is now lower than the arriving mainstream demand. Hence, the flow at the O1 merge area (Figure 5.7) is seen to not recover fully after the third VSL switch at L1 (Figure 5.8). This leads to a stronger and more durable flow reduction, because of which the O2 merge area density is maintained near critical values (with maximum motorway exit flow) over a longer period and the (unavoidable) congestion appearing there around $t = 1.4$ h is seen (Figure 5.7) to

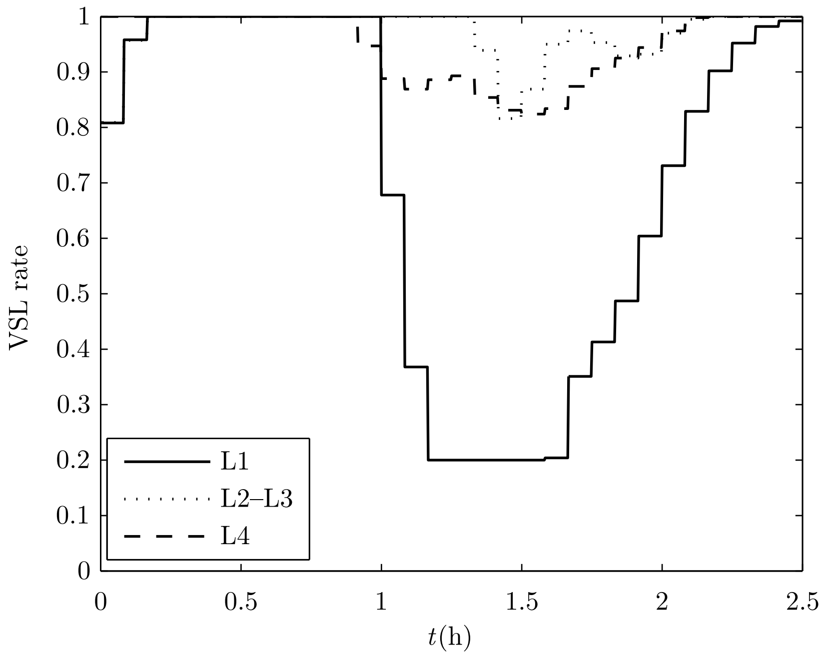

Figure 5.8: Optimal VSL rates for MTFC via VSLs ($b_{\mathrm{min},m} = 0.2$).

be weaker than in previous cases. Note also the more prolonged VSL application at L1 (Figure 5.8) and its gradual switch off leading to increased flow in the O1 merge area at $t \in [1.6, 2]$ h because of opposite state transitions (from lower to higher VSL values).

5.1.5 Integrated Control

When both coordinated ramp metering and MTFC via VSLs with $b_{\mathrm{min},m} = 0.5$ are applied, i.e., integrated traffic control, TTS is reduced to 992 veh·h, which is a 15.0 percent improvement compared to the no-control case. The related profiles are omitted for the sake of brevity.

The optimal results indicate a similar behaviour of each control measure (ramp metering and VSLs) to previous control scenarios. Because the integration of both measures increases the possibilities to hold more traffic back from the O2 merge area, the density there can be maintained close to its (now VSL modified) critical value up to $t = 1.4$ h after which an unavoidable (but less strong) congestion appears.

Finally, when both coordinated ramp metering and VSL control with $b_{\mathrm{min},m} = 0.2$ are applied, TTS is reduced further to 939 veh·h, which is a 19.5 percent improvement compared to the no-control case. The related ramp queue, density, speed, and flow profiles for both merge areas are shown in Figure 5.9 and the optimal VSL rate trajectories are shown in Figure 5.10.

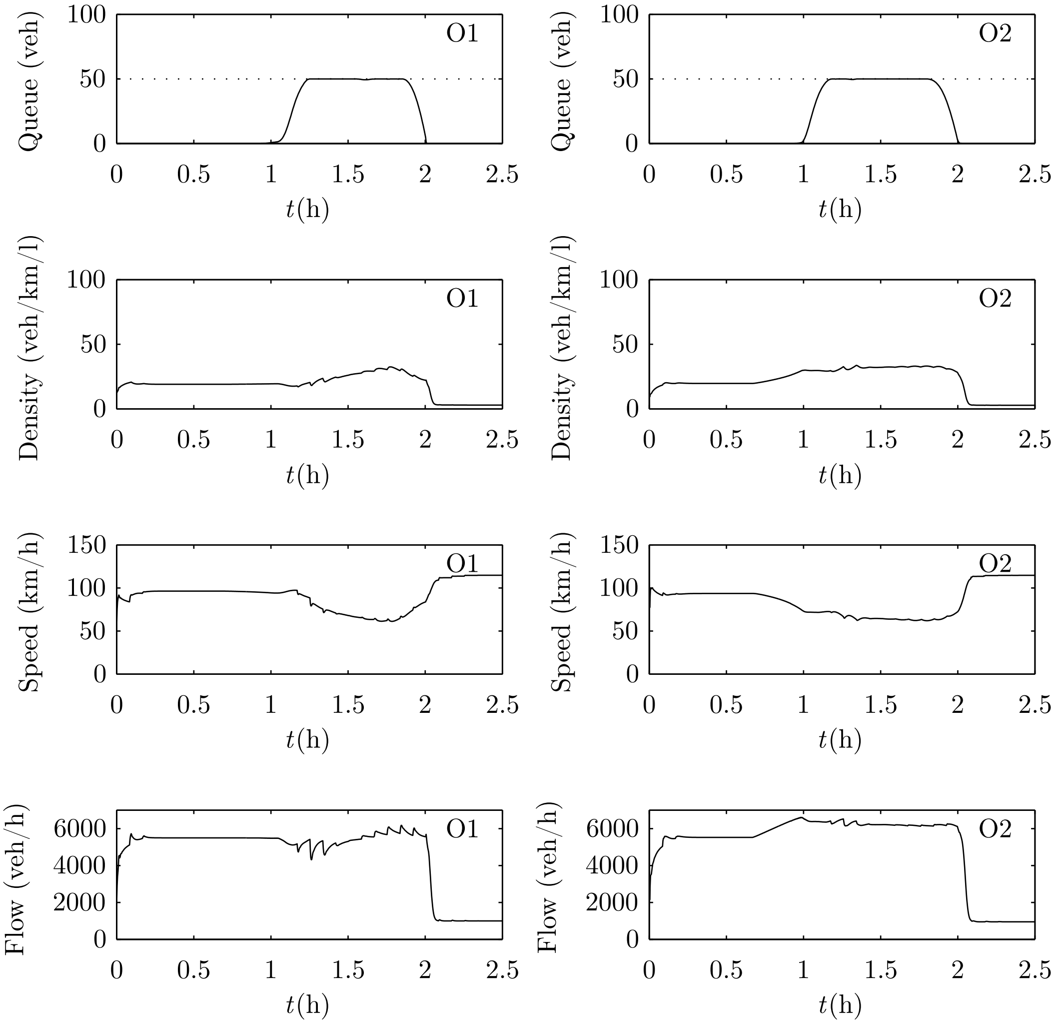

Figure 5.9: Integrated control, i.e., coordinated ramp metering and MTFC via VSLs ($b_{\min,m} = 0.2$): conditions at the merge-areas.

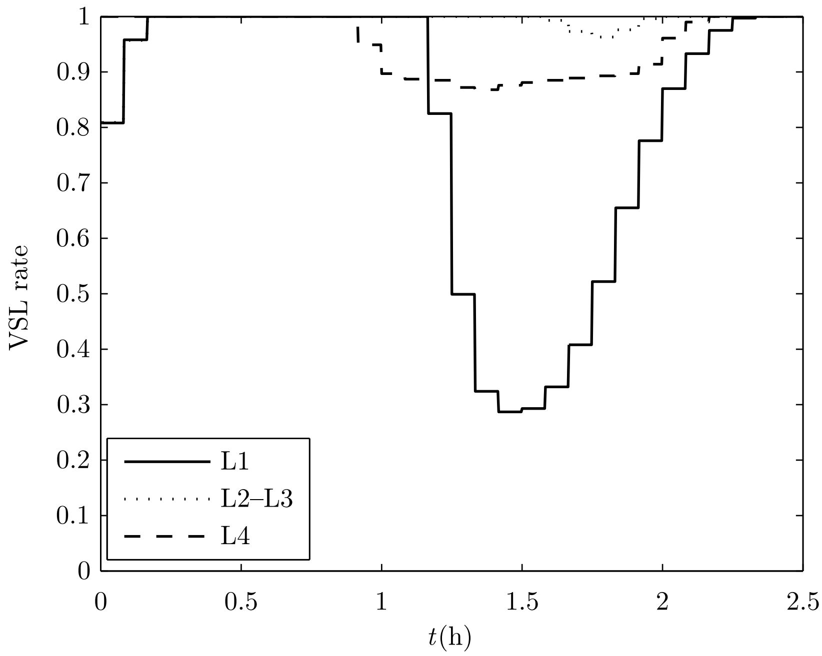

Figure 5.10: Optimal VSL rates for the integrated control, i.e., coordinated ramp metering and MTFC via VSLs ($b_{\min,m} = 0.2$).

The optimal results in Figures 5.9 and 5.10 indicate a similar control behaviour as in previous cases, with the notable difference that traffic can be held back at a sufficient level to completely avoid congestion. In fact, the O2 merge area density is maintained close to its (now VSL modified) critical value for as long as is necessary and the motorway exit flow is accordingly maximised, which lead to the above mentioned further decrease in TTS. Remarkably, the available storage space for ramp metering is fully utilised while the L1 VSL rate values (which are responsible for creating the mainstream bottleneck) do not reach the admissible lower bound of 0.2 because that is not needed.

5.2 Network Control

In this section a large-scale motorway network based on a real infrastructure with realistic demand is investigated. Ramp metering and VSLs are compared and their integration is evaluated.

5.2.1 The Amsterdam Network

For the purposes of this study, the counter-clockwise direction of the Amsterdam ring-road A10, which is about 32 km long, is considered. There are 21 on-ramps on this motorway, including the motorway-to-motorway (mtm) junctions with the merging motorways A8, A4, A2 and A1 and 20 off-ramps, including the connections with A8, A4, A2 and A1. The topological network model may be seen in Figure 5.11. The ring-road has been divided into 76 segments with average length of 421 m. This means that the state vector is 173-dimensional (including the 21 on-ramp queues). The disturbance vector is 41-dimensional (21 on-ramp demands and 20 off-ramp exit rates) while the dimension of the control vector is equal to the number of controlled on-ramps plus the number of controlled VSL clusters.

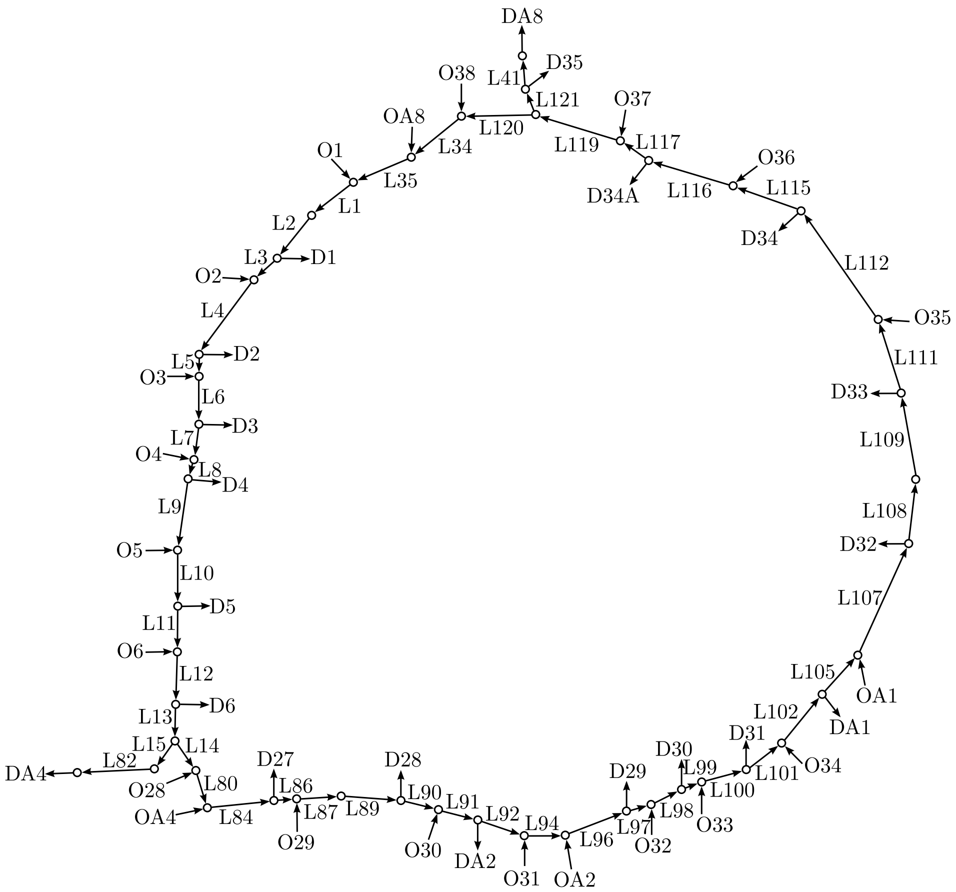

Figure 5.11: The Amsterdam ring-road A10.

The basic model parameters τ, ν, κ and ρ for all links in this network were determined from validation of the network traffic flow model against real data [37] and are provided in Section 2.3; while the specific parameters of the speed-density characteristic (2.9) were different for different groups of links according to Table 5.2. Since, for the study in this section, the interest is in exploiting the impact of MTFC without the possibility of capacity increase via VSLs, the parameter values of A and E were specified accordingly. In other words, the respective VSL-specific parameters A and E were chosen such that the VSL-induced capacity $q^*_{\mathrm{cap},m}(b_m)$ is not higher than the non-VSL $q_{\mathrm{cap},m}$ for any VSL value (Table 5.2). Figure 5.12

displays the b_m-dependent flow-density curves resulting from (2.9) with the values of the first row of Table 5.2. The simulation time step is $T = 10$ s.

The ring-road was studied for a time horizon of 4 h using realistic historical demands from the site.

Table 5.2: Non-VSL and VSL-related parameters.

Links m	$q_{\mathrm{cap},m}$ (veh/h/lane)	$v_{\mathrm{f},m}$ (km/h)	$\rho_{\mathrm{cr},m}$ (veh/km/lane)	α_m	E_m	A_m
L1, L2, L3, L4, L5, L6, L7, L8, L9, L10, L11, L12, L13, L14, L15, L82, L84, L86, L89, L90, L91	2212	102	33.3	2.34	1.82	0.67
L34, L35, L41	2390	102	35.9	2.34	1.82	0.67
L92, L94, L96, L97, L98, L99, L100, L101, L102, L105, L107, L108, L109, L111, L112, L115, L116, L117, L119, L120, L121	1840	102	27.7	2.34	1.82	0.67
L80	2212	102	35.9	1.98	1.69	0.67

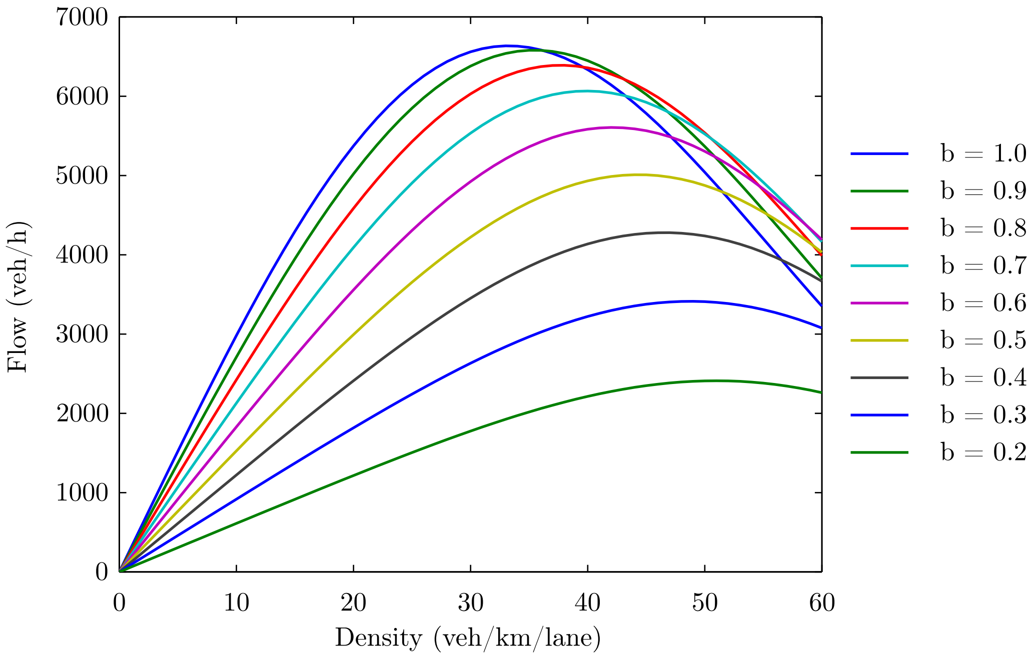

Figure 5.12: Fundamental diagrams for different VSL rates using the parameters of the first row of Table 5.2: $b = 1.0$ means no VSL applied, decreasing b-values correspond to decreasing VSLs.

5.2.2 Control Scenarios

In what follows, different control scenarios, introduced in Table 5.3, are considered. First the network is simulated without control serving as a reference for comparison of the benefits achieved with control. Scenarios 1–10 include ramp metering only, to enable comparisons with MTFC via VSLs as well as integrated traffic control. Scenario 1 reflects an (unrealistic) upper limit of traffic flow efficiency because all on-ramps are assumed to have unlimited storage space. Scenarios 2–6 consider an admissible storage limit of 30 veh for the, typically limited-size, urban on-ramps; while the usually more spacious mtm interconnections are considered either not controlled (Scenario 2) or with gradually increasing storage space of 100 veh, 200 veh, 300 veh, and 400 veh for scenarios 3, 4, 5 and 6, respectively. In Scenarios 7–10, the urban ramps are assumed not controlled while the mtm ramps have increasing respective storage spaces as above. Scenario 11 applies only MTFC via VSLs at all motorway links with a range of VSL rates $b_m \in [0.2, 1.0]$. Finally, Scenarios 12–21 are replications of the respective ramp metering Scenarios 1–10 but with the addition of MTFC via VSLs (integrated traffic control).

Clearly, all reported solutions for any controlled scenario are ideal in the sense that they consider a perfect model and perfect information with respect to the future disturbances for the entire time horizon. Practical application (e.g., by use of rolling horizon) would inevitably reduce the achievable performance as demonstrated in [67]. Nevertheless the conducted investigation and comparison is useful to demonstrate the potential of MTFC and its relative performance against optimal ramp metering actions.

5.2.3 No-control Case

When simulating the network by use of the METANET simulator without any control measures, heavy congestion appears in the motorway and large queues are built in some on-ramps. The density evolution and the corresponding queue profile are displayed in Figure 5.13. The excessive demand, coupled with the uncontrolled entrance of the drivers into the mainstream, causes congestion shortly after the beginning of the time horizon (Figure 5.13(a)). This congestion originates at the junction of A1 with A10 and propagates upstream, blocking A4 and a large part of the A10-West. After this congestion is partially dissolved, a new one appears and propagates upstream until it reaches the first congestion whose trend of resolving is thereby reversed leading to a single more severe congestion. This strong congestion keeps the

Table 5.3: Simulated control scenarios for the Amsterdam ring-road.

Scenario	Admissible ramp queues for controlled urban on-ramps (veh)	Admissible ramp queues for controlled mtm on-ramps (veh)	Range of VSL rates	TTS (veh·h)	%
No-control	Not controlled	Not controlled	Not controlled	14,163	-
1	∞	∞	Not controlled	7,017	−50.5
2	30	Not controlled	Not controlled	11,023	−22.2
3	30	100	Not controlled	7,856	−44.5
4	30	200	Not controlled	7,071	−50.1
5	30	300	Not controlled	7,081	−50.0
6	30	400	Not controlled	7,041	−50.3
7	Not controlled	100	Not controlled	8,913	−37.1
8	Not controlled	200	Not controlled	7,882	−44.3
9	Not controlled	300	Not controlled	7,161	−49.4
10	Not controlled	400	Not controlled	7,151	−49.5
11	Not controlled	Not controlled	0.2–1.0	7,454	−47.4
12	∞	∞	0.2–1.0	6,997	−50.6
13	30	Not controlled	0.2–1.0	7,256	−48.8
14	30	100	0.2–1.0	7,076	−50.0
15	30	200	0.2–1.0	7,018	−50.4
16	30	300	0.2–1.0	7,007	−50.5
17	30	400	0.2–1.0	7,002	−50.6
18	Not controlled	100	0.2–1.0	7,136	−49.6
19	Not controlled	200	0.2–1.0	7,029	−50.4
20	Not controlled	300	0.2–1.0	7,004	−50.5
21	Not controlled	400	0.2–1.0	6,998	−50.6

A4 entrance to A10 blocked, which results in the accumulation of many vehicles at the mtm on-ramp of A4, with a queue that exceeds 1200 veh (in real life the congestion spills back onto A4 itself), and at the surrounding on-ramps (Figure 5.13(b)). The TTS for this scenario is equal to 14,163 veh·h. The described no-control simulation results are very similar to the corresponding real traffic conditions [37].

5.2.4 Coordinated Ramp Metering

When AMOC is applied for coordinated ramp metering without maximum queue constraints (Scenario 1), the resulting TTS is 7,017 veh·h, which is an improvement of 50.5 percent compared to the no-control case. As mentioned earlier, this optimal solution serves as an "upper bound" for the achievable efficiency of any of the other ramp metering scenario as it relies on ideal conditions of unlimited ramp storage space. The related density evolution and queue profile are displayed in Figure 5.14. It is obvious that, when unlimited ramp storage

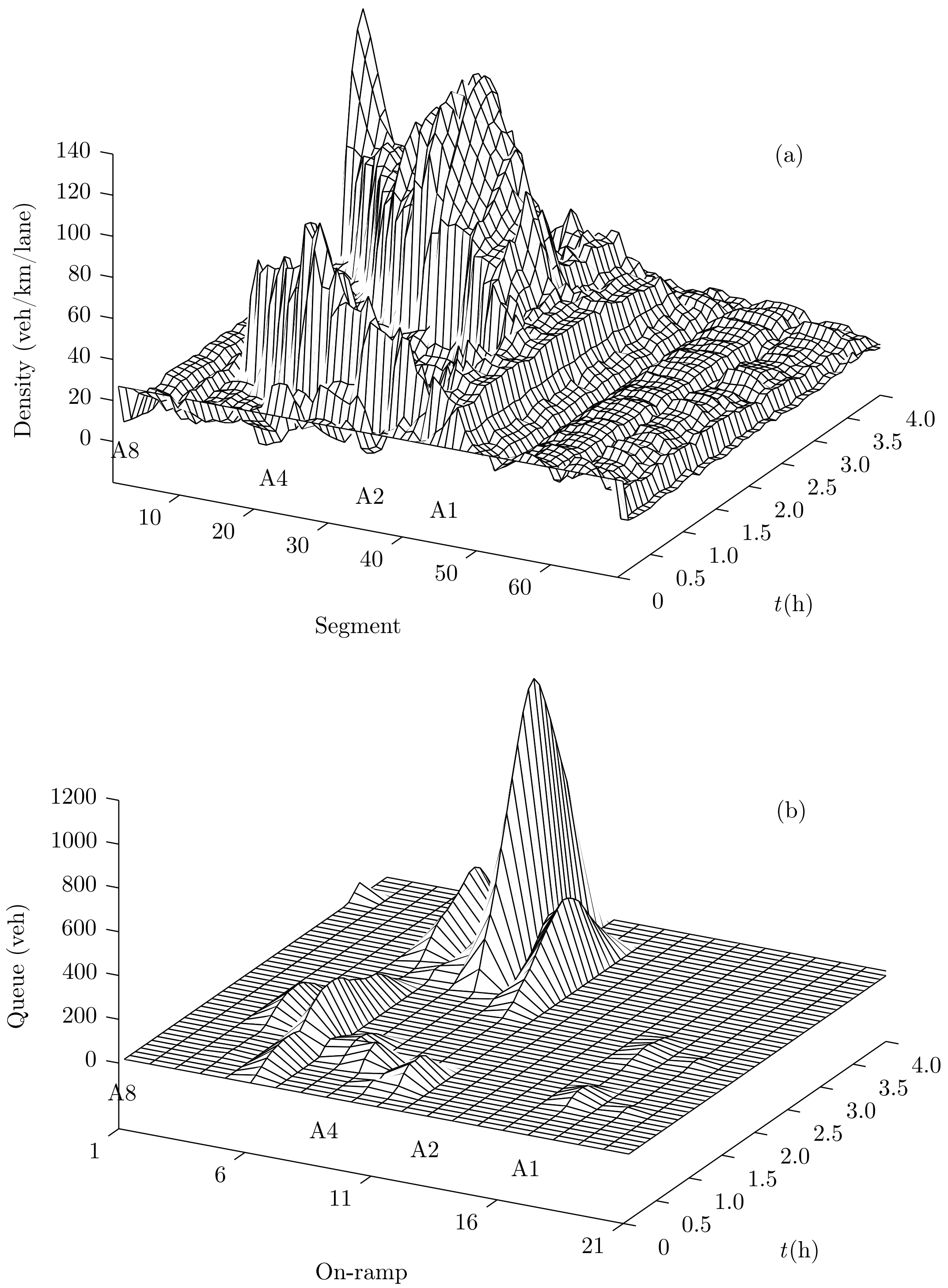

Figure 5.13: No-control case: (a) density profile and (b) ramp queue profile.

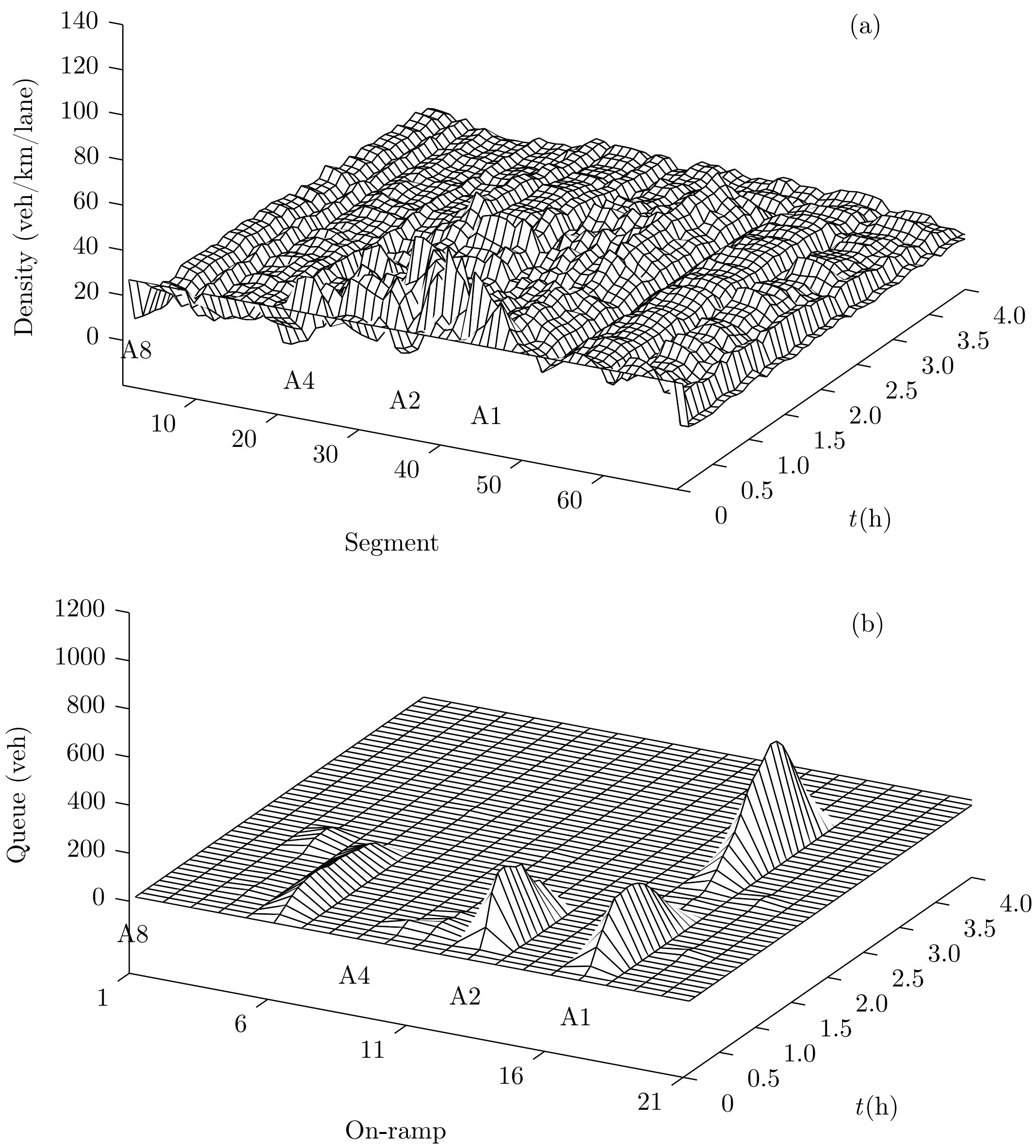

Figure 5.14: Scenario 1: (a) density profile and (b) ramp queue profile.

space is available, the mainstream congestion can be completely avoided (Figure 5.14(a)) at the cost of forming queues on the on-ramps, which, remarkably, are generally smaller than in the no-control case due to avoidance of the infrastructure degradation that leads to highest traffic flow efficiency. On the other hand, it may be concluded from Table 5.3 and Figure 5.15, that:

- When only urban on-ramps are controlled with maximum storage space of 30 veh (Scenario 2), the achieved improvement is moderate (22.2 %) as the congestions can be reduced but not fully resolved due to full ramps. But if the four mtm on-ramps are also controllable (Scenarios 3–6), the achievable performance increases and reaches the one

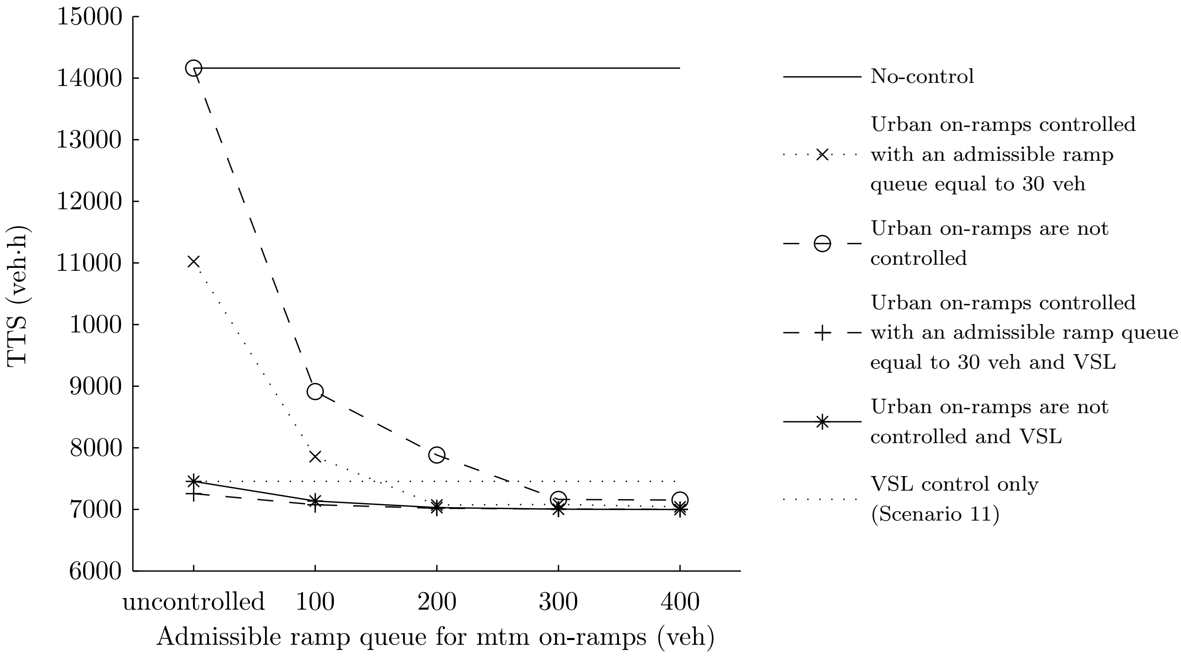

Figure 5.15: TTS values when coordinated ramp metering and integrated control are applied with different admissible ramp queues at the mtm on-ramps.

of Scenario 1 for a storage space of 200 vehicles (Scenario 4); while any further increase of the storage space (Scenarios 5 and 6) does not lead to further improvements.

- When urban on-ramps are not controllable but mtm ramps are (Scenarios 7–10), the achievable performance is reduced compared to the respective scenarios with controllable urban on-ramps; but the performance reduction becomes negligible for mtm ramp storages of 300 vehicles or more.

For further details and discussion of ramp metering results for the Amsterdam ring-road the reader is referred to [67].[1]

5.2.5 MTFC via VSLs

For the application of MTFC via VSLs, every link is considered as a cluster, that is, every link has its own VSL rate. This approach may not be needed or may not be acceptable in real applications, e.g., in the case of short links, but allows here to extract maximum information about the optimal MTFC application (under maximum flexibility) and potential impact. The VSL rates are allowed to change every 300 s with a minimum admissible VSL

[1] Note that the TTS values in this section differ slightly from [67], due to numerical improvements in METANET and AMOC tools.

rate of $b_{\min,m} = 0.2$ which is chosen sufficiently low to enable the maximum achievable impact of this control measure. Maximum ramp queue constraints are not taken into account when only VSL control is applied.

The resulting TTS value when only VSLs are applied (Scenario 11) is equal to 7,454 veh·h, which is a 47.4 percent improvement compared to the no-control case. The related density and ramp queue profiles are shown in Figure 5.16, while the optimal VSL rate trajectories are shown in Figure 5.17.

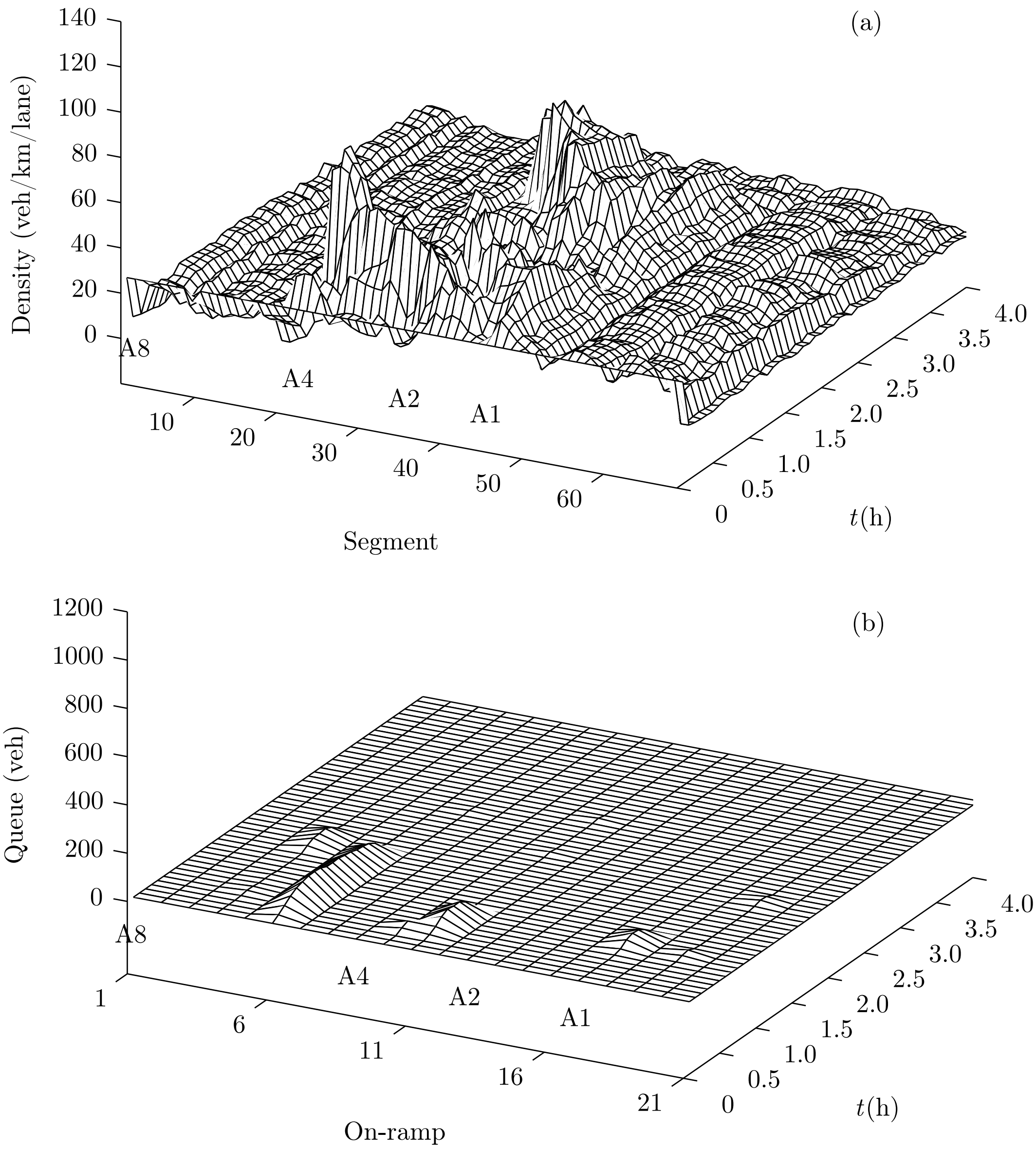

Figure 5.16: Scenario 11: (a) density profile and (b) ramp queue profile.

Figure 5.16(a) indicates that there are two congestions forming, but, in contrast to the no-control case, these congestions are much less extended in space and time. Note that, up to

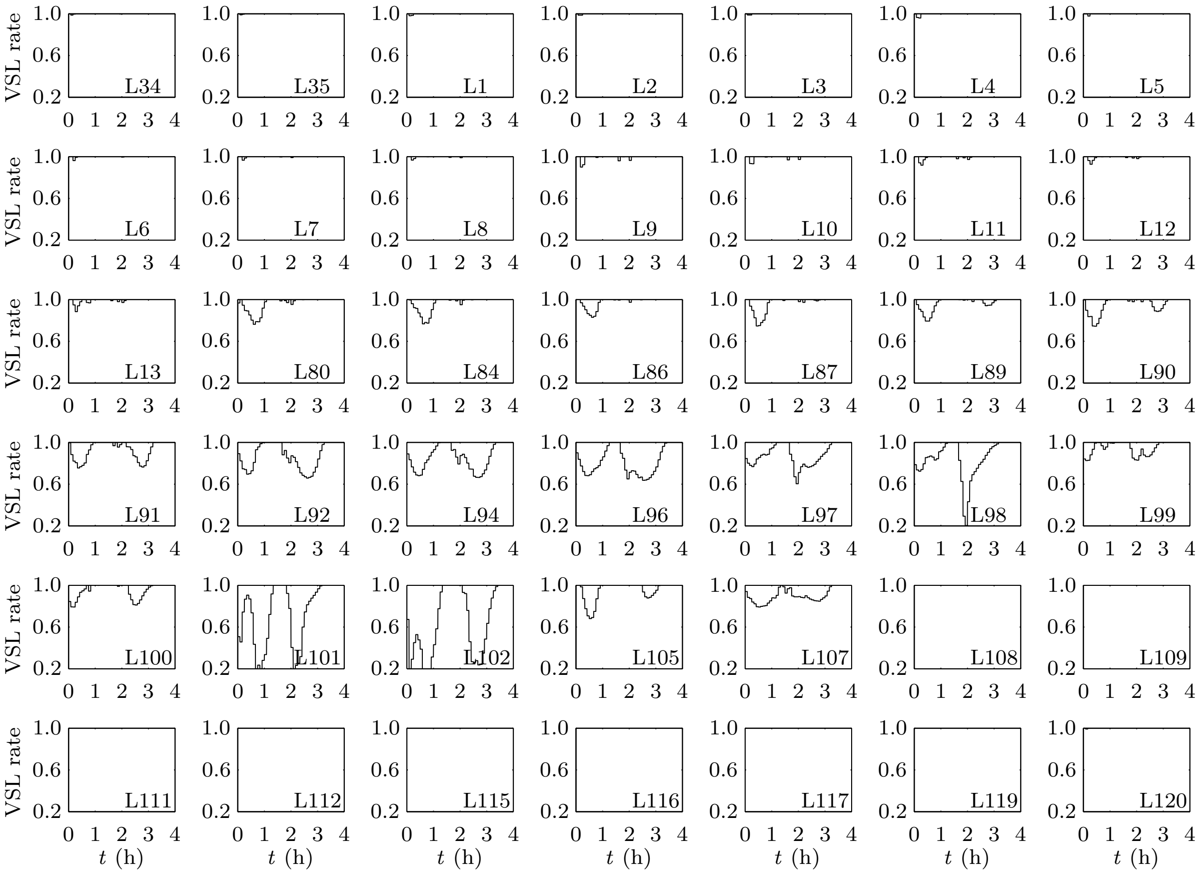

Figure 5.17: Scenario 11: VSL rate trajectories.

$t = 0.3$ h (Figure 5.16(a)) the traffic density at the A1 merge area is around or below the critical value and a congestion is formed a few segments upstream. In fact, this controlled congestion is not the direct result of the bottleneck in the merge area of A1 with A10 (as in the no-control case), but due to holding back of traffic upstream of the A1/A10-junction bottleneck via appropriate (optimal) VSL control. However, a light congestion starts forming at the merge area of A1, despite the fact that the VSL rates have not reached the lower bound. As a matter of fact, this light congestion forming at the merge area of A1 could have been completely avoided by MTFC via VSLs. Instead, AMOC decides to use the space at the merge area, and also at some of the upstream links (L105 alone is 1200 m long), to store more vehicles via higher densities. In that way, AMOC manages the congestion length and intensity so as to reduce the BOR effect, particularly at the exit to A4. This more than counterbalances the reduction of throughput due to the short term infrastructure degradation at the merge area of A1 and the reduced outflow of off-ramps immediately upstream of the bottleneck. Next, just after $t = 0.6$ h (Figure 5.17), VSLs are strongly applied at links L101 and L102 (located one link upstream of the A1/A10-junction) dissolving the congestion in order to maintain critical density and speed for as long as possible in the A1 merge area (link L107) (i.e., up to $t = 1.4$ h), with the aim of recovering from the traffic breakdown and capacity drop to enable maximum motorway throughput (which eventually leads to TTS minimisation). At the same time period, VSL rates of around $b_m \approx 0.8$ are applied at links L105 and L107, which allow the A1 merge area to accommodate a higher number of vehicles (due to higher critical density) (Figure 5.12). Ramp queues forming in some on-ramps (Figure 5.16) due to congestion spill-back are rather small, not exceeding 80 vehicles.

Remarkably, AMOC decides to create a mainstream congestion by use of VSLs at links L101 and L102 rather than at link L105 which is the one located immediately upstream of the problematic bottleneck A1/A10. The reason for this intelligent behaviour may be found in Section 3: whenever congestion at the merge area of A1 is avoided, the link L105 is used as an acceleration area for vehicles exiting the low-VSL (hence low-speed) link L102, in order to avoid capacity drop at the A1 merge area which is located 1200 m further downstream.

Further analysis of the VSL trajectories in Figure 5.17 shows that from link L34 to link to L13 and from link L108 to link L120, VSL is virtually not applied at all. These links comprise segments 1–21 and 48–69 which remain at undercritical densities (Figure 5.16(a)); hence there is no need for the application of VSLs there. On the other hand, at links L80–L97, VSLs are applied with increasingly stronger VSL rates from upstream to downstream, thereby increasing the respective links' critical densities.

The outlined and interpreted optimal MTFC via VSLs actions during the period $t \in [0.3, 1.4]$ h cease when the deliberately created mainstream congestion is also dissolved, but the increased demand at around $t = 2$ h leads to a second period of MTFC via VSLs activation that ends at around $t = 3.3$ h with the resolution of the related mainstream congestion. This second control-activation period is very similar in form and interpretation to the first period analysed above, with one minor exception: a second bottleneck at link L100 is about to be activated due to the merging of on-ramp O33 (Figure 5.11) and lower capacity (Table 5.2). To address this potential bottleneck, AMOC applies a strong VSL rate at link L98 at the start of this second control period (Figure 5.17) while the immediately downstream link L99 with $b_m \approx 0.8$ acts as an acceleration area to avoid capacity drop at the L100 bottleneck. Some 10 min later, strong VSL actions are applied to address again the A1/A10 bottleneck as in the first control period. The created controlled congestion propagates backwards and covers the upstream located O33/A10 bottleneck thus rendering the strong MTFC action there obsolete. Indeed, AMOC is seen (Figure 5.11) to rapidly increase the applied VSL rates at link L98, and eventually the whole situation becomes very similar as in the first control period, i.e., all control actions are focused again on the major bottleneck A1/A10. Note that, by the end of the congestion period VSLs are released and a light congestion is again formed in the merge area of A1, so as to reduce the BOR effect. In contrast to the previous congested period, VSLs are not applied again and the congested is dissolved due to the reduction of the demand.

As a global remark, optimal MTFC via AMOC is seen to render a rather complex no-control traffic situation (Figure 5.13) quite simple: there is only one major bottleneck identified during the studied period of the afternoon peak, and all MTFC actions are directed towards highest possible throughput at that location in a way that was expected on the basis of the discussion of Section 2.2.3, except when it is beneficial to manage the congestion length and intensity so that the BOR effect at important off-ramps is reduced. Note that the BOR effect by creating short term congestions at the merge area of A1 is reduced compared to an MTFC application that would completely avoid congestion at the same location. Even in the latter case, the BOR effect would still be smaller than the no-control case as discussed in Section 3.2. Remarkably, despite the inherent inability of MTFC to completely avoid mainstream congestion (in contrast to ramp metering with sufficient storage space), the achieved TTS improvement is very close to the one of Scenario 1, albeit with only minor creation of on-ramp queues.

In summary, optimal MTFC via VSLs for the studied peak period may be grouped as follows: strong VSL control at L101, L102 creates the mainstream bottleneck for MTFC; weak VSL control is applied to L105 (acceleration area just upstream of the addressed bottleneck A1/A10), to L107 (merge bottleneck A1/A10), and to L80–L100 (upstream of the MTFC bottleneck); light congestion is timely created at the merge area of A1 so as to manage the congestion length and intensity, and its impact on the off-ramps outflows; all other links remaining without VSL activation. An interesting arising question refers to the individual importance and contribution of each of these groups for the achieved significant amelioration. To answer this question, several sub-scenarios of Scenario 11 were created, whereby VSLs are enabled at only few selected links in each sub-scenario according to Table 5.4.

The reported TTS results of Table 5.4 indicate that the major part of the improvement is due to the VSL control in links L101 and L102; in fact, Scenario 11.4 (with VSL control enabled only at L101 and L102) leads to an improvement of 39.5 percent (TTS of 8,551 veh·h) compared to the no-control case. The impact of enabling VSL control also at the downstream (acceleration) link L105 (Scenario 11.5) is negligible, whereas controlling in addition to L101 and L102, both links L105 and L107 (Scenario 11.6) leads to a TTS of 7,834 veh·h, i.e., an additional five percent improvement. Enabling VSL control at upstream links in addition to links L101 and L102 in various combinations (Scenarios 11.1–11.3) leads to very small TTS improvements for each additional link. In terms of congestion length, the impact of removing VSL control from some links is more significant (Table 5.4) and affects also the ramp queue lengths in the congestion-covered areas.

Table 5.4: TTS values when only selected links are VSL-controlled.

Scenario	Controlled links	TTS (veh·h)	%	Extent of mainstream congestion: from L102 until
11	All	7,454	−47.4	L12
11.1	L98–L102	8,119	−42.7	L6
11.2	L99–L102	8,195	−42.1	L6
11.3	L100–L102	8,240	−41.8	L6
11.4	L101–L102	8,567	−39.5	L4
11.5	L101–L105	8,551	−39.6	L4
11.6	L101–L107	7,834	−44.7	L8/L7

A further interesting scenario (not displayed in Table 5.4) was to disable VSLs in the critical links L101 and L102, but allow it anywhere else. In this case, the optimal solution selects the immediately upstream links L98–L100 to apply strong VSL actions, i.e., to create an MTFC bottleneck, while similar VSL actions as in Scenario 11 are applied in all other controllable links. In other words, AMOC recognises MTFC upstream of the A1/A10 bottleneck as the major control measure to undertake and applies it to L98–L100 since L101 and L102 are not available for control. The resulting TTS in this case amounts to 7,566 veh·h, slightly higher than in Scenario 11.

In conclusion, the sub-scenarios of Table 5.4 underline the importance and potential of MTFC, i.e., the possibility to obtain a significant amelioration of the motorway traffic conditions by creating deliberately controlled mainstream congestion at the right time(s) and location(s).

5.2.6 Integrated Traffic Control

The application of both ramp metering and MTFC via VSLs, i.e., integrated traffic control, is considered in this section, with different combinations of available ramp storage. The results for the corresponding Scenarios 12–21 are presented in Table 5.3 and Figure 5.15. Scenario 12 achieves the best TTS among all presented scenarios, 6996 veh·h, which is an improvement of 50.6 percent compared to the no-control case. The TTS values in the other scenarios converge to Scenario 12 as ramp storage is increased. As a matter of fact, Scenario 12 has very similar queue and density profiles as Scenario 1, since VSL control is barely applied; with unlimited ramp queue storage, coordinated ramp metering is preferable to MTFC via VSLs since, as discussed in Section 3, ramp metering with sufficient storage space dissolves the mainstream congestion completely and hence avoids blocking of off-ramps upstream of the bottleneck location.

When on-ramps have very limited storage space, integrated control is seen to substantially improve the TTS compared to scenarios with ramp metering only (compare TTS values for Scenarios 2 versus 13, and Scenarios 3 versus 14). Density and ramp queue profiles for Scenario 13 are shown in Figure 5.18 while the optimal corresponding VSL rate trajectories are shown in Figure 5.19. As expected the mainline (controlled) congestion in Scenario 13 is smaller than in Scenario 11 (Figure 5.18) because, roughly speaking, the vehicles stored in the on-ramps are taken out of the mainline congestion. The resulting (not controlled) mtm on-ramp queues are very small or non-existent and admissible ramp queues are respected, except for O5 (on-ramp 6 in Figure 5.18(b)) where some exceed the queue constraints seems unavoidable due to limited ramp storage, high ramp demand and the spill-back of downstream congestion. However, compared to the corresponding fellow Scenario 2 where queues were exceeding 600 vehicles at the O4 mtm on-ramp, results are significantly better thanks to the addition of MTFC.

The VSL rates for Scenario 13 (Figure 5.19) are very close to the VSL rates of Scenario 11 (Figure 5.19). The main area for strong VSL-application remains at links L101 and L102, upstream of the A1/A10 bottleneck. The strong and short VSL activation at L98 during the second congestion period that was observed in Scenario 11 is not present here while a new one is now created at L87. Evidently, these minor control variations result due to the additional application of ramp metering.

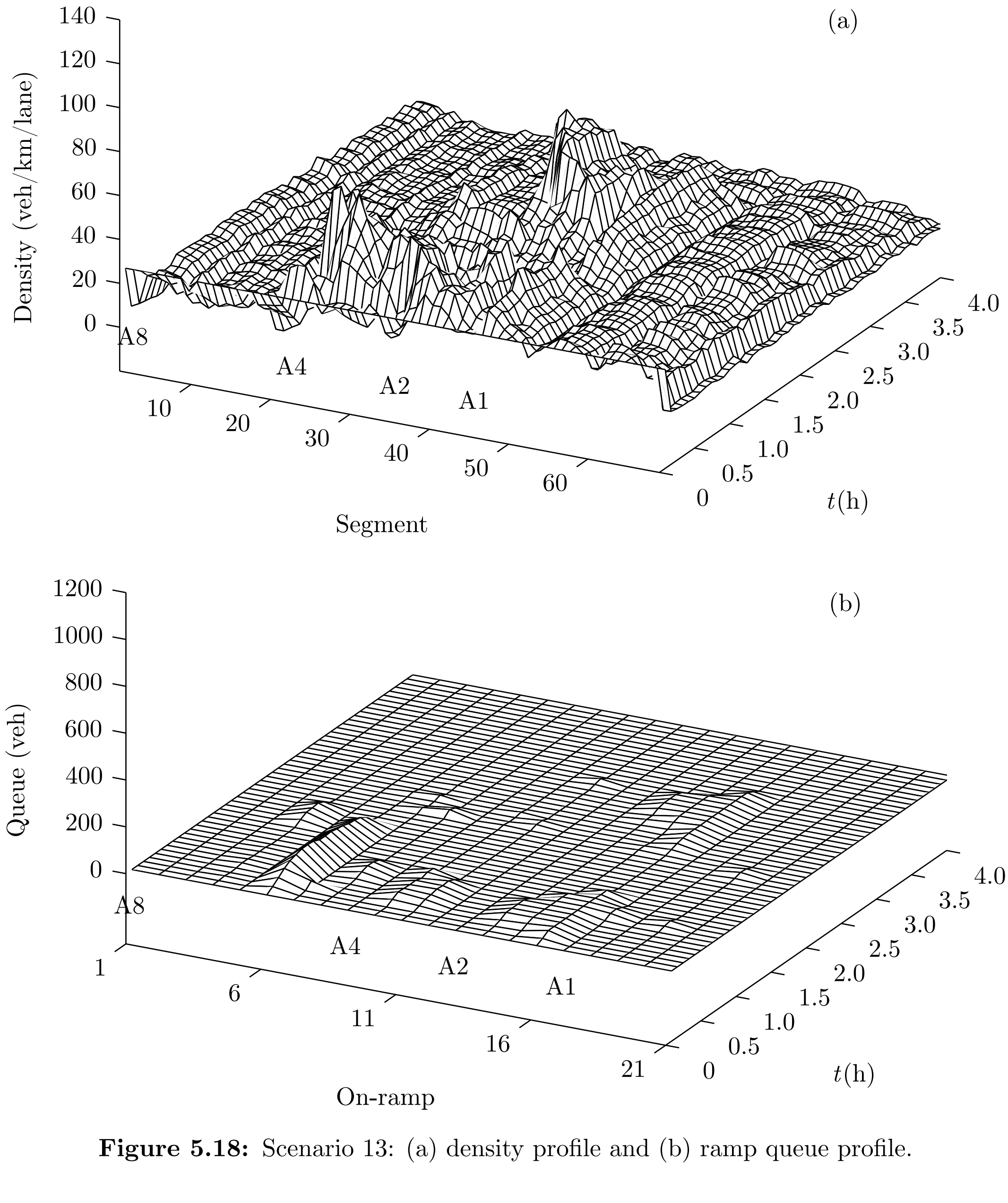

Figure 5.18: Scenario 13: (a) density profile and (b) ramp queue profile.

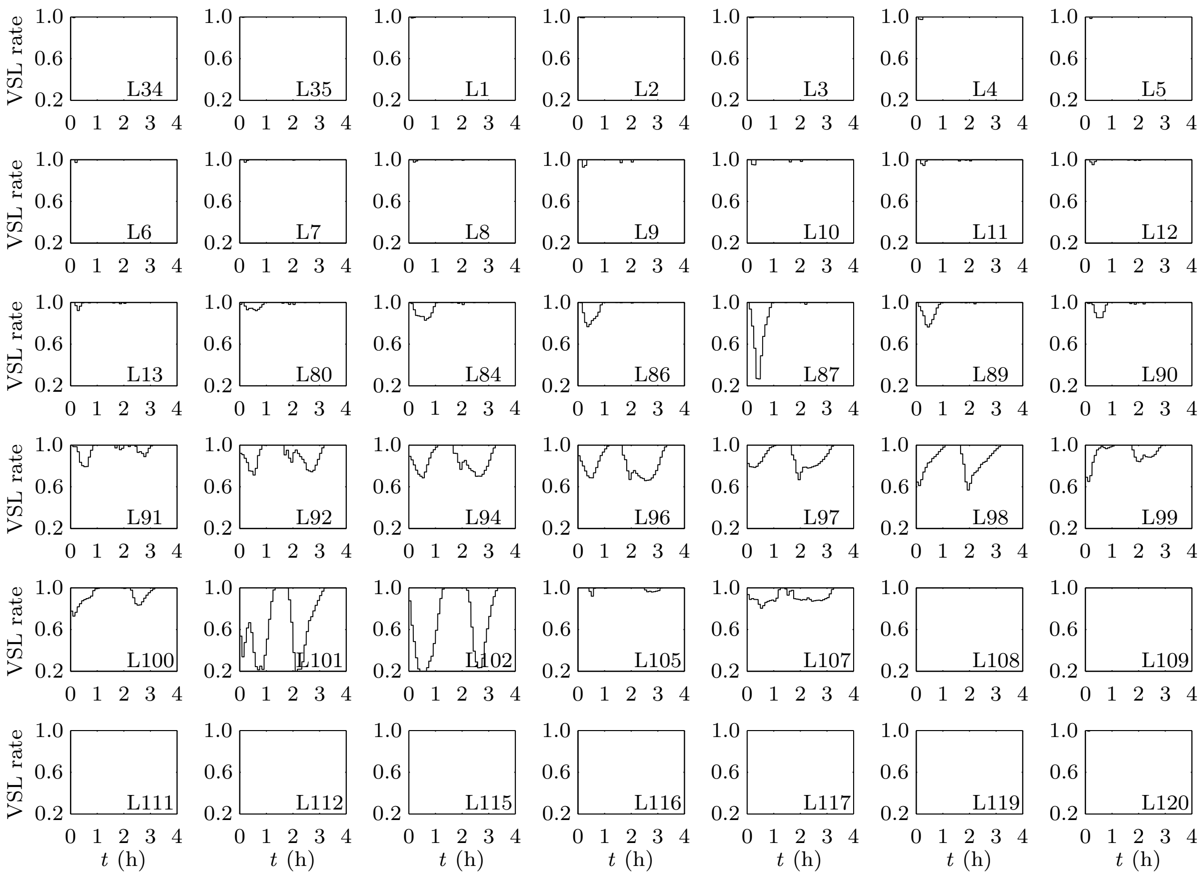

Figure 5.19: Scenario 13: VSL rate trajectories.

Chapter 6

Feedback Control Results

In some cases, proposed traffic control strategies are not even thoroughly and properly tested via simulation (...)

M. Papageorgiou [52]

In this chapter the feedback controllers developed in Chapter 4 are evaluated and compared in simulation. The feedback controllers also have their efficiency compared to the optimal control approach of Section 2.4. In Section 6.1 the Cascade Controller is first evaluated for an hypothetical motorway and hypothetical demand under all possible traffic flow conditions (free flow, critical, and congested). The analysis in this section covers several aspects and the capabilities of MTFC by the use of feedback control and VSLs. In Section 6.2 all three feedback controllers and the optimal controller are evaluated and compared using more strongly time-varying demands and turning rates with added noise. The aim is at demonstrating the feedback controller performance under more dynamically changing conditions. Several of the practical aspects discussed in Section 4.7 are investigated in this section and, based on the simulations results, additional recommendations are provided for the operation of the feedback controllers.

6.1 Cascade Feedback Control

This section presents the simulation results obtained with the METANET simulator and the AMOC optimal control tool presented in Sections 2.3 and 2.4 for various control scenarios, including application of the Cascade Controller developed in Chapter 4.

6.1.1 Network Model and Demand

A hypothetical 21.5 km long three-lane motorway stretch, depicted in Figure 6.1 (upper part), is used in the simulations that follow. The mainstream is divided in 15 links (L00–L14). There are two on-ramps (O1 and O2) and one off-ramp (D1) in-between. The main area where congestion is formed and MTFC is applied is zoomed in Figure 6.1 (lower part). The long stretch upstream of this area was added to allow for the application of upstream VSLs due to safety reasons. In Figure 6.1 (lower part) the potentially active bottleneck is the merge area of on-ramp O2, which receives both the mainstream flow from upstream and the O2 merging flow. Only the arriving mainstream flow is controlled (using MTFC via VSLs) in the reported simulations while (in absence of ramp-metering), the O1 and O2 flows are not controlled in the investigations that follow. The VSL application area (for MTFC) and the acceleration area, as well as both measurements for cascade control are also indicated in the lower part of Figure 6.1.

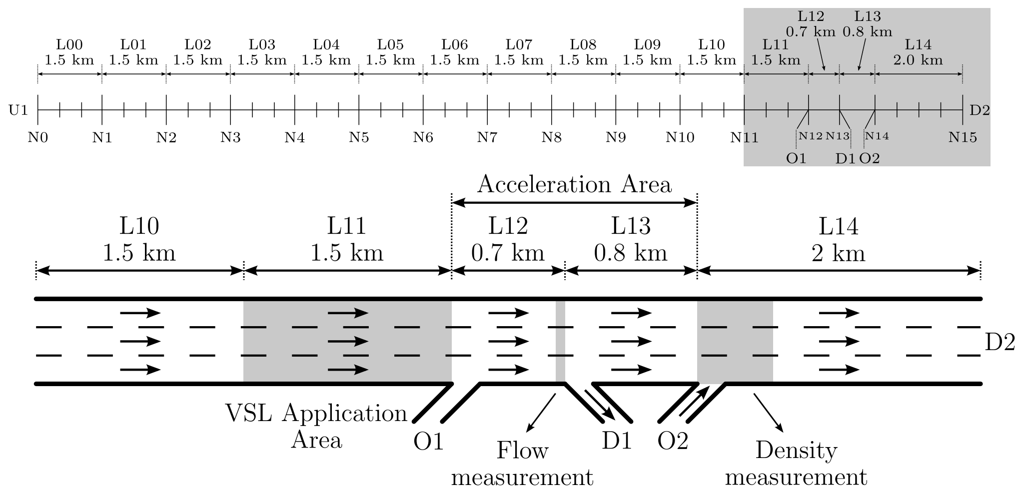

Figure 6.1: Hypothetical motorway stretch.

The demand profiles displayed in Figure 6.2 are used for the motorway input (U1) and for both on-ramps and extend over a 2.5-hour simulation horizon, whereby the last 30 min represent a cool-down period with reduced flows in the network entrances, which was introduced in order to have equal traffic conditions on the stretch at the end of the simulation, and hence comparable TTS values for all investigated scenarios. The demand scenario allows for control testing under all possible traffic flow conditions (free, critical, congested). The exit rate, i.e., the percentage of the mainstream flow that leaves the motorway at the off-ramp D1, is set to 8 percent; the model time step is $T = 10$ s, while the control time step is $T_c = 60$ s for all controlled scenarios. The model parameters were provided in Section 2.3. In particular, the

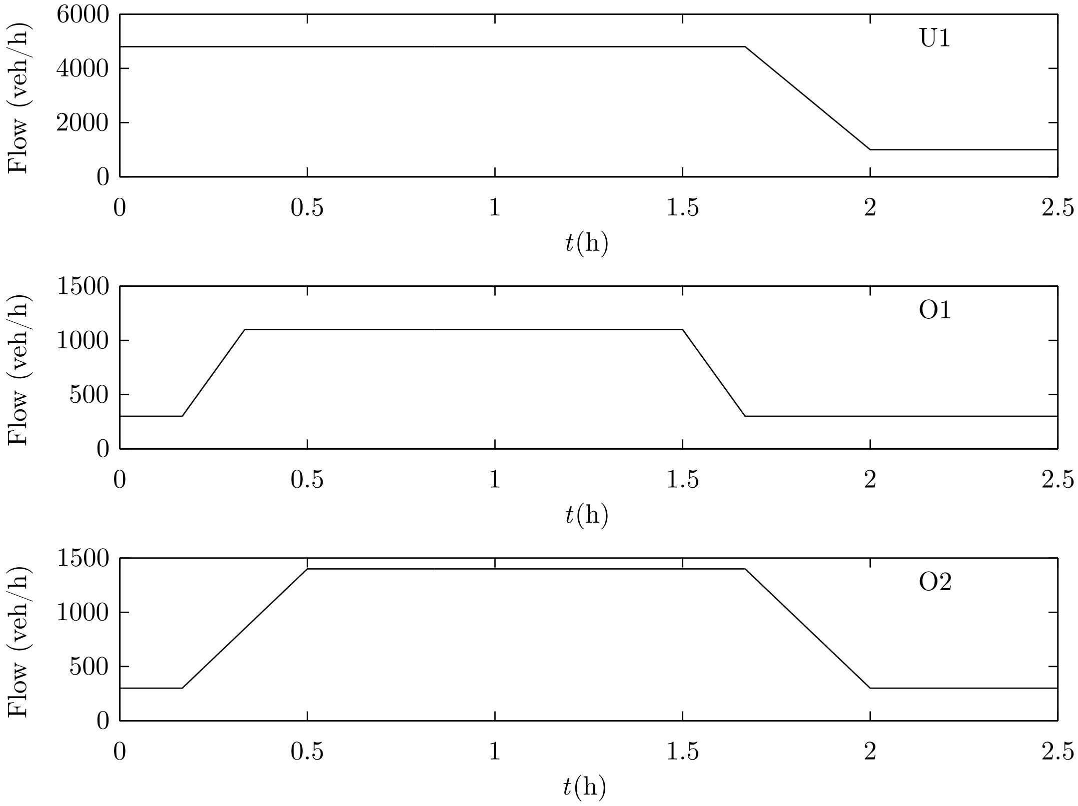

Figure 6.2: Demands at the network origins.

modelled impact of VSLs on the fundamental diagram is according to Figure 2.6.

A number of different control scenarios are examined in the following, each for a time horizon of 2.5 hours, using METANET for no-control and feedback control, and AMOC for optimal control. First the network is simulated for no-control (as a basic reference case) and then for optimal control (as an upper limit of achievable performance under ideal conditions). Next, three scenarios are simulated for feedback control, starting with the MTFC system in its simplest form and incorporating gradually features necessary to address practical concerns. This gradual investigation allows for the quantification of the impact of specific practical procedures on the efficiency (TTS) of the feedback concept. The scenarios and the respective TTS results are summarised in Table 6.1.

6.1.2 No-control

This is the basic reference case that allows any potential improvements of MTFC to be quantified. When no control measures are applied, the resulting density, speed and flow profiles for both on-ramp merge areas are shown in Figure 6.3. The flow in the merge area

Table 6.1: Summary of simulated control scenarios.

Strategy	Description	TTS (veh·h)	%
No-control	-	3,540	-
Scenario 1	Optimal MTFC via VSLs (AMOC) applied at L11 and at L12-L13-L14.	2,993	−15.4
Scenario 2	Feedback MTFC via VSLs applied at L11.	3,015	−14.8
Scenario 3	As Scenario 2, but with discrete speed limits and limited rate of change.	3,016	−14.8
Scenario 4	As Scenario 3, but with lower speed limit downstream (L12-L13-L14).	3,021	−14.7
Scenario 5	As Scenario 4, but with safety speed limits upstream.	3,004	−15.1

of O2 is seen to reach the factual capacity (6,240 veh/h) at $t = 0.4$ h but, as arriving flows continue to increase, a mainstream congestion appears after $t = 0.5$ h in the merge area of the O2 on-ramp; this leads to a visible gradual mainstream flow decrease (capacity drop). The created congestion (shock wave) travels upstream and reaches the merge area of the O1 on-ramp at around $t = 0.7$ h, leading to a visible speed drop and flow decrease there as well. The congestion lasts for 1.7 h and extends about 13 km upstream of the O2 on-ramp. The resulting TTS is equal to 3,540 veh·h.

6.1.3 Scenario 1 (Optimal Control)

As stated earlier, the derivation of optimal MTFC (via AMOC) is based on ideal assumptions (perfect model and demand/turning rate predictions) and provides therefore an upper limit of achievable performance that allows for simpler feedback concepts to be assessed in terms of efficiency (TTS) and control reactions.

For the application of MTFC via VSLs using optimal control, the concerned mainstream area in Figure 6.1 is divided into two clusters of links. The first cluster comprises L11, and the second cluster comprises L12, L13 and L14. All other links are left uncontrolled. Although AMOC achieves similar performance for higher control periods (see Chapter 5), the same control period T_c that will be used for feedback control is used here, i.e., the VSL rates are allowed to change every 60 s. The minimum admissible VSL rate is $b_{\min,m} = 0.2$. Note that, in this section of the thesis, results for higher values of minimum admissible VSL rate, e.g., $b_{\min,m} = 0.5$, are omitted. Higher values limit the performance of MTFC, since, for the severe congestions seen in the no-control scenario above, the resulting improvement would be

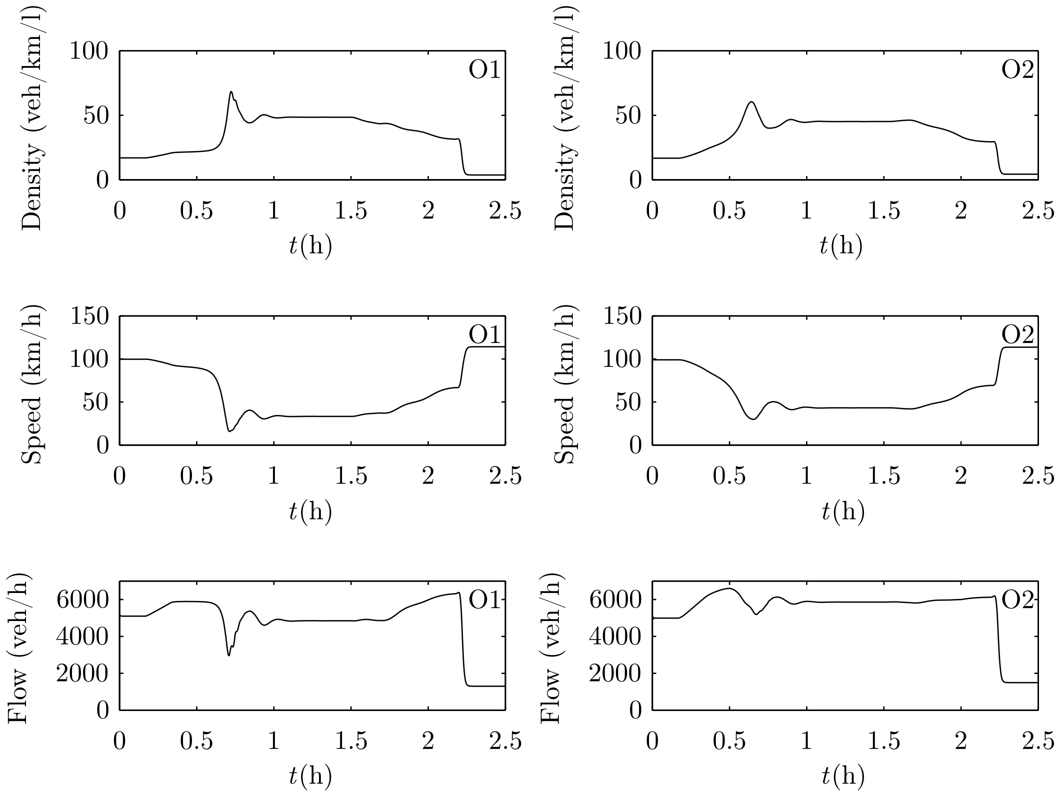

Figure 6.3: No-control: traffic conditions at the merge-areas.

limited to postponing (rather than avoiding) the bottleneck congestion, as already observed in 5.1.

The resulting TTS for this scenario is 2,993 veh·h, which is a 15.4 percent improvement compared to the no-control case. The related density, speed and flow profiles for both merge areas are shown in Figure 6.4, while the optimal VSL rate trajectories are shown in Figure 6.5(a).

The situation is identical to the no-control case until short before $t = 0.5$ h, but eventually the optimal solution maintains the density and flow at the O2 merge area close to the critical density and factual capacity value, respectively, in order to maximise the motorway exit flow (which leads to minimisation of TTS). At around $t = 0.5$ h, the VSL rate at the L12-L13-L14 cluster is seen to switch gradually to values around 0.95; this allows the O2 merge area to accommodate a higher number of vehicles (due to higher critical density) with hardly any loss in flow capacity (Figure 2.6).

In order to keep the O2 merge area density close to its (increased) critical density, the VSL rate for L11 is seen in Figure 6.5(a) to switch gradually from 1.0 to almost 0.2 (the lower admissible bound), thus creating a controlled mainstream congestion upstream of the acceleration area. In fact, the (factual) mainstream capacity under MTFC control is lower

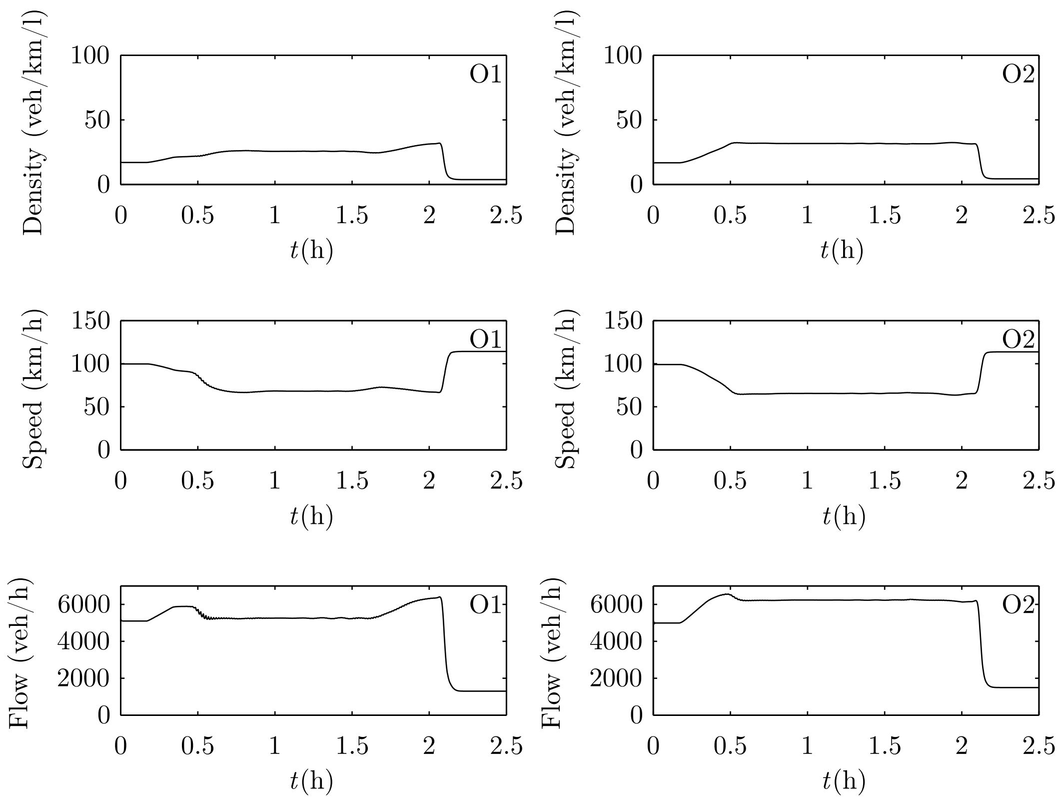

Figure 6.4: Scenario 1: traffic conditions at the merge-areas.

than the arriving demand, leading to a durable flow reduction, such that the O2 merge area density is maintained near critical values with capacity flow. The controlled congestion extends over some 8 km for some 1.5 h, which is smaller (in space and time) than in the no-control case, but has also higher internal speed (due to higher outflows).

6.1.4 Scenario 2

Cascade feedback MTFC via VSLs is now applied in its simplest form, i.e., speed limits assume real values within the admissible VSL rates range, as in Scenario 1 (Optimal Control), but are applied only at the application area (L11). The set-point for the primary controller is $\hat{\rho}_{\mathrm{out}} = 30$ veh/km/lane.

The resulting TTS for this scenario is 3,015 veh·h, which is a 14.8 percent improvement compared to the no-control case, and very close to Scenario 1, even though the cluster L12–L13–L14 is left uncontrolled. The related density, speed and flow profiles for both merge areas are shown in Figure 6.6 while the feedback VSL rate trajectories are shown in Figure 6.5(b).

The interpretation of these results is very similar to the previous scenario with some slight

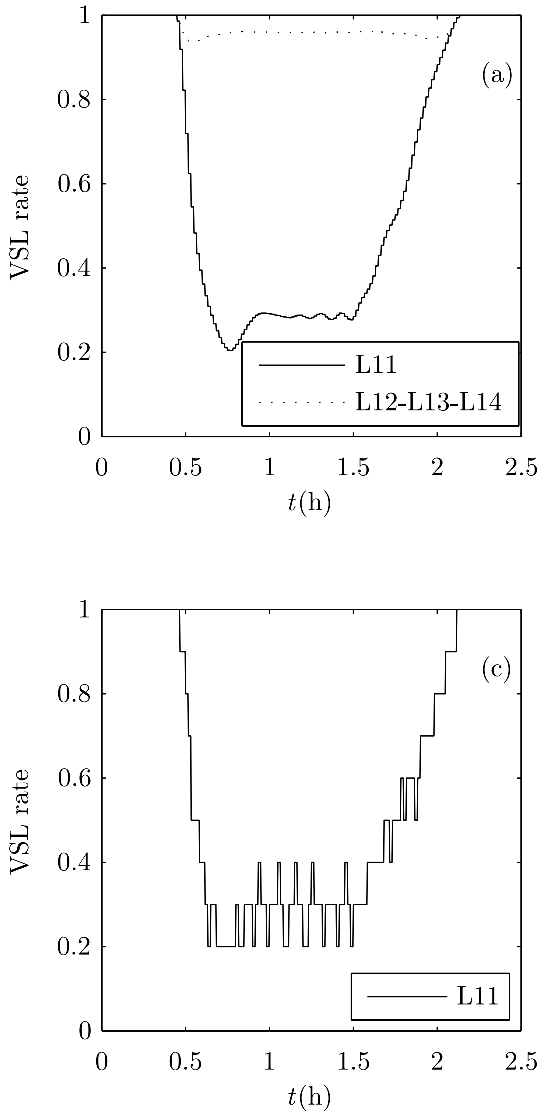

Figure 6.5: VSL rates: (a) Scenario 1; (b) Scenario 2; and (c) Scenario 3.

differences. In this scenario, the density at the O2 merge-area (Figure 6.6) is seen to slightly overshoot the set-point $\hat{\rho}_{\mathrm{out}}$ (dashed line in the O2 merge-area density plot). This overshoot may be influenced by the choice of the integral gain K_{I}' of the primary controller, as is usual for PI controllers. The VSL rate at L11 (Figure 6.5(b)) is seen to gradually decrease from 1.0, but this time it stays on the lower bound for a few control periods. The effect of VSLs on the controlled variable q_{c} can be seen in the flow plot of the O1 merge-area (Figure 6.6). On the same diagram, the dashed line shows the output $\hat{q}_{\mathrm{c}}$ of the primary controller which serves as a reference for the secondary controller, and, indeed, is followed very closely by the controlled variable whenever possible (i.e., when there is sufficient demand). The VSL control starts releasing a few minutes later than in the previous scenario.

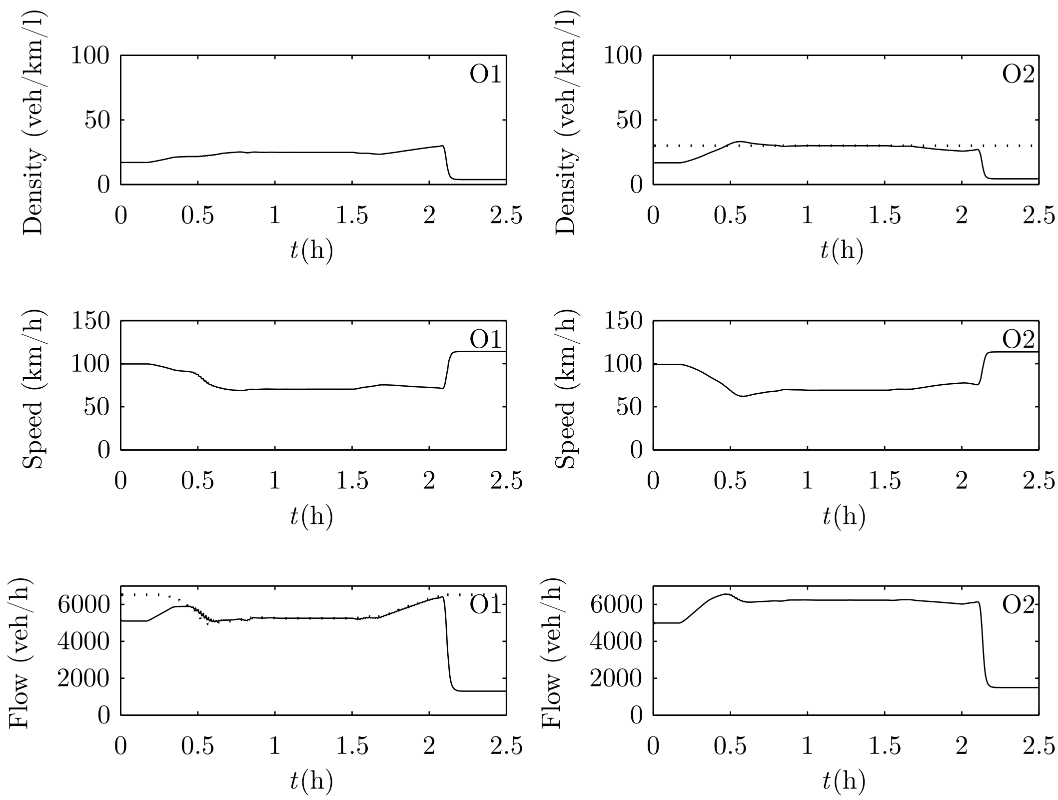

Figure 6.6: Scenario 2: traffic conditions at the merge-areas.

6.1.5 Scenario 3

In this scenario, cascade feedback MTFC via VSLs is applied in the same way as in Scenario 2, except that the speed limits assume discrete values according to Section 4.7.1, and the difference between two consecutive posted VSL rates at the same speed limit panel are limited, as discussed in Section 4.7.2.

The resulting TTS for this scenario is 3,016 veh·h, which is a 14.8 percent improvement compared to the no-control case, and virtually identical to Scenario 2. The related density, speed and flow profiles for both merge areas are omitted, since the only difference from the previous scenario is that the traffic variables are more scattered around the values observed in Figure 6.6 (see Section 6.2 for additional figures with scattered traffic variables). This is due to stronger (discrete-valued) changes of the VSL rate trajectory, as observed in Figure 6.5(c). Thus, constraining the VSL rates and their changes in time to discrete and maximum values, respectively, has hardly any impact on the controller efficiency.

6.1.6 Scenario 4

This scenario is similar to Scenario 3, the only difference being that VSLs are now also applied to links L12, L13 (the acceleration area) and L14 (the bottleneck area) according to Section 4.7.4. More specifically, the VSL rate in these links is set equal to 0.9, whenever a VSL is activated at L11. Note that:

- The optimal control solution (Scenario 1, Figure 6.5(a)) established a (virtually constant) value of 0.95 for links L12, L13, L14.
- In the present case, it is assumed, according to Figure 2.6, that no VSL value increases the motorway capacity.
- The set-point for the cascade controller was increased to $\hat{\rho}_{\text{out}} = 32$ veh/km/lane in this scenario to account for the increase of the critical density (according to Figure 2.6) due to the application of a VSL rate equal to 0.9.

The resulting TTS for this scenario is 3,021 veh·h, which is a 14.7 percent improvement compared to the no-control case, and again, virtually the same as Scenario 1 and Scenario 2. An additional improvement would be achievable if the employed VSLs would increase the motorway capacity as investigated in Section 6.2.4.

6.1.7 Scenario 5

Scenario 5 extends Scenario 4 by also applying VSLs upstream of the application area for safety reasons according to Section 3.4.4. Each upstream link from L01 to L10 is considered to include an individual VSL, and only L00 is left uncontrollable. These link-specific VSLs are operated in this scenario according to the rules of Section 4.7.3.

The resulting TTS for this scenario is 3,004 veh·h, which is a 15.1 percent improvement compared to the no-control case and virtually the same as in Scenario 1. The related density, speed, and flow profiles are quite similar to the previous ones and are, therefore, omitted. Figure 6.7 depicts the VSL rates for all links in this scenario. It can be seen that, as long as the VSL of the application area (L11) is active, the downstream VSLs (L12–L13–L14) are switched to a constant value of 0.9 according to Section 4.7.4. The upstream VSLs, on the other hand, are activated gradually to values that are in accordance with the rules of Section 4.7.3, so as to reduce the speed gradients and improve the safety conditions for

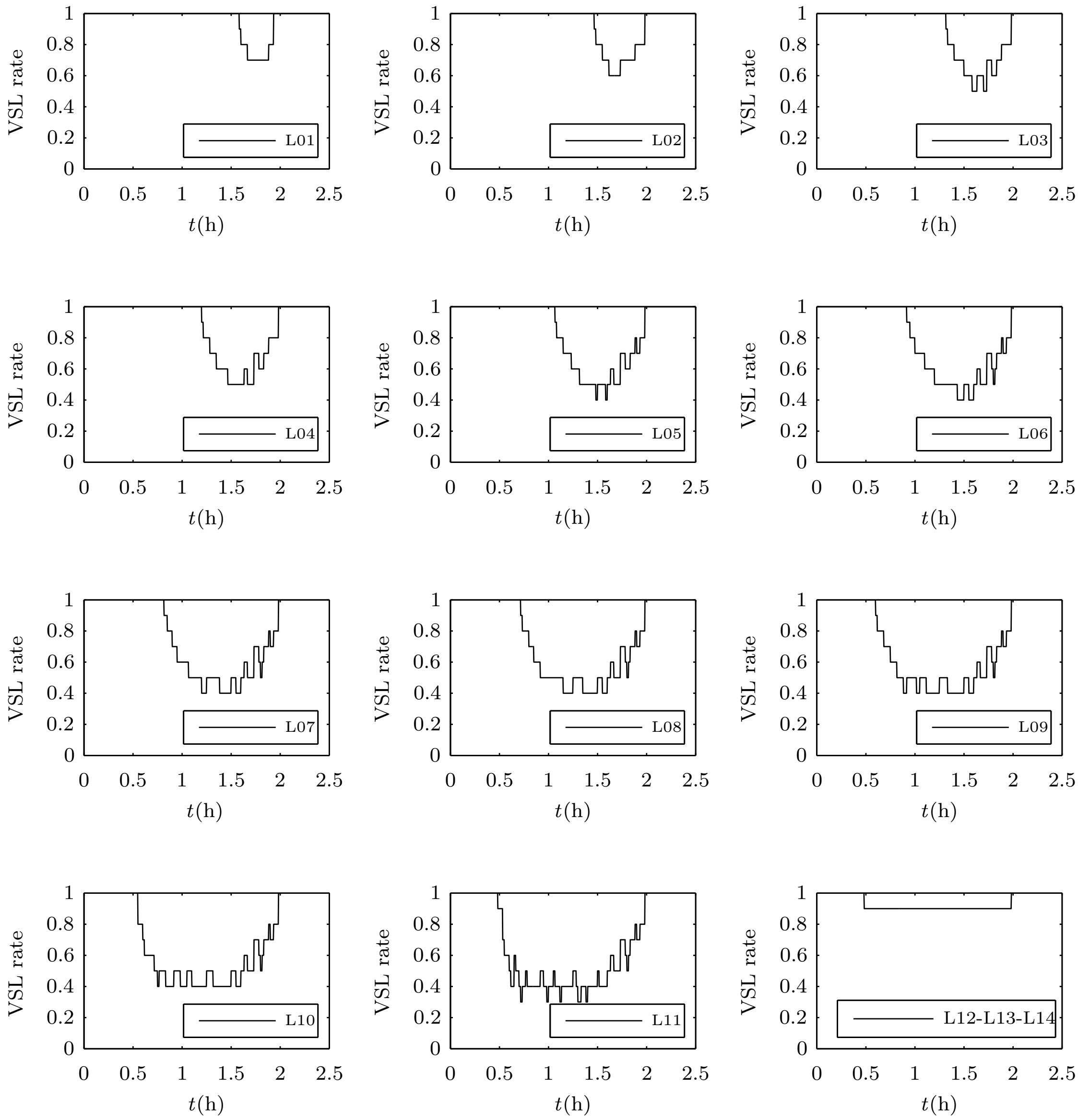

Figure 6.7: Scenario 5: VSL rates given by the feedback controller.

vehicles arriving from upstream. In fact, Figure 6.8 compares this scenario with the no-control scenario by means of a snapshot of speeds at $t = 1.5$ h. This time instant is close to the time of the maximum reach of the congestion in the no-control case and also close to the start of the gradual release of the feedback controller. It may be seen that the VSLs comply with the rules of Section 4.7.3 and that the spatial speed gradients are accordingly moderate in the MTFC case. In contrast, a huge gradient (from 100 km/h to 20 km/h within 1 km) is observed at distance 8–9 km in the no-control case, which may bear safety risks for vehicles approaching the tail of the uncontrolled congestion. It may also be seen in Figure 6.8 that the MTFC controlled congestion has higher internal speed than the uncontrolled congestion. This

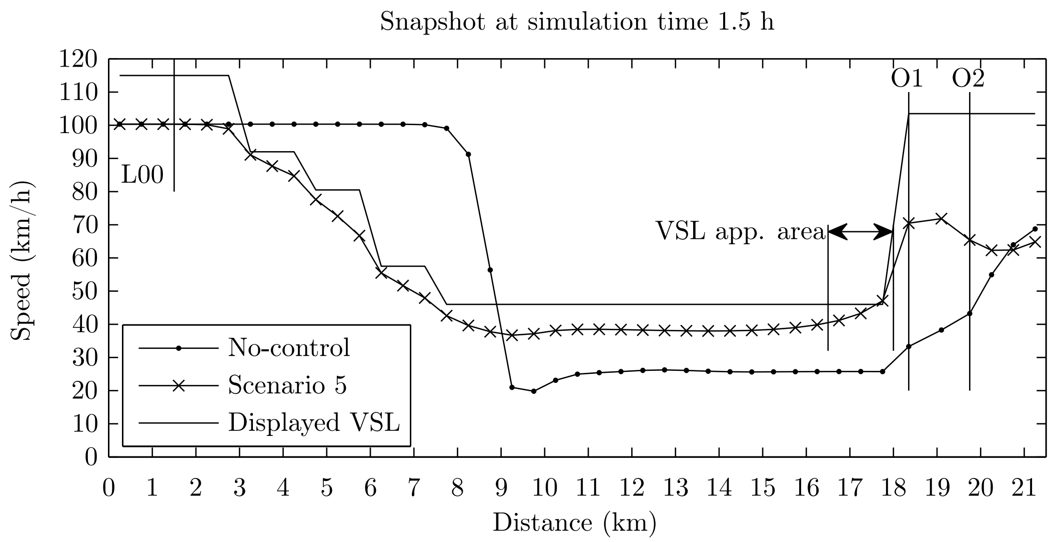

Figure 6.8: Comparison of speeds between Scenario 5 and No-control at simulation time 1.5 h.

was indeed observed for every controlled scenario and is visible in Figure 6.8 for kilometres 9.0–20.0.

The source of the demonstrated benefits of MTFC can be evidenced by contrasting the outflows at D1 (off-ramp) and D2 (mainstream exit) of the no-control scenario with the controlled scenarios as in Figure 6.9. The no-control case features clearly lower throughput at both motorway exits, which is due to capacity drop (at D2) and due to lower congestion flow (at D1) compared with the control scenarios. As a consequence, Scenario 1 and Scenario 5 are seen to have vehicles exiting the network earlier than in the no-control case which is the reason for the accordingly reduced TTS. At D1, the outflow of Scenario 5 is seen to vary around the outflow established by the optimal control (Scenario 1) due to the discretisation of the VSL rates delivered by the feedback controller; while at D2 the outflows of both control scenarios are very close to each other.

The absence of on/off-ramps in the long stretch upstream of the O1 merge area is certainly an unrealistic simplification. However, this simplification is "harmful" for MTFC since, except for D1, there is no further degradation due to BOR effects.

6.2 Comparison of MTFC Feedback Controllers

In this section, the features of all three proposed MTFC feedback controllers are demonstrated and evaluated in a simulation-based test for a hypothetical motorway stretch using the METANET simulator (Section 2.3). The feedback controllers are compared between

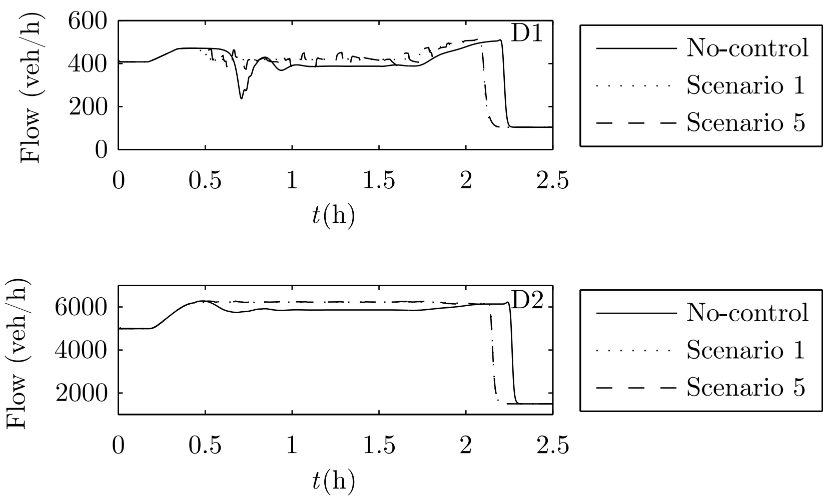

Figure 6.9: Motorway outflows for No-control, Scenario 1 and Scenario 5.

them, and their efficiency is also compared against an optimal control approach, via the optimal control tool AMOC [38] (Section 2.4).

In the previous section, the control scenarios explored MTFC via VSLs in a motorway under all possible traffic conditions, free flow, critical and congested. However, the used demands and exit rates (at D1) were deterministic and indeed constant over long periods. In this section a new demand scenario that reflects a more realistic situation where the demand and exit rate are noisy and also subject to strong time-variations. Hence, the dynamic properties of the feedback controllers are more challenged by this case.

A number of different control scenarios are examined for a hypothetical motorway network and demand, each for a time horizon of 3 hours, using METANET for the no-control and feedback control cases, and AMOC for optimal control.

First, the network is simulated for five basic control scenarios: for no-control as a base reference, for optimal control as an upper limit of achievable performance under ideal conditions, and for each of the three feedback controllers, i.e., the Cascade Controller, the Lookup Controller and the PI Controller.

Eventually, additional simulations elaborate on the issues discussed in Section 4.7, namely the choice of the control period, the exploitation of possible VSL-induced capacity increases, and the robustness of the Lookup Controller to mismatches in the lookup table. Finally, based on the achieved results, some recommendations are given with respect to the use and operation of the feedback controllers.

The model parameters used in the simulation were taken from Section 2.3, and the modelled impact of VSLs on the fundamental diagram is according to Figure 2.6 for all scenarios without capacity increase. In the case of increase of capacity, appropriate parameter values, as obtained from real data (see Section 6.2.4), are used, and the modelled impact of VSLs on the fundamental diagram is according to Figure 4.7.

6.2.1 Network Model and Demand

The simulated hypothetical network is exactly the same as the one used in Section 6.1 and depicted in Figure 6.1. The demand profiles and exit rates displayed in Figure 6.10 are used for the motorway input (U1) and for both on-ramps (O1 and O2) and the off-ramp (D1); and extend over a 3-hour simulation horizon, whereby the last hour represents a cool-down period with reduced flows in the network entrances and constant (average) exit rates, which was introduced in order to have equal traffic conditions on the stretch at the end of the simulation, and hence comparable TTS values, for all investigated scenarios. The demand scenario allows for control testing under all possible traffic flow conditions (free, critical, congested), including dynamic transitions among them. The model time step is $T = 10$ s. The minimum admissible VSL rate is $b_{\min,m} = 0.2$ for all scenarios. The control period, that determines the frequency of posted VSL changes, is chosen as $T_c = 60$ s, except where otherwise stated.

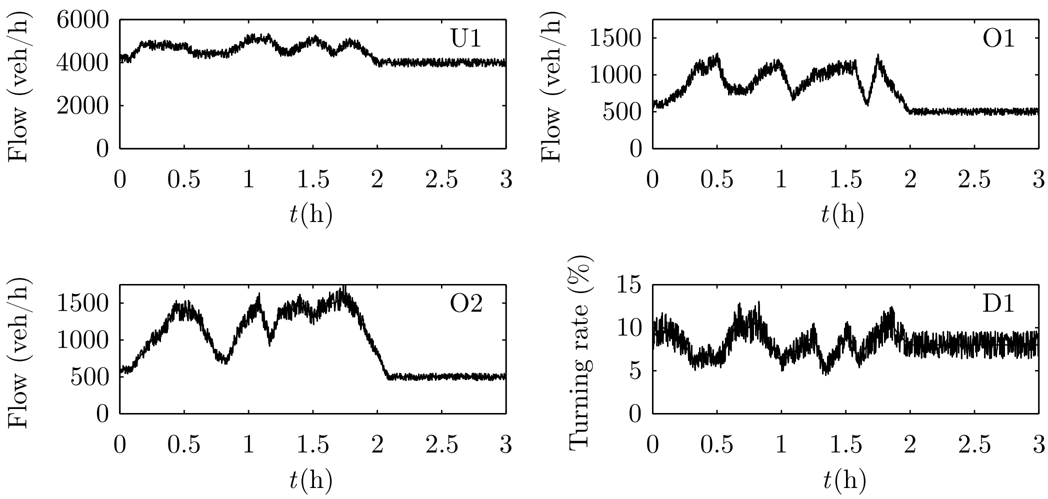

Figure 6.10: Demands at the network origins and turning rates.

6.2.2 Basic Scenarios

The simulated basic scenarios and respective results are summarised in Table 6.2.

Table 6.2: Summary of simulated basic scenarios.

Strategy	Description	TTS (veh·h)	%
No-control	-	4,196	-
AMOC	Optimal MTFC via VSLs applied at L11 and at L12-L13-L14.	3,363	−19.8
Cascade Controller	Feedback MTFC via VSLs applied at L11 with the VSLs restrictions of Section 4.7.	3,370	−19.7
Lookup Controller	Feedback MTFC via VSLs applied at L11 with the VSLs restrictions of Section 4.7.	3,376	−19.5
PI Controller	Feedback MTFC via VSLs applied at L11 with the VSLs restrictions of Section 4.7.	3,410	−18.7

6.2.2.1 No-control

This is the basic reference case that allows for any potential improvements of MTFC to be quantified. In absence of control, the resulting density and flow profiles for both on-ramp merge areas are shown in Figure 6.11. The flow in the merge area of O2 reaches the factual capacity (6,240 veh/h) at $t = 0.4$ h, and, despite the strong reduction of inflow at the origins and increase of exit rate at D1 that follows, a continuous mainstream congestion appears there after $t = 0.5$ h; this leads to a visible gradual mainstream flow decrease (capacity drop). The tail of the created congestion (shock wave) travels upstream and reaches the merge area of the O1 on-ramp at around $t = 0.6$ h, leading to a visible flow decrease there as well. Note that, despite the low demand entering the network after $t = 2$ h, it takes about 40 minutes before congestion is completely dissolved. The resulting TTS is equal to 4,196 veh·h.

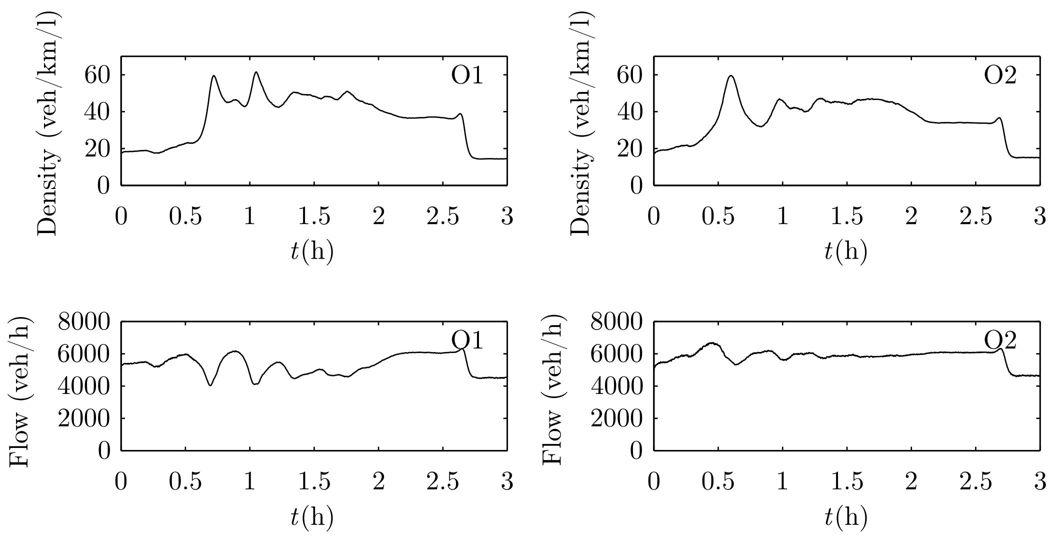

Figure 6.11: No control: traffic conditions at the merge areas.

6.2.2.2 Optimal Control (AMOC)

The control setup is the same that was applied in Section 6.1.3. The resulting TTS for this scenario is 3,363 veh·h, which is a 19.8 percent improvement compared to the no-control case. The related density and flow profiles for both merge areas are shown in Figure 6.12, while the optimal VSL rate trajectories are shown in Figure 6.13(a). The situation is identical to the no-control case until $t = 0.4$ h, when VSL is first activated (Figure 6.13(a)) at both clusters of links so as to increase the critical density in the merge area of O1 and to decrease the flow arriving at the bottleneck, respectively. This short VSL action is sufficient to avoid the onset of congestion, and thus further VSL action is barely needed for the next 20 minutes. (Recall that in the no-control case the first demand peak creates a congestion that lasts uninterrupted for the next two hours despite the intermediate decrease in the demand.) A second control action is started short before $t = 1.3$ h, this time stronger and more durable, leading to VSL rates lower than 0.3. The bottleneck congestion is again avoided and the outflow is maintained close to capacity (Figure 6.12) by maintaining the bottleneck density close to its critical value.

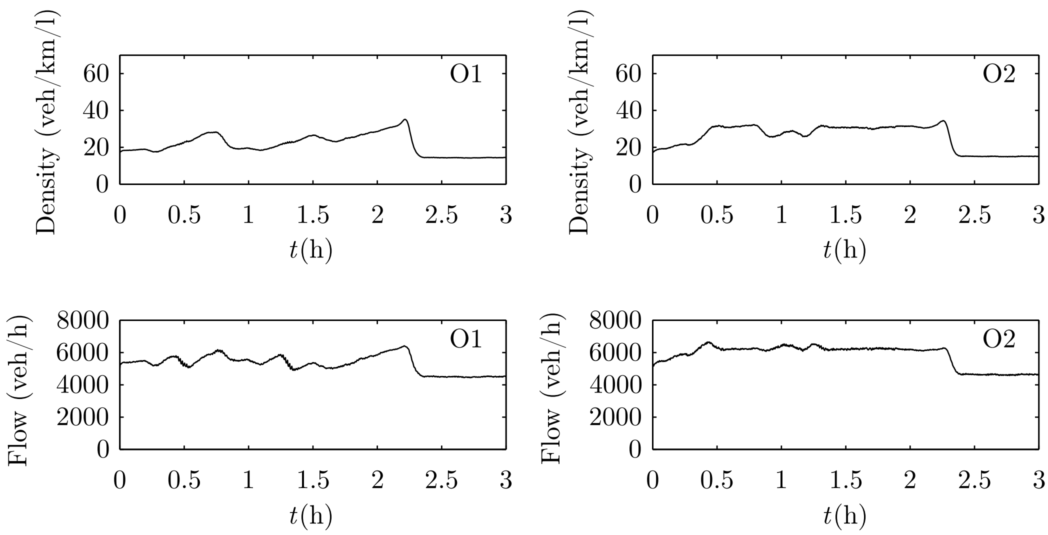

Figure 6.12: AMOC: traffic conditions at the merge areas.

6.2.2.3 Cascade Controller

The control setup is the same that was applied in Section 6.1.7. The resulting TTS is 3,370 veh·h, which is a 19.7 percent improvement compared to the no-control case and very close to the corresponding optimal control scenario. The related density and flow profiles for both merge areas are shown in Figure 6.14, while the feedback VSL rate trajectories are shown in

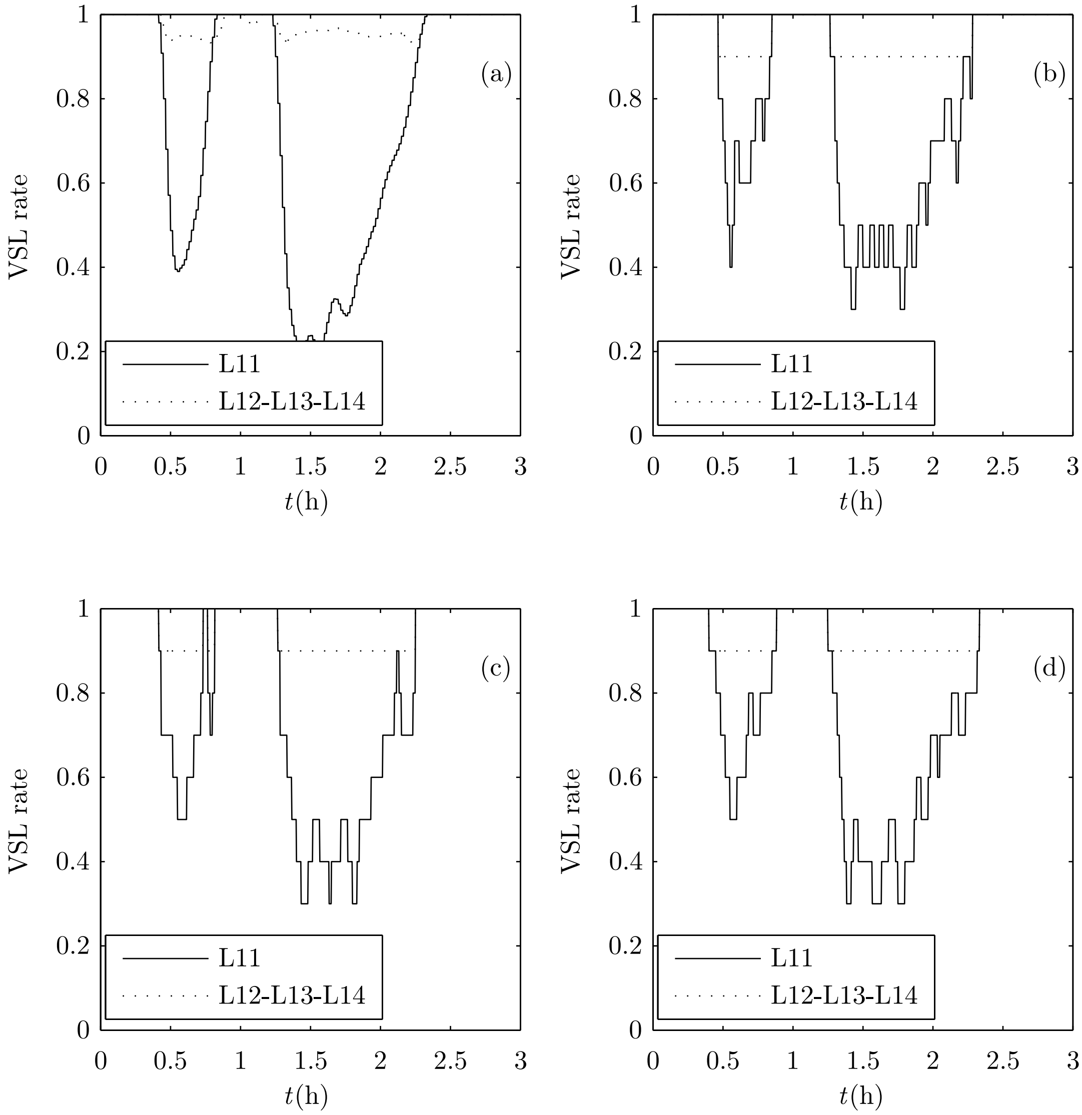

Figure 6.13: VSL rates: (a) AMOC; (b) Cascade Controller; (c) Lookup Controller; and (d) PI Controller.

Figure 6.13(b). The interpretation of these results is similar to the previous scenario with some slight differences. In this scenario, the density at the O2 merge-area (Figure 6.14) is seen to slightly overshoot the set-point $\hat{\rho}_{\text{out}}$ (dashed line in the density plot) at both occasions where VSL is first activated. Also, the traffic variable values are more scattered around values close to the ones of Figure 6.12 because of the discrete-valued changes of the VSL rate trajectory (Figure 6.13(b)). The effect of VSLs on the controlled variable q_{c} can be seen in the flow plot of the O1 merge-area (Figure 6.14). On the same diagram, the dashed line shows the output $\hat{q}_{\text{c}}$ of the primary controller which serves as a reference for the secondary controller, and, indeed, is followed very closely by the controlled variable whenever possible.

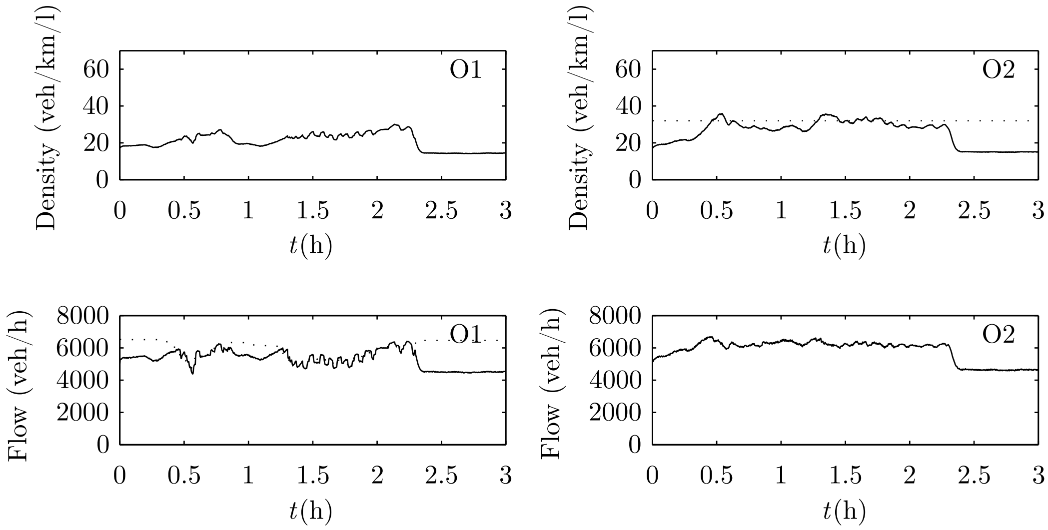

Figure 6.14: Cascade Controller: traffic conditions at the merge areas.

6.2.2.4 Lookup Controller

In this section, the Cascade Controller is replaced by the Lookup Controller (Section 4.4). The clusters of links are the same as before and the VSL rate delivered by the controller by means of the lookup table (Figure 4.6) is applied at L11. The set-point remains unchanged. The density measurement is taken as shown in Figure 6.1, while the flow measurement is not needed. The controller gains are the same as for the primary controller of the cascade structure.

The resulting TTS is 3,376 veh·h, which is a 19.5 percent improvement compared to the no-control case and very close to the Cascade Controller case. The related density and flow profiles for both merge areas are shown in Figure 6.15, while the feedback VSL rate trajectories are shown in Figure 6.13(c). Again, the interpretation of these results is very similar to the previous control scenarios with some slight differences. In this scenario, the density at the O2 merge-area (Figure 6.15) exhibits a stronger overshoot over the set-point $\hat{\rho}_{\text{out}}$, along with some more pronounced departures from the set-point at the second VSL action. Remarkably, the Lookup Controller (Figure 6.13(c)) VSL rate is subject to (slightly) less variation than the corresponding trajectory of the Cascade Controller (Figure 6.13(b)). This may be due to the fact that the lookup table is insensitive to variations of flow in the acceleration area, while the Cascade Controller has some sensitivity, because of the flow measurement of the secondary controller.

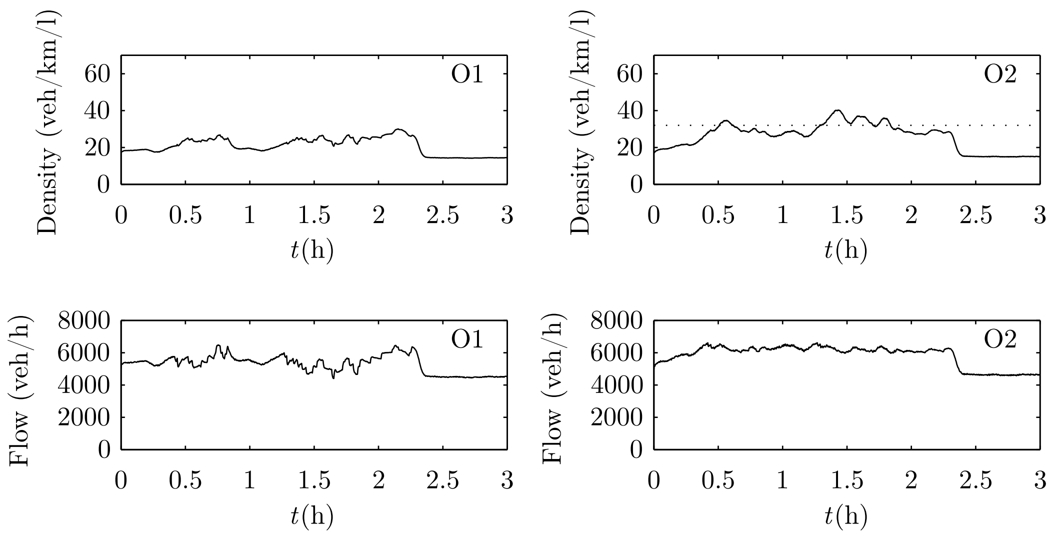

Figure 6.15: Lookup Controller: traffic conditions at the merge areas.

6.2.2.5 PI Controller

In this section, the PI Controller (Section 4.5) is applied. The system setup remains unchanged compared to the Lookup Controller, the controller itself being the only difference.

The resulting TTS is 3,410 veh·h, which is a 18.7 percent improvement compared to the no-control case and slightly worse than the Cascade and Lookup Controllers. The related density and flow profiles for both merge areas are shown in Figure 6.16, while the feedback VSL rate trajectories are shown in Figure 6.13(d). In this case, the density at the O2 merge-area (Figure 6.16) overshoots the set-point $\hat{\rho}_{\text{out}}$ slightly stronger than in the Lookup case at the first VSL control action; and, at the second VSL control action, it takes slightly longer to approach and stay in the vicinity of the set-point. Finally, the VSL rate trajectory for the PI Controller case (Figure 6.16(d)) shows a slightly slower reaction for high VSL rates compared to the other two feedback controllers.

6.2.3 VSL Control Period

The choice of the control period T_c in an MTFC via VSLs system determines the frequency of posted VSL changes, which should be limited. Defining a good control period may be a non-trivial task, and several generic guidelines and rules of thumb have been developed to assist control engineers in this task [73]. Several of these rules are based on characteristics of the time response of the system. However, other aspects should be considered as well. In the case considered here, the controllers have to reject disturbances in traffic flow that

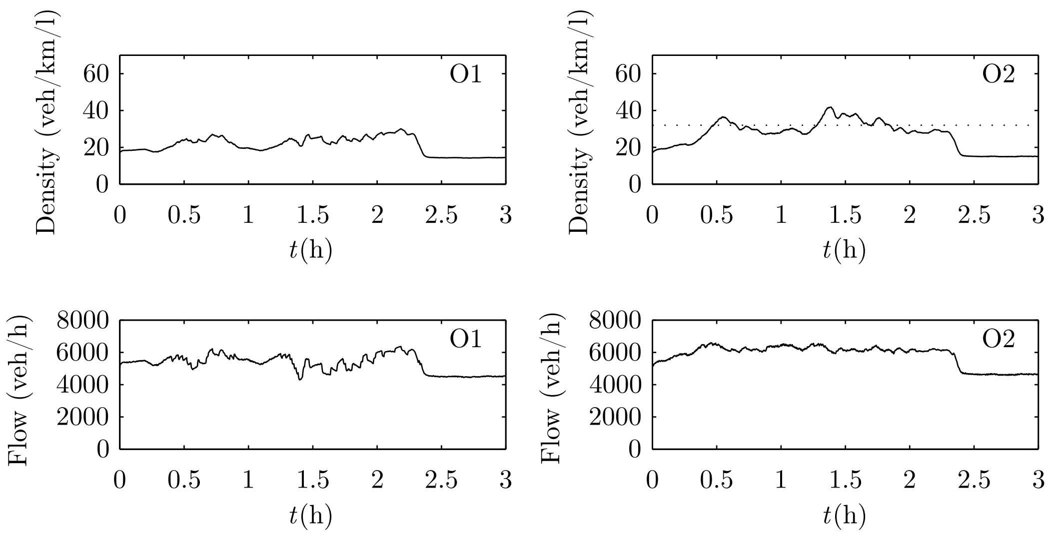

Figure 6.16: PI Controller: traffic conditions at the merge areas.

may cause serious variations within few minutes. Moreover, the adoption of discrete VSL rates introduces noise and errors, that may also affect the performance for a given control period. Finally, the system is non-linear and the chosen control period must be suitable for the whole VSL operating range. A thorough analysis of the choice of the control period is beyond the scope of this thesis and may indeed not be necessary from a practical point of view. Therefore, the investigation that follows is limited to the empirical evaluation of the controllers' behaviour for different control periods.

To evaluate the effect of the control period in the controllers' performance the simulations of Section 6.2.2 were repeated for eight further control periods, ranging from 90 s to 300 s at intervals of 30 s. For this experiment the gains of the feedback controllers were not retuned, since any efforts of retuning the controllers for larger control periods resulted in minor improvements in the smoothness of the output and no improvement in TTS. The resulting TTS values are plotted in Figure 6.17.

In Figure 6.17 it is seen that AMOC's TTS remains virtually unchanged as the control period is increased from 60 to 300 s; all model and external disturbance predictions being accurate within AMOC, a more dynamic VSL variation does not seem necessary to preserve the achieved level of beneficial VSL impact on traffic flow. Thus the open-loop optimal control approach (AMOC) with perfect knowledge would probably maintain a good performance even for longer control periods.

The feedback controllers, on the other hand, lack any predictive mechanisms; thus they exhibit a clear and increasing drop of performance for increasing control periods, because the

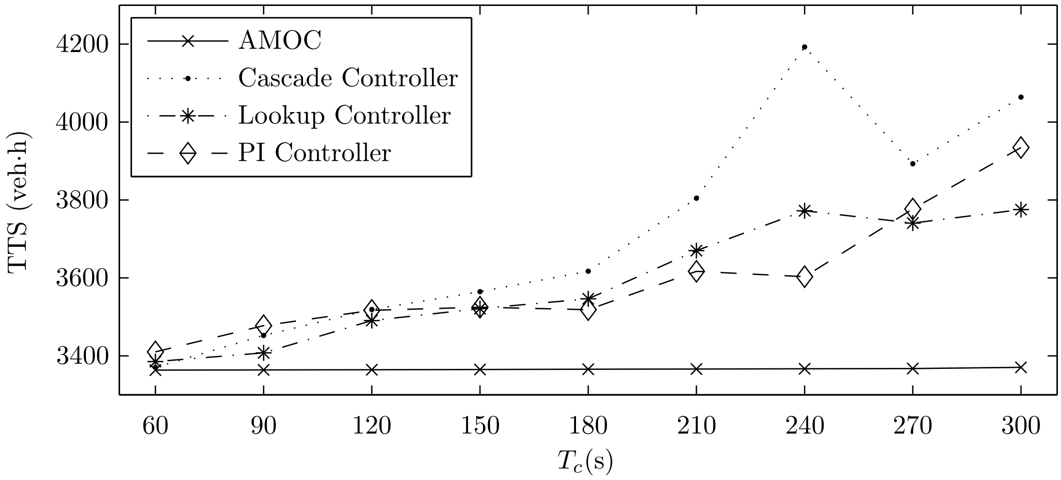

Figure 6.17: TTS for increasing control periods.

real-time measurements they rely on for their action become increasingly outdated due to the dynamics of the disturbances and the traffic flow process.

Besides the TTS, the smoothness of the output is a major requirement in traffic control systems to decide on a suitable control period. Although not shown, the system output is smooth with AMOC for the whole range of investigated control periods. On the other hand, the feedback controllers cannot really cope with much longer control periods, as their output deteriorates considerably (exhibiting increasingly strong time variations) for increased control periods, despite the relatively reasonable TTS values shown in Figure 6.17. As a matter of fact, the output of the PI and Lookup Controllers may be unacceptable for control periods longer than 90 s; while 120 s is the corresponding limit in the Cascade Controller case. Any attempt to re-tune the feedback gain values to reduce output oscillations for longer control periods leads to an accordingly slower control behaviour and TTS deterioration. In conclusion, T_c = 60 s is a suitable choice, and care must be taken when choosing longer control periods.

6.2.4 Increase of Capacity

In this section the case of possible VSL-induced capacity increases (for high VSL values according to Figure 4.7) is investigated. The simulation scenario (network and demand) remains unchanged compared to Section 6.2.2, except for the two constants A_m and E_m that affect two out of three b_m-dependent parameters of (2.9) according to (2.7) and (2.8), respectively. The new parameter values were also obtained via real-data fitting, albeit from a different motorway location than the previous ones, and are $A_m = 0.67$ and $E_m = 2.4$ and for all links m. The resulting fundamental diagrams obtained from (2.9) for these parameters give a maximum capacity at around $b = 0.89$ with an increase of approximately 1.7 percent (see Figure 4.7).

The network is simulated for Optimal Control and the Cascade, Lookup and PI Controllers, and the results are roughly comparable with the previous ones (Section 6.2.2). The figures showing the traffic variables are omitted, since the only outstanding difference is the increased outflows (leading to slightly shorter periods of operation at capacity), which are translated in the correspondingly reduced TTS in Table 6.3.

Table 6.3: Summary of simulated scenarios with increase of capacity.

Strategy	Description	TTS (veh·h)	%
AMOC	Optimal MTFC via VSLs applied at L11 and at L12-L13-L14.	3,280	−21.8
Cascade Controller	Feedback MTFC via VSLs applied at L11 with the VSL restrictions of Section 4.7.	3,283	−21.8
Lookup Controller	Feedback MTFC via VSLs applied at L11 with the VSL restrictions of Section 4.7.	3,301	−21.3
PI Controller	Feedback MTFC via VSLs applied at L11 with the VSL restrictions of Section 4.7.	3,315	−21.0

The resulting TTS for Optimal Control is 3,280 veh·h, which is a 21.8 percent improvement compared to the no-control case and better than the corresponding scenario without increase of capacity. Figure 6.18 shows the optimal VSL rates for this scenario. The VSL rates at L11 have a similar profile to the ones in Figure 6.13(a) (optimal control without capacity increase) but are slightly shorter in time and have higher values, since the possibility of increasing the bottleneck capacity renders the case less critical. The cluster L12-L13-L14 is seen to reach a value near $b = 0.87$ that corresponds to the VSL rate with maximum factual VSL-induced capacity, with an increase of approximately 1.3 percent in capacity. These values differ slightly from the ones resulting from (2.10) because of the contribution of the other terms of the dynamic speed equation (2.3).

The Cascade Controller is applied in the same way as in Section 6.2.2. Because discrete values of VSL rates are used (Section 4.7.1), the VSL rate applied at the acceleration and bottleneck areas is kept at 0.9 and the controller set-point remains unchanged. The consequence is a smaller capacity increase compared to the optimal control. Nevertheless, the resulting TTS for this scenario is 3,283 veh·h, which is an improvement of 21.8 percent and virtually the same as the capacity-increased optimal control scenario.

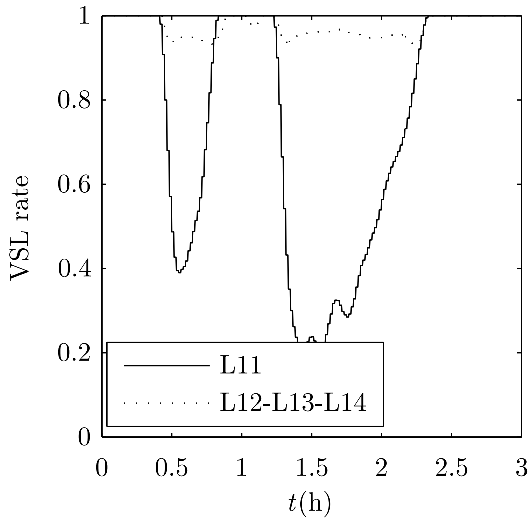

Figure 6.18: VSL rates: AMOC (with increase of capacity).

For the application of the Lookup Controller, a new lookup table is needed, and the same remarks provided for the Cascade Controller apply here also. New values were obtained in the same way as described in Section 4.4, and the resulting curve used for the generation of a lookup table is shown in Figure 6.19. Since the curve is now not monotonically increasing for increasing VSL rates, care must be taken to avoid overlapping flow ranges that would yield non-unique VSL rates; to this end, the curve is used only up to the (discrete) VSL rate b^* that yields highest capacity; while even higher flows are mapped to $b = 1$, i.e., no VSL application; and no (discrete) VSL rates are allowed between b^* and 1. It should be noted that, in the present case, $b^* = 0.9$, and hence no discrete VSL rate needs to be omitted. The resulting TTS for this scenario is 3,301 veh·h which is an improvement of 21.3 percent.

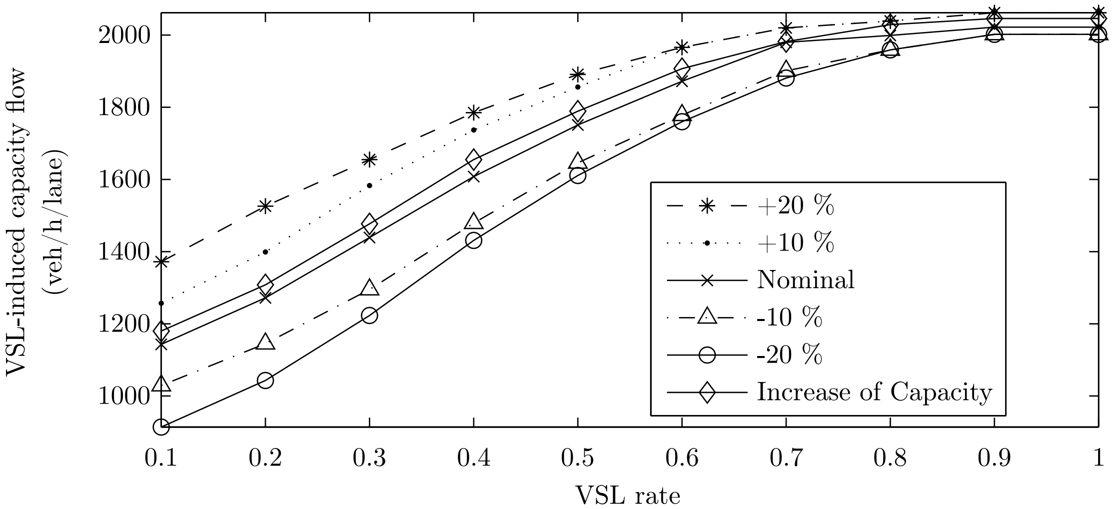

Figure 6.19: Simulated VSL-induced capacity flow with increase of capacity, and modified curves for robustness assessment of the Lookup Controller.

The PI Controller is applied in the same way as in Section 6.2.2 and the same remarks provided for the Cascade Controller apply here also. The resulting TTS for the PI Controller is 3,315 veh·h, which is an improvement of 21.0 percent and very close to the other controllers.

In conclusion, the possibility of a VSL-induced capacity increase does not affect the feedback controllers. In fact, they prove capable of exploiting this feature (wherever and whenever it may appear in practice) to improve their performance accordingly, while their outputs remain as smooth as in the case without increase of capacity.

6.2.5 Robustness of the Lookup Controller

The performance of the Lookup Controller is dependent on the design of the lookup table. Any mismatch in these values acts as a disturbance that, in absence of a secondary loop (as in the Cascade Controller), can only be compensated by the PI controller in the (primary) loop. In this section, the robustness of the Lookup Controller is evaluated with respect to mismatches in the lookup table. To this end, the (accurate) flow capacity values corresponding to specific VSL rates, obtained in Section 4.4 (Figure 4.5), are replaced by inaccurate values. More specifically, four scenarios are created, with respective capacity changes of −20 %, −10 %, 10 %, 20 %; albeit without allowing an increase of the non-VSL capacity (see Figure 6.19). Then, the new values are used to generate corresponding lookup tables, similar to the one in Figure 4.6.

The simulation results are shown in Table 6.4. All the scenarios show a merely slight decrease in performance with respect to TTS, compared to the nominal case. On the other hand, as Figure 6.20 indicates, the actual control results may differ in a more visible way; in this particular scenario, the 20 %-increase case looks even slightly better (from a set-point control point of view) than the nominal case.

In summary, a non-accurately designed lookup table can still provide good performance for

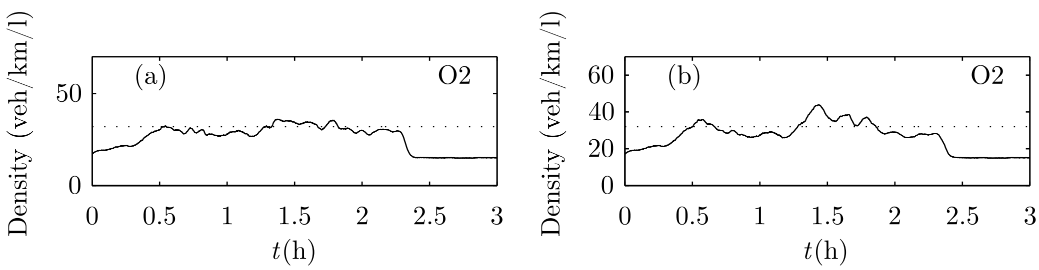

Figure 6.20: (a) Lookup Controller (+20 %); and (b) Lookup Controller (-20 %).

Table 6.4: Summary of simulated scenarios with modified lookup tables.

Strategy	Description	TTS (veh·h)	%
Lookup (+20 %)	As Lookup Controller, but the values of the lookup table are bigger than the nominal lookup table by up to +20 %.	3,380	−19.4
Lookup (+10 %)	As Lookup Controller, but the values of the lookup table are bigger than the nominal lookup table by up to +10 %.	3,391	−19.2
Lookup (-10 %)	As Lookup Controller, but the values of the lookup table are smaller than the nominal lookup table by up to -10 %.	3,393	−19.1
Lookup (-20 %)	As Lookup Controller, but the values of the lookup table are smaller than the nominal lookup table by up to -20 %.	3,406	−18.8

the Lookup Controller; further improvements may be attempted eventually via lookup table fine-tuning.

6.2.6 Remarks and Recommendations

The performance of the feedback controllers was found to be consistent also for other demand scenarios that are not reported here, with the Cascade Controller usually performing slightly better and faster. The Lookup Controller tends to perform slightly worse than what was shown in this section when compared to the Cascade Controller, having most of the time its performance in-between the Cascade and PI Controllers.

There are some minor differences between the presented controllers that should nevertheless be pointed out. The first one is that the Lookup and PI Controllers have one less controller gain to be tuned because of the suppression of the secondary loop. Even if there is little or no need for major re-tuning of the secondary loop from one location to another, this may be seen as a potential advantage of both (simpler) controllers, as controller tuning requires qualified personnel and should be performed with care, to avoid poor performance or even system instability. The investigations in Section 6.2.5 have shown that the Lookup Controller is fairly robust with respect to mismatches in the lookup table, but an initial, at least roughly accurate table is still needed, along with a possible limited fine-tuning effort.

Another difference is that the Lookup and PI Controllers, again because of the suppression of the secondary loop, do not need the flow measurement; however the cost related to the addition of such a measurement, if it is not available, is rather negligible. On the other hand, in some cases, the measurement of flow may help for early detection and compensation of possible disturbances, which is a potential advantage for the Cascade Controller.

Note that at the location of the mainstream flow measurement in Figure 6.1, the inflow from the on-ramp to the motorway has already merged with the flow delivered from the application area. This gives the opportunity for the secondary loop of the cascade controller to reject this on-ramp disturbance faster. If the detector was placed upstream of the on-ramp, the performance of the Cascade Controller would worsen slightly, since the disturbance would be rejected only after reaching the merge area of O1, as with the Lookup and PI Controllers. If a detector is not present downstream of the on-ramp merge, but a dedicated detector measures the outflow of the on-ramp into the motorway, this measurement can be added to the measured flow upstream of the on-ramp, with appropriate treatment for the number of lanes, before being fed to the Cascade Controller. Analogous reasoning applies in the case of an off-ramp. However, the placement of the detector even further downstream than immediately after the application area, should be considered with care; a sensor placed too far downstream might shift most of the dynamics between q_{c} and q_{out} (Figure 4.2)) into the secondary loop, thus spoiling the design of the Cascade Controller.

Assuming that the Cascade Controller is adopted, the Lookup or the PI Controllers can be implemented as back-up controllers that would enter in operation in case of failure of the flow detector used by the Cascade Controller. Given the good performances reported in this thesis, the developed feedback controllers could be used as an element in other control schemes as outlined in Section 4.8.

Chapter 7

Conclusions and Future Work

(...) the major challenge in the coming decade is the deployment of advanced and efficient traffic control strategies in the field.

M. Papageorgiou [52]

In this final chapter, the findings and results of this thesis are summarised, along with comments on further research on the topic. Section 7.1 gives a summary of the mains findings while the main contributions of this thesis are highlighted in Section 7.2. Finally, in Section 7.3, aspects that should be considered for further research are presented.

7.1 Concluding Remarks

Mainstream traffic flow control (MTFC), along with several related issues, is proposed and analysed as a new and innovative control measure for motorway traffic management. MTFC is aimed at avoiding the capacity drop that sets in case of uncontrolled bottleneck activation, thereby increasing the motorway throughput and significantly alleviating motorway congestion. Among several potential actuators for MTFC, variable speed limits (VSLs) are employed in this thesis in order to demonstrate the potential efficiency of the new control measure.

After the qualitative elaboration of the opportunities offered by the operation of VSLs to improve the traffic flow efficiency on motorways, a quantitative model for the impact of VSLs on aggregate traffic flow behaviour, which resulted from a related previous validation study with real traffic data, was proposed. VSLs were incorporated in a general macroscopic second-order traffic flow model as an additional control component leading to an accordingly extended general optimal control formulation and its numerical solution via the also-extended AMOC tool.

Optimal MTFC via VSLs was applied in simulation to a hypothetical motorway and also to a busy large-scale motorway ring road either as a standalone control tool or in combination with ramp metering. A series of appropriately designed control scenarios shed light on the properties and application procedures of MTFC and allowed to reveal, analyse and demonstrate the benefits of MTFC, which stem from its potential to avoid the capacity drop and its detrimental effects on traffic flow efficiency. In particular, it was shown in detail that traffic flow efficiency can be substantially improved when VSL control measures are used appropriately (particularly in integration with coordinated ramp metering) mainly by retarding or avoiding the capacity drop at active bottlenecks. The appropriate application of VSLs on motorways was shown to resemble ramp metering actions, albeit by holding traffic back on the mainstream rather than on the ramps. Conditions for temporary or durable mainstream flow reduction with VSLs were elaborated. The mainstream flow reduction via VSLs was exploited within the MTFC concept to avoid the appearance of the detrimental capacity drop at active bottlenecks.

Because of various inherent uncertainties, the open-loop optimal solution delivered by optimal control approaches becomes suboptimal when directly applied to the motorway traffic process [67]. However, the optimal results can be used in a rolling horizon mode or can be utilised to extract useful conclusions for the development of similarly efficient but simpler feedback control strategies.

Indeed, three simple MTFC feedback controllers using VSLs as an actuator were developed, examined and compared to the sophisticated optimal control approach. The proposed feedback control strategies are simple yet efficient as evidenced by their evaluation using the METANET macroscopic traffic simulator and their comparison with the optimal control approach for a hypothetical motorway stretch. All feedback controllers were found to be stable and robust, and to approach the optimal control performance without any need for on-line model calculations or future demand predictions. The feedback strategies consider several practical and safety requirements that may be necessary for the application of MTFC via VSLs in the field and, thanks to their simplicity, they are suitable for ready field implementation. Some recommendations for the choice and operation of the feedback controllers were also provided.

7.2 Main Contributions

The main contributions of this thesis can be summarized as follows:

- A new control method for traffic management on motorways that can drastically improve current traffic conditions on known otherwise active bottlenecks called mainstream traffic flow control (MTFC). MTFC is complementary to existing measures and can be applied to different types of motorway bottlenecks via different types of actuators.
- A better understanding of the impact of VSLs on aggregate traffic flow behaviour and how it can be appropriately used for motorway traffic flow control.
- An extended general second-order traffic flow model and corresponding optimal control formulation that can be solved efficiently even for large-scale networks, and that was validated against real field data with VSLs.
- Three MTFC feedback controllers developed based on methods of the control theory. The proposed feedback controllers take into account several safety and practical requirements and are simple yet efficient and robust, and are deemed suitable for immediate application in the field.

7.3 Further Research

In this thesis, MTFC was applied to on-ramp merge bottlenecks with the use of VSLs as an actuator. Investigations using other MTFC actuators such as traffic lights or VII systems and the application to other types of bottlenecks should be carried out for both the optimal control and feedback control approaches.

The integration of MTFC via VSLs with ramp metering was studied for the optimal control case. The integration of feedback MTFC with feedback ramp metering control at the local level was outlined. The integrated control via feedback control strategies at the local and global levels, along with a single coordinated MTFC strategy for large-scale networks are necessary and worth further investigation. The extension and integration of the feedback controllers with other motorway control strategies and measures should be also investigated. Additionally, the optimal control problem presented in Chapter 2 could be cast into a rolling horizon mode and be applied to large-scale networks and lead to additional insights.

The outlined extension of MTFC for merging motorways could benefit from a queue management scheme. This scheme would override the delay balancing in order to avoid, for as long as possible, situations where controlled congestion in one motorway covers an important off-ramp while a longer controlled congestion would not be harmful in the other motorway.

Further research could address the detailed application of MTFC at local level by use of microscopic simulation, along with a rigorous validation effort of the microsimulation model.

As already mentioned in Chapter 2, more investigation and validation work with VSL data are necessary for a quantitatively accurate and reliable description of the VSL impact on traffic flow.

Finally, and most importantly, a field test of the MTFC concept by the presented feedback strategies should be attempted in the near future.

Bibliography

[1] PTV AG. VISSIM - Multi-Modal Traffic Flow Modeling, July 2011. URL `http://www.vissim.de/`. 6

[2] P. Albertos and I. Mareels. *Feedback and Control for Everyone*. Springer, Berlin, 2010. 49

[3] A. Alessandri, A. Di Febbraro, A. Ferrara, and E. Punta. Optimal control of freeways via speed signalling and ramp metering. *Control Engineering Practice*, 6(6):771–780, June 1998. 26, 36

[4] R. C. Carlson, A. Ragias, I. Papamichail, and M. Papageorgiou. Mainstream traffic flow control of merging motorways using variable speed limits. In *Proceedings of The 19th Mediterranean Conference on Control and Automation*, pages 674–681, Corfu, Greece, 2011. 67

[5] M. Cassidy and J. Rudjanakanoknad. Increasing the capacity of an isolated merge by metering its on-ramp. *Transportation Research Part B: Methodological*, 39(10):896–913, December 2005. 2, 13, 35, 38

[6] H. Chang, Y. Wang, J. Zhang, and P. Ioannou. An integrated roadway controller and is evaluation by microscopic simulator VISSIM. In *Proceedings of The European Control Conference*, pages 2436–2441, Kos, Greece, 2007. 37

[7] C. Chen, Z. Jia, and P. Varaiya. Causes and cures of highway congestion. *IEEE Control Systems Magazine*, 21(6):26–32, 2001. 1, 2, 14

[8] L. Chen, A. M. May, and D. M. Auslander. Freeway ramp control using fuzzy set theory for inexact reasoning. *Transportation Research Part A: General*, 24(1):15–25, January 1990. 36

[9] O. Chen, A. Hotz, and M. Ben-Akiva. Development and evaluation of a dynamic ramp metering control model. In *Proceedings of the 8th IFAC/IFIP/IFORS Sympos. Transportation Systems*, Chania, Greece, 1997. 14

[10] Y. H. Chiang and J. C. Juang. Control of freeway traffic flow in unstable phase by H-infinity theory. *IEEE Transactions on Intelligent Transportation Systems*, 9(2):193–208, June 2008. 37

[11] K. Chung, J. Rudjanakanoknad, and M. Cassidy. Relation between traffic density and capacity drop at three freeway bottlenecks. *Transportation Research Part B: Methodological*, 41(1):82–95, January 2007. 13, 39

[12] S. Cohen, M. Ayot, and N. Duc. Guide méthodologique: enjeux des mesures de régulation dynamique de vitesses. Technical report, INRETS and LEE, 2008. 3, 15, 45

[13] European Comission. Roadmap to a single european transport area – towards a competitive and resource efficient transport system. WHITE PAPER, European Comission, Brussels, Belgium, 2011. 1

[14] M. Cremer. *Der Verkehrsfluß auf Schnellstraßen*. Springer, Berlin, 1979. xxiii, 19, 26, 36

[15] K. W. Crowley and H. Greenberg. Holland tunnel study aids efficient increase of tube's use. *Traffic Engineering*, 35:20–41, 1965. 36

[16] C. F. Daganzo. The nature of freeway gridlock and how to prevent it. In *Traffic and Transportation Theory*, pages 629–646. Pergamon, Lesort, J. B. (ed.), 1996. 13

[17] C. Diakaki and M. Papageorgiou. Design and simulation test of coordinated ramp metering control (METALINE) for A10-West in amsterdam. Internal Report 1994-2, Dynamic Systems and Simulation Laboratory, Technical University of Crete, Chania, Greece, 1994. 14

[18] G. Ellis. *Control System Design Guide: a practical guide*. Elsevier Academic Press, Amsterdam, 2004. 56

[19] R. S. Foote. Instruments for road transportation. *High Speed Ground Transportation Journal*, 18(1501):260–281, 1968. 36

[20] R. S. Foote and K. W. Crowley. Developing density controls for improved traffic operations. *Highway Research Board Record*, 154(1430):24–37, 1967. 36

[21] G. F. Franklin, J. D. Powel, and M. L. Workman. *Digital Control of Dynamic Systems*. Addison-Wesley, Menlo Park Calif., 3rd edition, 1998. 52

[22] D. C. Gazis and R. S. Foote. Surveillance and control of tunnel traffic by an on-line digital computer. *Transportation Science*, 3(3):255–275, August 1969. 35, 36

[23] G. Gomes and R. Horowitz. Optimal freeway ramp metering using the asymmetric cell transmission model. *Transportation Research Part C: Emerging Technologies*, 14(4): 244–262, August 2006. 14

[24] H. Greenberg and A. Daou. The control of traffic flow to increase flow. *Operations Research*, 8(4):524–532, 1960. 35

[25] K. A. Haboian. A case for freeway mainline metering. *Transportation Research Record*, 1494:11–20, 1995. 36, 40

[26] F. L. Hall. Chapter 2: Traffic stream characteristics. In *Traffic Flow Theory: State-of-the-art Report*. FHWA/TRB/ORNL, Gartner, N., Messer, C. J., Rathi, A. K. (eds.), USA, 2001. 39

[27] A. Hegyi. *Model predictive control for integrating traffic control measures*. PhD Thesis, TRAIL Thesis Series T2004/2, Delft University of Technology, The Netherlands, 2004. xxiii, 19, 20, 21, 22, 26, 36

[28] A. Hegyi and S. P. Hoogendoorn. Dynamic speed limit control to resolve shock waves on freeways - field test results of the SPECIALIST algorithm. In *13th International IEEE Conference on Intelligent Transportation Systems*, pages 519–524, Funchal, Madeira Island, Portugal, September 2010. 14, 37

[29] A. Hegyi, M. Burger, B. De Schutter, J. Hellendoorn, and T. J. J. van den Boom. Towards a practical application of model predictive control to suppress shock waves on freeways. In *Proceedings of The European Control Conference 2007 (ECC'07)*, pages 1764–1771, Kos, Greece, 2007. 36

[30] A. Hegyi, S.P. Hoogendoorn, M. Schreuder, H. Stoelhorst, and F. Viti. SPECIALIST: a dynamic speed limit control algorithm based on shock wave theory. In *2008 11th International IEEE Conference on Intelligent Transportation Systems*, pages 827–832, Beijing, China, October 2008. 14, 37

[31] B. G. Heydecker and J. D. Addison. Analysis and modelling of traffic flow under variable speed limits. *Transportation Research Part C: Emerging Technologies*, 19(2):206–217, April 2011. 19

[32] L. Intpanis, S. Broekx, and R. Liu. Modelling instantaneous traffic emission and the influence of traffic speed limits. *Science of The Total Environment*, 371(1-3):270–285, December 2006. 17

[33] E. Jacobson and J. Landsman. Case studies of US freeway-to-freeway ramp and mainline metering and suggested policies for Washington State. *Transportation Research Record*, 1446:48–55, 1994. 36

[34] K. Kampitaki. *Integrated control of traffic flow using ramp metering an variable speed limits (in Greek)*. MSc Thesis, Department of Production Engineering and Management, Technical University of Crete, Chania, Greece, 2008. 26, 27, 28

[35] V. L. Knoop, A. Duret, C. Buisson, and B. van Arem. Lane distribution of traffic near merging zones: influence of variable speed limits. In *13th International IEEE Conference on Intelligent Transportation Systems*, pages 485–490, Funchal, Madeira Island, Portugal, September 2010. 19

[36] A. Kotsialos and M. Papageorgiou. Efficiency and equity properties of freeway network-wide ramp metering with AMOC. *Transportation Research Part C: Emerging Technologies*, 12(6):401–420, December 2004. 2, 14

[37] A. Kotsialos, M. Papageorgiou, C. Diakaki, Y. Pavlis, and F. Middelham. Traffic flow modeling of large-scale motorway networks using the macroscopic modeling tool METANET. *IEEE Transactions on Intelligent Transportation Systems*, 3(4):282–292, December 2002. 23, 27, 82, 85

[38] A. Kotsialos, M. Papageorgiou, M. Mangeas, and H. Haj-Salem. Coordinated and integrated control of motorway networks via non-linear optimal control. *Transportation Research Part C: Emerging Technologies*, 10(1):65–84, February 2002. 14, 31, 33, 71, 108

[39] A. Kouvelas, K. Aboudolas, E. B. Kosmatopoulos, and M. Papageorgiou. Adaptive performance optimization for large-scale traffic control systems. *IEEE Transactions on Intelligent Transportation Systems*, 2011. doi: 10.1109/TITS.2011.2159002. 57

[40] J. P. Lebacque and H. Haj-Salem. Speed limit control: a problem formulation and theoretical discussions. In *Proceedings of the 4th Triennial Symposium in Transportation Analysis*, pages 421–426, São Miguel, Azores, 2001. 21

[41] J. P. Lebacque and H. Haj-Salem. Ramp metering, speed management, and braess-like paradoxes. In *Proceedings of the 5th Triennial Symposium in Transportation Analysis*, Le Gosier, Guadaloupe, French West Indies, 2004. 21

[42] P. W. Lin, K. P. Kang, and G. L. Chang. Exploring the effectiveness of variable speed limit controls on highway work-zone operations. *Journal of Intelligent Transportation Systems*, 8(3):155–168, July 2004. 37, 41

[43] M. Lorenz and L. Elefteriadou. Defining freeway capacity as function of breakdown probability. *Transportation Research Record*, 1776:43–51, January 2001. 45

[44] X. Y. Lu, P. Varaiya, R. Horowitz, D. Su, and S. E. Shladover. A new approach for combined freeway variable speed limits and coordinated ramp metering. In *13th International IEEE Conference on Intelligent Transportation Systems*, pages 491–498, Funchal, Madeira Island, Portugal, September 2010. 37, 54

[45] M. S. McCalden Jr. A traffic management system for the San Francisco-Oakland bay bridge. *ITE Journal*, 54(5):46–51, 1984. 36, 42

[46] A. Messmer and M. Papageorgiou. METANET: a macroscopic simulation program for motorway networks. *Traffic Engineering and Control*, 31(8):466–470, 1990. 23

[47] M. Mirshahi, J. Obenberger, C. A. Fuhs, C. E. Howard, R. A. Krammes, B. T. Kuhn, R. M. Mayhew, M. A. Moore, K. Sahebjam, and C. J. Stone. Active traffic management: The next step in congestion management. Technical Report FHWA-PL-07-012, Federal Highway Administration, July 2007. 15

[48] M. Morari and E. Zafiriou. *Robust process control*. Prentice Hall, Englewood Cliffs, N.J., 1989. 54

[49] H. Okamura, S. Watanabe, and T. Watanabe. An empirical study on the capacity of bottlenecks on the basic suburban expressway sections in Japan. In *Fourth International Symposium on Highway Capacity*, pages 120–129, Maui, Hawaii, 2000. 42

[50] M. Papageorgiou. *Optimierung*. Oldenbourg, München, 2nd edition, 1996. 31

[51] M. Papageorgiou. Reduction of total time spent in a freeway system by on-ramp metering. Internal Report 1997-11, Dynamic Systems and Simulation Laboratory, Technical University of Crete, Chania, Greece, 1997. 13

[52] M. Papageorgiou. Traffic control. In *Handbook of Transportation Science*, volume 56, pages 243–277. Kluwer Academic Publishers, Hall, R. W. (ed.), Boston, 2003. 11, 49, 97, 123

[53] M. Papageorgiou and A. Kotsialos. Freeway ramp metering: an overview. *IEEE Transactions on Intelligent Transportation Systems*, 3(4):271–281, 2002. 1, 12, 13, 14

[54] M. Papageorgiou and M. Marinaki. A feasible direction agorithm for the numerical solution of optimal control problems. Internal Report 1995-4, Dynamic Systems and Simulation Laboratory, Technical University of Crete, Chania, Greece, 1995. 31

[55] M. Papageorgiou and R. Mayr. Optimal decomposition methods applied to motorway traffic control. *International Journal of Control*, 35(2):269–280, February 1982. 14

[56] M. Papageorgiou and I. Papamichail. Handbook of ramp metering. Deliverable 7.5, Report for the European IST Office, Brussels, Belgium, 2007. 14, 68

[57] M. Papageorgiou and I. Papamichail. Overview of traffic signal operation policies for ramp metering. *Transportation Research Record: Journal of the Transportation Research Board*, 2047:28–36, December 2008. 61, 68

[58] M. Papageorgiou, J. M. Blosseville, and H. Haj-Salem. Modelling and real-time control of traffic flow on the southern part of Boulevard Peripherique in Paris: Part II: coordinated on-ramp metering. *Transportation Research Part A: General*, 24(5):361–370, September 1990. 14

[59] M. Papageorgiou, J. M. Blosseville, and H. Haj-Salem. Modelling and real-time control of traffic flow on the southern part of Boulevard Peripherique in Paris: Part I: modelling. *Transportation Research Part A: General*, 24(5):345–359, September 1990. 23, 25

[60] M. Papageorgiou, H. Haj-Salem, and J. M. Blosseville. ALINEA: a local feedback control law for on-ramp metering. *Transportation Research Record*, 1320:58–64, 1991. 50, 53

[61] M. Papageorgiou, H. Hadj-Salem, and F. Middelham. ALINEA local ramp metering: Summary of field results. *Transportation Research Record*, 1603:90–98, January 1997. 50, 61

[62] M. Papageorgiou, E. Kosmatopoulos, M. Protopappas, and I. Papamichail. Effects of variable speed limits (VSL) on motorway traffic. Internal Report 2006-25, Dynamic Systems and Simulation Laboratory, Technical University of Crete, Chania, Greece, 2006. 4, 18, 22, 26

[63] M. Papageorgiou, E. Kosmatopoulos, and I. Papamichail. Effects of variable speed limits on motorway traffic flow. *Transportation Research Record: Journal of the Transportation Research Board*, 2047:37–48, December 2008. 3, 4, 20, 22, 26, 50, 65

[64] M. Papageorgiou, I. Papamichail, A. Spiliopoulou, and A. Lentzakis. Real-time merging traffic control with applications to toll plaza and work zone management. *Transportation Research Part C: Emerging Technologies*, 16(5):535–553, October 2008. 35, 38, 41, 44, 45

[65] I. Papamichail and M. Papageorgiou. Balancing of queues or waiting times on metered dual-branch on-ramps. *IEEE Transactions on Intelligent Transportation Systems*, 12(2): 438–452, 2011. 67

[66] I. Papamichail, K. Kampitaki, M. Papageorgiou, and A. Messmer. Integrated ramp metering and variable speed limit control of motorway traffic flow. In *Proceedings of The 17th IFAC World Congress*, pages 14084–14089, Seoul, Korea, 2008. 23, 39, 65

[67] I. Papamichail, A. Kotsialos, I. Margonis, and M. Papageorgiou. Coordinated ramp metering for freeway networks – a model-predictive hierarchical control approach. *Transportation Research Part C: Emerging Technologies*, 18(3):311–331, June 2010. 2, 14, 40, 84, 88, 124

[68] I. Papamichail, M. Papageorgiou, V. Vong, and J. Gaffney. Heuristic Ramp-Metering coordination strategy implemented at Monash freeway, Australia. *Transportation Research Record: Journal of the Transportation Research Board*, 2178:10–20, 2010. 62

[69] A. Popov, R. Babuska, A. Hegyi, and H. Werner. Distributed controller design for dynamic speed limit control against shock waves on freeways. In *Proceedings of The 17th IFAC World Congress*, pages 14060–14065, Seoul, Korea, 2008. 37

[70] K. J. Åström and B. Wittenmark. *Adaptive Control*. Addison-Wesley, 2nd edition, 1995. 58

[71] M. Robinson. Examples of variable speed limit applications, 2000. URL `http://ntl.bts.gov/lib/jpodocs/briefing/12164.pdf`. 15

[72] D. Schrank, T. Lomax, and S. Turner. Urban mobility report 2010. Technical report, Texas Transportation Institute, The Texas A&M University System, 2010. URL http://mobility.tamu.edu. 1

[73] D. Seborg, T. F. Edgar, and D. A. Mellichamp. *Process Dynamics and Control*. Wiley, New York, 1989. 54, 67, 114

[74] F. G. Shinskey. *Process control systems: application, design, and tuning*. McGraw-Hill, New York, 4th edition, 1996. 54, 57, 69

[75] S. Skogestad. Simple analytic rules for model reduction and PID controller tuning. *Journal of Process Control*, 13(4):291–309, June 2003. 57

[76] E. Smaragdis and M. Papageorgiou. Series of new local ramp metering strategies. *Transportation Research Record*, 1856:74–86, 2003. 21

[77] S. Smulders. Control of freeway traffic flow by variable speed signs. *Transportation Research Part B: Methodological*, 24(2):111–132, April 1990. 19

[78] A. D. Spiliopoulou, I. Papamichail, and M. Papageorgiou. Toll plaza merging traffic control for throughput maximization. *Journal of Transportation Engineering*, 136(1):67, 2010. 36

[79] G. Stephanopoulos. *Chemical process control: an introduction to theory and practice*. Prentice-Hall, Englewood Cliffs, N.J., 1984. 54, 66, 68

[80] TSS-Transport Simulation Systems. Aimsun, July 2011. URL http://www.aimsun.com/. 6

[81] G. Toulminet, J. Boussuge, and C. Laurgeau. Comparative synthesis of the 3 main european projects dealing with cooperative systems (CVIS, SAFESPOT and COOPERS) and description of COOPERS demonstration site 4. In *2008 11th International IEEE Conference on Intelligent Transportation Systems*, pages 809–814, Beijing, China, October 2008. 14

[82] Y. Wang and M. Papageorgiou. Local ramp metering in the case of distant downstream bottlenecks. In *2006 IEEE Intelligent Transportation Systems Conference*, pages 426–431, Toronto, ON, Canada, 2006. 61, 62

[83] Y. Wang, M. Papageorgiou, and A. Messmer. RENAISSANCE – a unified macroscopic model-based approach to real-time freeway network traffic surveillance. *Transportation Research Part C: Emerging Technologies*, 14(3):190–212, June 2006. 67

[84] Y. Wang, M. Papageorgiou, G. Sarros, and W. Knibbe. Feedback route guidance applied to a large-scale express ring road. *Transportation Research Record*, 1965:79–88, 2006. 3, 14

[85] D. Warren. Variable speed limits, 2000. URL http://safety.fhwa.dot.gov/speedmgt/vslimits/docs/warren_vsl.ppt. 15

[86] D. Warren. Variable speed limits, 2003. URL http://ops.fhwa.dot.gov/wz/workshops/originals/Warren.ppt. 15

[87] H. Wei and M. Pavithran. Concept of dynamic merge metering approach for work zone traffic control. pages 374–379, Delft, The Netherlands, August 2006. 41

[88] S. Xiaotian and R. Horowitz. A localized switching ramp-metering control with queue length estimation and microscopic simulation results. In *Proceedings of the 16th IFAC World Congress, 2005*, Prague, Czech Republic, 2005. 21

[89] S. Xiaotian and R. Horowitz. A localized switching ramp-metering controller with a queue length regulator for congested freeways. In *Proceedings of the 2005, American Control Conference, 2005.*, pages 2141–2146, Portland, OR, USA, 2005. 21

[90] H. Zackor. Beurteilung verkehrsabhängiger geschwindigkeitsbeschränkungen auf autobahnen. *Forschung Strassenbau und Strassenverkehrstechnik*, 128:1–61, 1972. 18, 19

[91] H. Zackor. Speed limitation on freeways: traffic-responsive strategies. In *Concise Encyclopedia of Traffic and Transportation Systems*, pages 507–511. M. Papageorgiou (ed.). Pergamon, Oxford, UK, 1991. xxiii, 18, 19, 21

[92] S. K. Zegeye, B. De Schutter, H. Hellendoorn, and E. A. Breunesse. Model-based traffic control for balanced reduction of fuel consumption, emissions and travel time. In *2010 12th IFAC Symposium on Control for Transportation Systems*, Redondo Beach, CA, USA, September 2009. 17

[93] S. K. Zegeye, B. De Schutter, J. Hellendoorn, and E. A. Breunesse. Variable speed limits for area-wide reduction of emissions. In *13th International IEEE Conference on Intelligent Transportation Systems*, pages 507–512, Funchal, Madeira Island, Portugal, September 2010. 17

[94] H. M. Zhang and W. W. Recker. On optimal freeway ramp control policies for congested traffic corridors. *Transportation Research Part B: Methodological*, 33(6):417–436, August 1999. 14

[95] J. Zhang, H. Chang, and P. A. Ioannou. A simple roadway control system for freeway traffic. In *2006 American Control Conference*, pages 4900–4905, Minneapolis, MN, USA, 2006. 36, 39, 58